

---

Masters Theses

Student Theses and Dissertations

---

1951

## Investigation of vacuum tubes as four terminal networks

Vasil Uzunoglu

Follow this and additional works at: [https://scholarsmine.mst.edu/masters\\_theses](https://scholarsmine.mst.edu/masters_theses)



Part of the [Electrical and Computer Engineering Commons](#)

Department:

---

### Recommended Citation

Uzunoglu, Vasil, "Investigation of vacuum tubes as four terminal networks" (1951). *Masters Theses*. 3016.  
[https://scholarsmine.mst.edu/masters\\_theses/3016](https://scholarsmine.mst.edu/masters_theses/3016)

This thesis is brought to you by Scholars' Mine, a service of the Missouri S&T Library and Learning Resources. This work is protected by U. S. Copyright Law. Unauthorized use including reproduction for redistribution requires the permission of the copyright holder. For more information, please contact [scholarsmine@mst.edu](mailto:scholarsmine@mst.edu).

INVESTIGATION OF VACUUM TUBES AS  
FOUR TERMINAL NETWORKS

BY  
VASIL UZUNOGLU

---

A  
THESIS

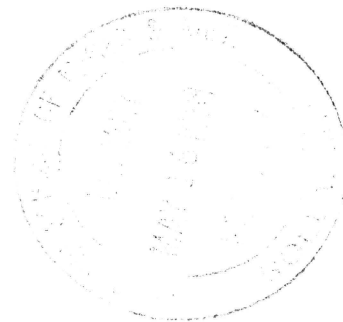
submitted to the faculty of the  
SCHOOL OF MINES AND METALLURGY OF THE UNIVERSITY OF MISSOURI

in partial fulfillment of the work required for the  
Degree of

MASTER OF SCIENCE, ELECTRICAL ENGINEERING

Rolla, Missouri

1951



Approved by

*Gabriel G. Skitek*

Professor of Electrical Engineering

79638

### Acknowledgment

The writer of this thesis is deeply grateful to Mr. G. G. Skitek, Professor of Electrical Engineering, University of Missouri, School of Mines and Metallurgy, for his valuable suggestions and assistance in the preparation of this paper.

The writer of this thesis is also grateful to Mr. C. Grimm, Instructor in Electrical Engineering for his valuable assistance in preparing the graphs and diagrams used in this thesis.

## CONTENTS

Acknowledgments.....	ii
List of Tables.....	iv
Introduction.....	1
Classical Methods of Equivalent Circuit Representation.....	4
Electron Theories.....	30
Vacuum Tubes Equivalent Circuits When Transit Time is Taken Into Account.....	41
Electron Stream Theory as Applied to Vacuum Tubes.....	57
Four Terminal Networks in General.....	97
Application of Four Pole Terminal Admittances to Vacuum Tubes.....	102
Admittance Measurement of Vacuum Tubes.....	118
Conclusions.....	155
Appendix 1.....	158
Appendix 2.....	163
Appendix 3.....	168
Bibliography.....	169
Index.....	172
Vita.....	175

## LIST OF ILLUSTRATIONS

<u>No.</u>	<u>Title</u>	<u>Page</u>
1.....	Triode Tube.....	8
2.....	Plot of Plate Current Versus Plate Voltage of Triode Tube.....	9
3.....	Equivalent Grid and Plate Circuit of a Triode Tube.....	11
4.....	Equivalent Circuit of Negative Grid Triode at Low Frequencies.....	12
5.....	Equivalent Circuit of Negative Grid Triode at Low Frequencies with a Current Source.....	13
6.....	Equivalent Circuit of Positive Grid Triode at Low Frequencies.....	13
7.....	Equivalent Circuit of Triode with Con- sideration of Displacement Currents.....	18
8.....	Equivalent Circuit Representing Displace- ment Currents.....	18
9.....	Triode Showing the Interelectrode and Capacitances and Lead Inductances.....	20
10.....	Equivalent Circuit of Triode Including the Internal Lead Effects and the Inter- electrode Capacitances.....	22
11.....	Schematic Diagram of Triode Including Outside Pin and Lead Effects as well as Stray Capacitances.....	23
12.....	Equivalent Circuit of Triode with Internal and External Tube Effects Taken Into Account.....	24
13.....	A Charge Between Two Parallel Plates....	33
14.....	Potential Distribution Between Two Para- llel Planes of Positive Potentials.....	36

15.....	Current Flow Lines Between Two Parallel Planes.....	41
16.....	Plot of Internal Plate Impedance Versus Frequency.....	51
17.....	Plot of Total Impedance Versus Frequency.....	51
18.....	Plot of Amplification Factor Versus Frequency.....	52
19.....	Plot of Phase of Amplification Factor Versus Frequency.....	52
20.....	Equivalent Circuit of Plate Cathode Path of Negative Grid Triode at Low Values of Transit Time.....	53
21.....	Plot of                      Versus Space Charge Factor.....	67
22.....	Plot of Diode Resistance and Reactance Versus Transit Time.....	77
23.....	General Diagram of Multielement Vacuum Tube.....	78
24.....	Equivalent Circuit of Third Region.....	82
25.....	Equivalent Network of Electron Stream of Figure No. 23.....	83
26.....	Plot of Magnitude and Phase of Versus Transit Angle.....	88
27.....	Electron Stream Equivalent Circuit of a Triode.....	92
28.....	Electron Stream Equivalent Circuit of a Negative Grid Triode.....	94
29.....	General Four Pole Equivalent Circuit.....	98

30.....	General Four Pole Network.....	99
31.....	Representation of the Bilateral Equivalent Vacuum Tube Circuit.....	106
32.....	Equivalent Circuit of a Positive Grid Triode at Moderately Low Frequencies.....	107
33.....	Electron Stream Equivalent Circuit of a Triode with Negative Grid.....	109
34.....	A Different Representation of Fig. No.33.....	109
35.....	Transformation of Current Source to Voltage Source of Fig. No. 34.....	110
36.....	Representation of Electron Stream Equivalent Circuit by Four Pole Network.....	113
37.....	Representation of Electron Stream Equivalent Circuit by Four Pole Network at Moderately High Frequencies.....	115
38.....	Potential Distribution in a Diode.....	118
39.....	Equivalent Circuit of Diode Measuring Equipment.....	121
40.....	Plot of Values Versus $\frac{Y}{Y_0}$ .....	125
41.....	Four Pole Representation of a Negative Grid Triode.....	126
42.....	Diagram for the Measurements of Admittances.....	128
43.....	Schematic Diagram of a System for Phase Angle and Transfer Impedance Measurements.....	130
44.....	Equivalent Circuit of a Triode and its Associated Measuring Equipment.....	133
45.....	Equivalent Circuit of a Triode Based on Experimental Results.....	138
46.....	Plot of Experimental and Theoretical Values of Phase of Transadmittance for a 1553 Triode.....	140

47.....	A Short Circuited Transmission Line.....	143
48.....	Semi-Schematic Diagram for Susceptance Variation Method.....	150
49.....	A Hybrid Device.....	158
50.....	Spreading of a Wave Front Into a Compound Junction from the Series Arm.....	159
51.....	T Junction in a Wave Guide in the E Plane....	160
52.....	Spreading of a Wave Front Into a Compound Junction from the Parallel Arm.....	161
53.....	T Junction in the Wave Guide in the H Plane..	162
54.....	Compound T Junction of a Wave Guide.....	162
55.....	Plot of Electron Trajectories Versus $x$ and $t$ When Two Electrons Cross.....	165
56.....	Plot of Electron Trajectories Versus $x$ and $t$ When Two Electrons Cross.....	166



## LIST OF TABLES

<u>No.</u>	<u>Title</u>	<u>Page</u>
I	Values of Alternating Current Components of Electron Stream.....	70
II	Complete Space Charge.....	71
III	Zero Space Charge.....	72
IV	Symbols used in the Derivation of Electron Stream Equivalent Circuit.....	72
V	Limiting Values of Admittances for Electron Stream Equivalent Circuit.....	86

## INTRODUCTION

The concept of the equivalent plate to cathode circuit <sup>of a vacuum tube</sup> is about as old as the tube itself. The work of Van der Bijl and Nichols showed that for purposes of circuit analysis, the plate to cathode circuit could be replaced by a fictitious generator of voltage  $\mu e_g$ , in series with a resistance whose magnitude is equal to the reciprocal of the slope of the static  $i_b - e_b$  characteristics. In this concept, where the vacuum tube is replaced by its equivalent network, one outstanding feature is exemplified, namely the separation of the alternating and direct current components. The equivalent network is applicable to the alternating components of the currents only.

As long as the frequency remained low the above representation gave results comparable to actual operation. However, as the frequency range was increased, complications arose. The complications were due to the interelectrode capacitance existing between the various elements of the vacuum tube.

As time progressed, higher and higher frequencies were desired. This range of frequencies brought about changes in the equivalent circuit of the vacuum tube that included the internal lead effect of the tube and the transit time.

These early equivalent circuits were derived by purely mathematical means and no thought was given to the electron stream itself. The first undertaking of the problem of developing a generally valid system based on <sup>the</sup> electron stream

was made by W. E. Benham. This work was a great contribution toward the development of the equivalent circuit of the vacuum tube based on the electron stream theory.

Following Benham's work, many investigators such as Llewellyn, Peterson, and Ferris, have extended the ideas formulated by Benham for the representation of vacuum tube circuits. The first outstanding work comes from Llewellyn who, by the use of Maxwell's equations, derived one equivalent circuit which can be considered as an extension of the classical equivalent vacuum tube representation. The above derivation was not complete and <sup>the</sup> most pronounced defect was the assumption of zero space charge, and the single valued electron velocity.

A more vigorous attack was made by Llewellyn and Peterson and the result was quite dependable with the only assumption of the single valued electron velocity. In order to make the complex equivalent circuit derived by Llewellyn and Peterson more suitable for practical purposes, the four pole network theorems were applied to the results of Llewellyn and Peterson's work.

Still, the representation of vacuum tubes by equivalent four pole networks was not a final and rigorous solution to the problem as far as practical use was concerned. This was due to the fact that the evaluation of the four pole parameters were real lengthy and tedious.

---

(1) Benham, W. E., Theory of Internal Action of Thermionic Systems at Moderately High Frequencies, Phil. Mag., Vol. 11, p. 457, Feb. 1931.

A final solution to the problem was the experimental determination of the four pole parameters which made the equivalent four pole representation of the vacuum tube of practical significance.

This thesis was undertaken with the aim of consolidating the most important work that has been done in the field of equivalent vacuum tube circuits which has been found to be highly disassociated.

The author of this thesis feels that this thesis is the most complete consolidation of information on equivalent vacuum tube circuits.

## SECTION I

## Classical Methods of Equivalent Circuit Representation

(A) The First Concept of Equivalent Circuit

The art of equivalent network representation has grown considerable since its inception by Dr. G. A. Campbell in his paper "Cissoidal Oscillations", which was published in 1911. He proved that any passive network made up of a finite number of invariable elements and have one pair of input terminals and one pair of output terminals is externally equivalent to a  $T$  or  $\Pi$  network. From this modest beginning the field of applications of the equivalent circuit concept has steadily expanded so that by now the whole field of linear passive circuit theory has been subjected to equivalent circuit interpretation.

With the advent of the thermionic vacuum tube amplifier, linear active network theory had to be considered and almost immediately the attempt was made to obtain an equivalent circuit whose performance would depict the linear characteristic of the tube.

Equivalent circuit concepts have played an important part in electrical engineering, particularly in communication engineering. In this paper we shall be concerned only with linear a.c. amplifier operation, where the term linear indicates that the analytical expressions connecting currents and voltages are linear and involve only the first power of any instantaneous current or its derivative.

Our first step will be to prove the general equivalent circuit theory concerning vacuum tubes. As an example we will consider a general triode with its grid positively biased. 2,3

The instantaneous plate current  $i_b$  and the instantaneous grid current  $i_c$  through a triode are functions of both instantaneous plate voltage  $e_b$  and grid voltage  $e_c$  as shown below.

$$i_b = \psi(e_b, e_c) \quad 1$$

$$i_c = \varphi(e_b, e_c) \quad 2$$

The total differential of  $i_b$  and  $i_c$  are

$$di_b = \frac{\partial i_b}{\partial e_b} de_b + \frac{\partial i_b}{\partial e_c} de_c \quad 3$$

$$di_c = \frac{\partial i_c}{\partial e_b} de_b + \frac{\partial i_c}{\partial e_c} de_c \quad 4$$

The first partial coefficient in equation 3 is called the incremental or variational plate conductance and is denoted by the letter  $k_p$ .

$$k_p = \left( \frac{\partial i_b}{\partial e_b} \right)_{e_c = \text{constant}} = \frac{1}{r_p} \text{ mhos} \quad 5$$

where  $r_p$  is the variational or incremental plate resistance.

(2) Chaffee, E. L., Equivalent Circuits for an Electron Triode and the Equivalent Input and Output Admittances, Proc. IRE, Vol. 12, p. 1633, Sept. 1929.

(3) Glasgow, Principal of Radio Engineering, P. 137

The second term is known as the incremental or variational mutual conductance and is denoted by  $g_p$ .

$$g_p = \left( \frac{\partial i_b}{\partial e_g} \right)_{e_b = \text{constant}} \text{ mhos} \quad 6$$

The first partial coefficient of equation 4 is intrinsically a negative quantity under actual conditions and hence the coefficient will be negative and it is defined as the incremental or variational inverse mutual conductance and is denoted by  $g_g$ .

$$-g_g = \left( \frac{\partial i_c}{\partial e_b} \right)_{e_c = \text{constant}} \text{ mhos} \quad 7$$

Finally the second partial coefficient is defined the incremental grid conductance and is denoted by the letter  $k_g$ .

$$k_g = \left( \frac{\partial i_c}{\partial e_c} \right)_{e_b = \text{constant}} \text{ mhos} \quad 8$$

Equations 3 and 4 can now be written

$$di_b = k_p de_b + g_p de_c \quad 9$$

$$di_c = -g_g de_b + k_g de_c \quad 10$$

Suppose  $e_b$  and  $e_c$  vary in such a way  $i_b$  remains constant. Then equation 9 becomes

$$0 = k_p de_b + g_p de_c \quad 11$$

The ratio

$$\frac{de_b}{de_c} = - \frac{g_p}{k_p} \quad 12$$

or

$$\frac{g_p}{k_p} = - \left( \frac{\partial e_b}{\partial e_c} \right)_{i_b = \text{constant}} \quad 13$$

This last ratio  $k_p$  is denoted by the letter  $\mu_p$  which is called the incremental amplification factor.

Then

$$g_p = k_p \mu_p \quad 14$$

Similarly we may assume that  $e_b$  and  $e_c$  vary in such a way that  $i_c$  remains constant. Then by equation 10 we obtain

$$\frac{g_g}{k_g} = \left( \frac{\partial i_c}{\partial e_b} \right)_{i_c = \text{constant}} \quad 15$$

and

$$\mu_g = \left( \frac{\partial i_c}{\partial e_b} \right)_{i_g = \text{constant}} \quad 16$$

also

$$g_g = \mu_g k_g \quad 17$$

The total space current is given by

$$i_s = i_c + i_b \quad 18$$

Since  $i_s$  is a function of  $e_b$  and  $e_c$  we may write

$$i_s = \gamma(e_b, e_c) \quad 19$$

The total differential of  $i_s$  is obtained by adding 9 and 10.

$$di_s = (k_p - g_p) de_b + (g_p + k_g) de_c \quad 20$$

Now if we define  $\mu_s$  as the negative of the ratio of the incremental in plate voltage to be incremental in grid voltage to maintain  $i_s$  constant, i.e.,

$$\mu_s = - \left( \frac{\partial e_b}{\partial e_c} \right)_{i_s = \text{constant}}. \quad 21$$



We have from equation 20,  $di_s = 0$ ,

$$\mu_s = \left( \frac{g_p + k_g}{k_p - g_g} \right) \quad 22$$

So long as there is no space charge effect  $\mu_s$  depends mostly upon the geometry of the tube and only slightly upon the space charge.

### (B) Equivalent Plate Circuit Theorem

The equivalent plate circuit theorem has been known since the first application of electron tubes but there was not a rigorous derivation for it. The first reference to this theorem was made by J. M. Miller in his article published in the Proc. of IRE, Vol. 6, p. 143, June 1918.

Figure No. 1 shows a triode with impedances  $Z_c$  and  $Z_b$  in the grid and plate circuit respectively. The values of the currents and electromotive forces are defined by the figure.

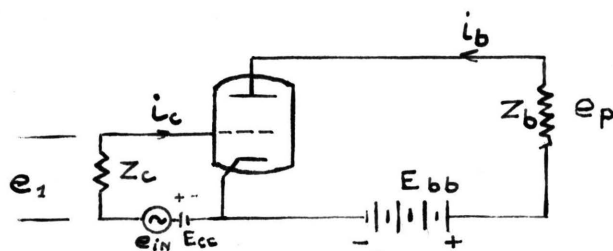


Figure No. 1  
A Triode Tube

In the Figure No. 2 if there is no varying potential impressed in the grid circuit the operating point Q is determined by the steady components of the grid and plate potential. If the grid voltage changes by a small amount  $de_c$

the operating point will move to some new position A and equation 3 gives the relation between change of plate current and the changes of grid and plate potentials.

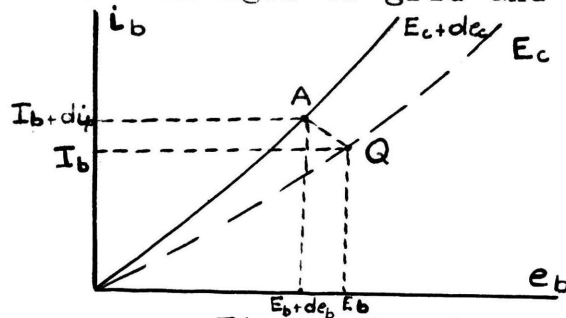


Figure No. 2

Plot of the Plate Current Versus Plate Voltage of a Triode Tube

Since  $E_b$  is constant  $dE_b = -dE_b$  and equation 9 becomes

$$dI_b = k_p(\mu_p dE_c - dE_b) \quad 23$$

letting  $k_p = \frac{1}{r_p}$

$$r_p dI_b + dE_b = \mu_p dE_c \quad 24$$

Usually  $e_g$  varies with time so the following differential equation can be written

$$r_p \frac{dI_b}{dt} + \frac{dE_b}{dt} = \mu_p \frac{dE_c}{dt} \quad 25$$

In deriving the above equation the origin coordinate was at zero. Since we are interested only in changes of current and potentials we may transfer the origin of coordinates to Q and consider but finite changes from the point of Q, the changes being always so small that  $r_p$  and  $\mu_p$  are essentially constant over the path travelled. Thus we may write equation 24 in the form

$$r_p \Delta I_b + \Delta E_b = \mu_p \Delta E_c \quad 26$$

since  $\Delta e_b = i_b Z_b$

$$r_p \Delta i_b + Z_b \Delta i_b = \mu_g \Delta e_c \quad 27$$

$$\Delta i_b = \frac{\mu_p \Delta e_c}{r_p + Z_b} \quad 28$$

which is the well known classical representation of plate circuit.

(C) Equivalent Grid Circuit Theorem

From equation 10 and 17 it can be seen that

$$di_c = k_g (de_c - \mu_g de_b) \quad 29$$

Now adding emf's in the grid circuit of Figure No. 1 we have

$$E_{cc} - e_1 - e_g + e_c = 0 \quad 30$$

$$de_c = de_{in} + de_1 \quad 31$$

where  $e_{in}$  is an impressed emf from an outside source.

Combining equation 31 and 29 and using  $r_g$  as the reciprocal of  $k_g$  we have

$$r_g di_c = de_{in} + de_1 - \mu_g de_b \quad 32$$

as before

$$r_g \Delta i_c = \Delta e_{in} + \Delta e_1 - \mu_g \Delta e_b \quad 33$$

$$\Delta i_c = \frac{\Delta e_{in} - \mu_g \Delta e_b}{r_g + Z_c} \quad 34$$

The grid circuit of a triode can be represented by a resistance  $r_g$ , an impedance or combination of circuit elements  $Z_c$  and an impressed emf of  $e_g$  minus a fictitious voltage of  $\mu_g \Delta e_b$ .

The equivalent plate and grid circuit can be drawn with the aid of equations 28 and 34.

Assuming there exists linear relationship between currents and voltages, we can write equations 28 and 34 as

$$i_p = \frac{\mu_p e_g}{r_p + Z_b} \quad 35$$

$$i_g = \frac{e_{in} - \mu_g e_p}{r_g + Z_c} \quad 36$$

and the equivalent circuit is given by Figure No. 3 below.

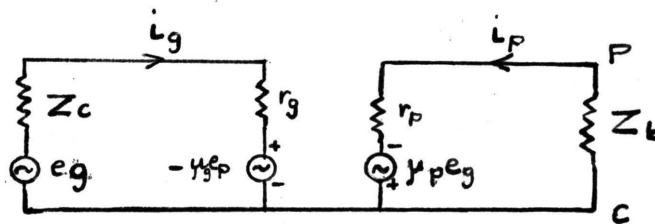


Figure No. 3

#### Equivalent Grid and Plate Circuit of a Triode Tube

#### (D) Application of Equivalent Circuit to Triode at Low Frequencies

Before starting with the representation of the equivalent circuits we have to point out that from now on we are

---

(4) Peterson, L. C., Equivalent Circuits of Linear Active Four Pole Terminal Networks, B.S.T.J., Vol. 23, p.593, Oct. 1948.

going to use different notations for voltages and currents than those used in the derivation of the equivalent plate and equivalent grid theorems. The input grid to cathode voltage will be denoted by  $V_1$  and the output plate to cathode voltage by  $V_2$ . We find it necessary to do this in order to have our notations the same as the standard ones used in the representation of four pole terminal networks. In studying the applications of the equivalent circuit, a grounded triode, operated at such a low frequency that all displacement currents can be disregarded, will be considered. Let us also assume that the grid is negatively biased with respect to cathode so that the grid current is absent. Applying equation 35 to the circuit in Figure No.1, we get the figure below.

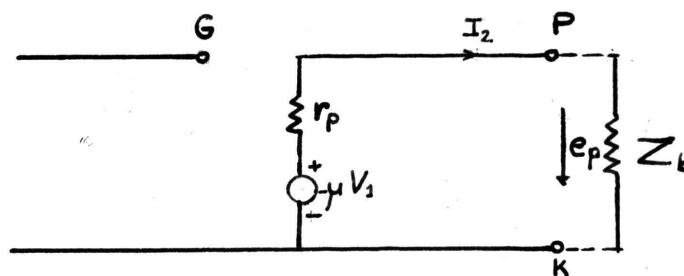


Figure No. 4

Equivalent Circuit of a Negative Grid Triode at Low Frequencies

In terms of mathematical analysis the circuit<sup>is</sup> described by the two equations

$$I_1 = 0$$

$$-\mu V_1 = I_2 r_p + V_2$$

37

By slight rearrangement of equation 37 a network representation based on current equilibrium may be obtained. For this

purpose equation 37 is written

$$I_1 = 0$$

$$I_2 = -\frac{\mu}{r_p} V_1 - \frac{1}{r_p} V_2 \tag{38}$$

The corresponding network representation is as shown in Figure No. 5, where the energizing source in the plate circuit consists of a constant current generator of magnitude  $\frac{\mu V_1}{r_p}$  impressed across the output terminals.

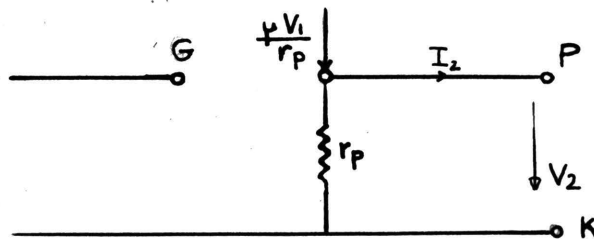


Figure No. 5  
Equivalent Circuit of a Negative Grid Triode at Low Frequencies with a Current Source

Let us now consider that the grid is positive so that grid current flows. Applying the "Equivalent-grid circuit theorem" to Figure No. 1, we get Figure No. 6 as shown below.

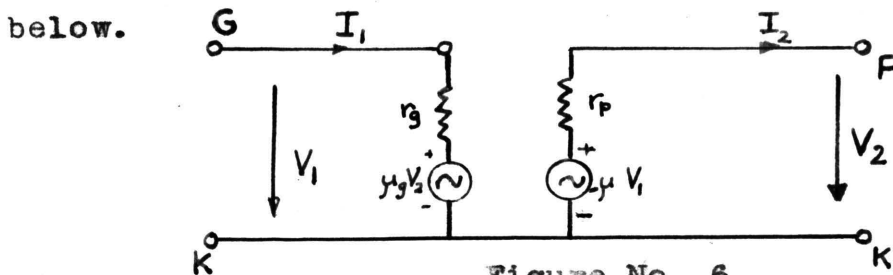


Figure No. 6  
Equivalent Circuit of a Positive Grid Triode at Low Frequencies.

Analytically, the circuit can be expressed by

$$V_1 = \mu_g V_2 + I_1 r_g$$

$$-\mu V_1 = I_2 r_p + V_2 \tag{39}$$

or

$$I_1 = \frac{1}{r_g} V_1 - \frac{\mu_g}{r_g} V_2$$

$$I_2 = -\frac{\mu}{r_p} V_1 - \frac{1}{r_p} V_2 \tag{40}$$

This equation will be very useful in applying the idea of equivalent networks to four pole network representation of a vacuum tube. Two observations can be made on the above representation of vacuum tubes.

1. These networks are not based on any study of the internal action of the tube, but rather on the purely formal mathematical process of differentiating the two functional relations which impress the broad fact that plate and grid currents are some unspecified linear continuous functions of the grid and plate potentials in the neighborhood of the operating point.
2. The last figure (Figure No. 6) represents in a sense two separate networks intersecting with each other by means of voltage or current generators.

#### (E) UHF Effects in Conventional Vacuum Tubes<sup>5</sup>

Before extending our ideas of vacuum tube equivalent circuits we shall first study the behavior of vacuum tubes at UHF. As the frequency is raised vacuum tubes get progressively less effective as amplifier and oscillators. Amplifiers at UHF require greater driving power, and the power output drops off considerable. If the frequency is raised high enough, the gain of the amplifier will drop to unity or less. At the same time the limitations on the output change. At low frequency the output for continuous operation is generally

---

(5) Spengenberg, Vacuum Tubes.

limited by plate dissipation. As the high frequency limit of oscillation is reached, the grid dissipation commonly becomes the limiting factor while the plate dissipation is far from its limiting value. All the above effects come about because of a combination of electronic and circuital phenomena associated with the vacuum tube.

(F) The Decrease of Output at UHF

In general there are three main factors effecting the output at UHF.

1. External and internal reactance effects
2. Circuit and tube loss limitations
3. Electron-transit time limitations

At low frequencies the external electrical circuit and vacuum tube is quite distinct. As the frequency increases, this is no longer true and it is found that part of the resonant circuit exist inside the tube. This is due to the electrode leads having a small but finite inductance. As frequency rises into the UHF ranges the reactance of this inductance becomes appreciable. This means that the same voltage doesn't appear across the external terminals and electrodes. Moreover there is a decrease inter-electrode capacitance at high frequencies<sup>6</sup> and these values calculated for low frequencies do not hold. The combination of the electrode-lead inductance and

---

(6) Strutt, M.J.O., Von der Ziel, A., The Causes for the Increase of the Admittances of Modern High Frequency Amplifier Tubes on Short Waves, Proc.IRE, Vol. 28, No. 8, p. 1011, 1938.



the interelectrode capacity may give rise to resonance in the UHF region. Even if resonances do not occur, the combination of the reactances within the tube may constitute a network that mismatches the equivalent tube generator and the load.

The power losses associated with a tube all tend to increase with frequency. Glass and other insulating supports have losses associated with the molecular movements produced by the electric fields. These losses are characterized as dielectric hysteresis losses and will vary as the first power of frequency. In addition there will be appreciable radiation from the leads and electrodes. The power radiated from a short length of wire carrying current increases with the frequency. All the above factors contribute to a general reduction in tube efficiency as frequency is increased.

In addition to all above effects, electron-transit-time effects can contribute to reduced tube output in many ways. If the transit time of the electrons are appreciable fractions of the UHF cycle, then <sup>the</sup> plate current will lag the negative grid voltage and there will be a reduced power output because <sup>the</sup> plate current and voltage are out of phase. Associated with increased transit time there is a debunching of electrons, which has the result that the plate current pulses are not as sharp as the pulses liberated from the cathode. In addition there will be an energy,

interchange between the electric fields and the electron in flight so that as frequency increases the grid input impedance will have a resistance component which decreases with frequency even though no electrons strike the grid. Furthermore, all the tube constants such as the amplification factor will become complex<sup>7</sup> instead of real numbers as a result of a shift in phase and what is generally a reduction in magnitude. There is not much that can be done about electron-transit-time effects except to raise the voltages and reduce the dimensions of the tube.

#### (G) Consideration of Displacement Current

The equivalent vacuum tube circuits discussed previously were satisfactory as long as the frequency was low enough for all displacement current to be disregarded. With the operation of circuits at higher frequencies, in the order of  $10^6$  cps and higher, it becomes necessary to take the internal tube capacitances into account. This was done by the superposition of a capacity network on Figure 6 as shown in Figure 7. It is interesting as well as instructive to formulate this network transition in analytical terms as will be seen later. The transition rests upon the physical fact that the total current entering or leaving the electrode is the sum of convection and displacement currents.

---

(7) Llewellyn, F. B., Operation of UHF Vacuum Tubes, B.S.T.J., Vol. 14, p.632, Oct. 1935.

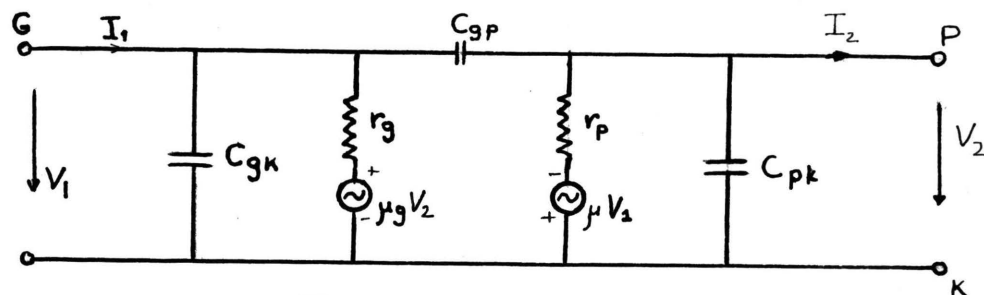


Figure No. 7  
Equivalent Circuit of a Triode With Consideration of Displacement Currents

Therefore Figure No. 7 is the superposition of Figures 6 and 8. As seen in Figure 7 the network for the displacement currents is passive.

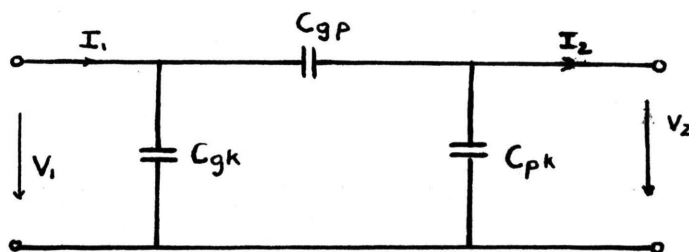


Figure No. 8  
Equivalent Circuit of Displacement Currents

#### (H) Consideration of Lead Effects<sup>5, 8</sup>

At frequencies about  $10^8$  cycles/sec it become necessary to take into account lead effects usually in the form of self and mutual inductances. At these high frequencies marked increases in the input, output, forward and feedback admittances\* occurs in excess of that caused by the inter-electrode capacitance. This means that we have to

(5) Spangenberg, op.cit

(8) Thompson, B. J., Review of UHF Vacuum Tube Problems, RCA Review, p. 146, Oct. 1938.

\*See Section on Four Terminal Networks of this Paper

modify Figure 7 to take this into account. Let us investigate how the lead effects are to be considered and their modification on the equivalent circuit. To start with, it has to be pointed out that there are two kinds of lead effects. First **effect** is due to the interaction of electron stream on the electrodes inside the tube, and second, the usual mutual and self inductances of the lead pins of the tube. Both of these effects will be investigated in this paper.

### 1. Internal Tube Lead Effects

The inductance of a wire increases as the wire diameter is made smaller or as the wire length is increased. As an example of how large lead reactances can be, consider the case of 100 mils in diameter and 1 inch in length, as found in most high frequency transmitting tubes. This lead is found to have an inductance of approximately 0.015 microhenry. As 500 mc this represents a reactance of 47 ohms, which is fairly high.

Since part of the lead reactances are internal to the tube, there will be coupling between the input and output circuits due to grid and plate currents flowing through the common cathode lead inductance. This will have the effect of introducing feedback into the stage involving the tube and will cause the grid input impedance to be effected. In general the effect of the internal tube reactance is to decrease the impedance presented at the tube input terminals.

Consider a triode as <sup>shown in</sup> Figure No. 9.

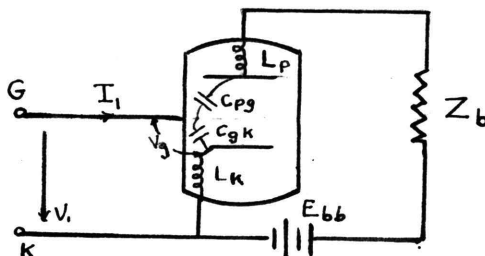


Figure No. 9  
Triode Showing the Interelectrode Capacitances and Lead Inductances

$L_k$  and  $L_p$  are the inductances of the internal tube cathode and plate leads respectively.

$C_{gk}$  and  $C_{gp}$  are the grid to cathode and grid to plate interelectrode capacitances respectively.

For simplicity let us take into account only the effect of the cathode lead inductances and the cathode grid capacity, and neglect any outside effect. The the voltage  $V_1$  differs from the voltage that appears between the grid and the cathode by the voltage drop in the cathode lead inductance.

Thus:

$$V_1 = V_g + j\omega L_k I_p \quad 41$$

But the plate current will be approximately proportional to the negative of the product of the grid voltage and the mutual conductance of the tube, since at UHF the plate load impedance will be very small.

$$I_p = -g_m V_g \quad 42$$

The voltage drop across the grid cathode capacity is:

$$V_g = \frac{I_i}{j\omega C_{gk}} \quad 43$$

Making the substitution into equations 41 and 42 we get

$$V_i = I_i \left( \frac{1 + j\omega L_k g_m}{j\omega C_{kg}} \right) \quad 44$$

Since the second term is very small we may write the input admittance as:

$$Y_{g_i} = \frac{I_i}{V_i} = j\omega C_{kg} (1 - j\omega L_k g_m) \quad 45$$

The first term of the input admittance will be recognized as the normal capacitive susceptance of the tube. The second term is a real positive term representing a conductive component of input admittance and having the value:

$$G_{iN} = \omega^2 L_k C_{kg} g_m \quad 46$$

The input conductance corresponds to a resistance whose value decreases as the square of the frequency in parallel with the input capacitance  $C_{kg}$  for a given driving voltage. This resistance consumes no power. There is no real power involved. The driving power consumed in this fashion is simply transmitted to the plate circuit. The equivalent input resistance encountered here can become very low due to this shunting conductance in the grid circuit. A similar admittance will be across the grid and plate. So the equivalent circuit including also the cathode to plate

capacitance would be as shown in Figure No. 10. Note that in Figure No. 10 we have the capacitance in series with the resistance; so it means that we have to convert the parallel parameters into their series equivalent.

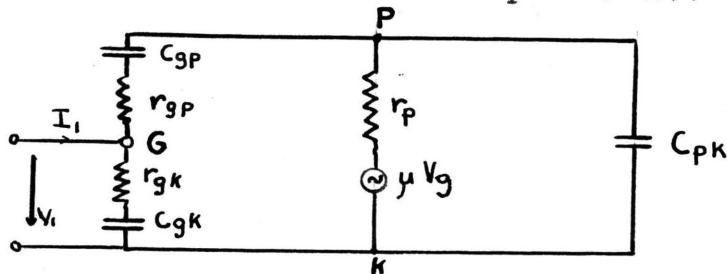


Figure No. 10

Equivalent Circuit of a Triode Including the Internal Lead Effects and the Interelectrode Capacitances

As it may be realized the lead inductances which are considered to be inside of the tube can be added to the electron transit time effect.<sup>9</sup>

In this case we have a similar component of conductance due to electron transit time effect as will be seen later. The transit time effect varies as the square of the frequency. The equivalent resistances that are due to cathode inductance feedback and electron transit time, are in parallel and any measurement will involve the effect of both. A brief outline of the W. R. Ferris<sup>10</sup> point of view on this matter will be given later.

## 2. Consideration of the Pin and Internal Circuit Effects of the Tube<sup>(6)</sup>

With the development of equivalent circuits at higher

- (9) Llewelyn, F.B., Equivalent Networks of Negative Grid Vacuum Tubes at UHF, B.S.T.J., Vol.15, p.575, 1936.  
 (10) Ferris, W. R., Input Resistance of Vacuum Tubes at UHF Amplifiers, Proc.IRE, Vol.24, p. 82, Jan. 1936.  
 (6) Strutt, Vonder Ziel, op. cit.

frequencies the outside lead effect had to be included in equivalent circuit. As it is obvious these effects are entirely outside effects and have to be considered separately from the internal tube lead effects. A schematic diagram of a triode including outside pin and lead effects as well as stray capacitances is given below in Figure No. 11.

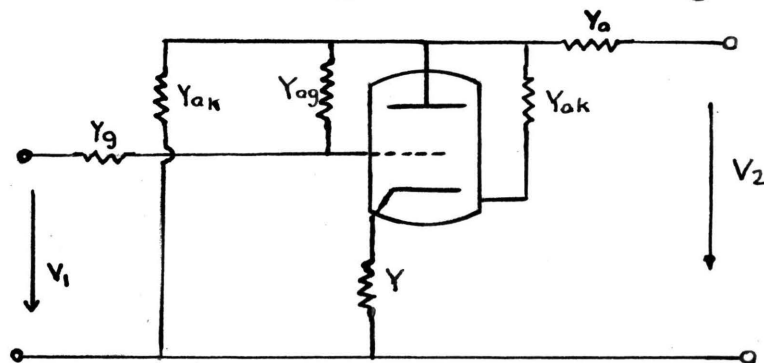


Figure No. 11  
Schematic Diagram of Triode Including Outside Pin and Lead Effects as Well as Stray Capacitances

The symbol  $Y$  is the admittance between cathode and ground,  $Y_{ak}$  the admittance between anode and cathode,  $Y_a$  the anode lead inductance,  $Y_{ag}$  the admittance between anode and grid and  $Y_g$  the grid lead inductance.

The various inductive parameter can be calculated by the well known self inductances and mutual inductances formulas respectively.

$$L = 2l \left( \ln \frac{4l}{d} - 1 \right) \times 10^{-9} \text{ henries} \quad 47$$

$$M = 2l \left( \ln \frac{2l}{a} - 1 \right) \times 10^{-9} \text{ henries} \quad 48$$

Where:  $l$  is the lead in centimeters

$d$  is the diameter of the lead in centimeters

$a$  is the distance between the corresponding leads



After the evaluation of lead effects we can include also the interelectrode capacitances in Figure No. 11. There arises another important point, what are the values of the interelectrode capacitances?<sup>11</sup> As Benham points out the grid to cathode as well as grid to anode capacitances differ considerable from those at cold stage.

They are given as follows:

$$C_{gk} = \frac{4\mu C_1}{3\mu - \gamma} \quad 49$$

$$C_{pk} = \frac{4C_1}{3\mu - \gamma} \quad 50$$

where:  $C_1$  is the cathode grid capacitance in the cold stage

$$\gamma \text{ is } 1 + \frac{C_1}{C_2}$$

$C_2$  is the grid anode capacitance in the cold stage

After the external lead effect and the stray capacitances between leads are included in Figure No. 11, an equivalent circuit for a positive grid for a positive grid triode is as shown in Figure No. 12.

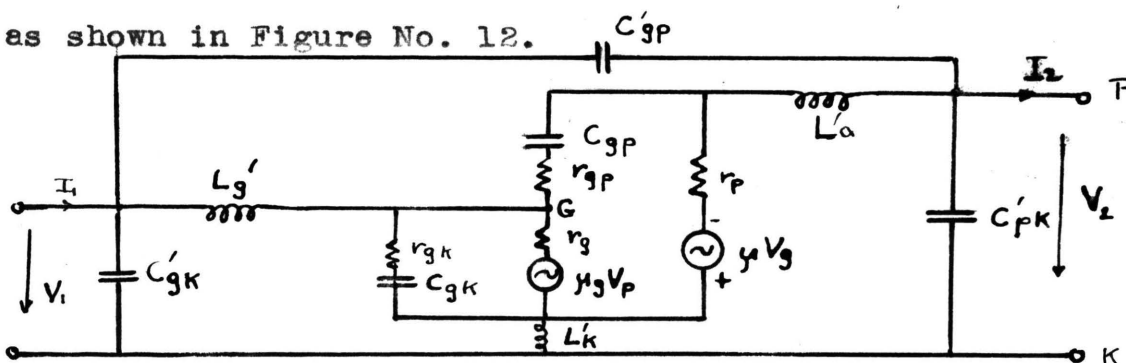


Figure No. 12  
Equivalent Circuit of a Triode With Internal and External Tube Effects Taken into Account

(11) Benham, Tubes and Amplifier Theory, Proc. IRE, Vol. 26, p. 1105, 1938.

The symbols with primes indicate external effects.

(I) Modification of the Above Circuit<sup>10</sup>

Modification of the above circuit can be made by including the transit time in the internal lead and interelectrode capacity effects. Such a derivation would be analytically analogous to the internal tube effects and could be included in the above circuit. Such a derivation has been carried out by W. R. Ferris. His point of view depends upon mathematical manipulations and assumptions and it doesn't consider any internal electron effects. This method will now be analyzed. Llewellyn's point of view and derivations on transit time effects in vacuum tubes is found to be more reliable and will be discussed later. The most pronounced effect at high frequencies is the transit time effect. This is evident with the appearance of a conductive component in the grid input admittance. That is, a definite amount of power is required to drive the grid even though it does not intercept any electrons. In addition the mutual conductance and amplification factor becomes complex and smaller in magnitude, having a negative phase angle that increases in magnitude with frequency. The grid current in this case will be proportional to the product of the mutual conductance, the frequency, the electron transit time and the grid voltage. Mathematically expressed:

$$I_{g_1} = K_{g_m} f T V_g$$

51

---

(10) Ferris, op.cit.

Where:  $K$  is a proportionality constant  
 $g_m$  is the grid mutual conductances  
 $T$  is <sup>the</sup> transit time  
 $V_g$  is grid input voltage

The grid input admittance will be defined by:

$$Y_g = \frac{I_{g1}}{V_g} = k_1 g_m f T \quad 52$$

This admittance will have a conductance component and a susceptance component. If the grid current leads the grid voltage by  $90^\circ$  the input admittance would be purely imaginary, corresponding to the susceptance of the cathode grid capacitance. Actually this will be the larger component of the input admittance. However, the admittance will have a conductance component of the form:

$$G_g = Y_g \sin \theta \quad 53$$

Where  $\theta$  is the angle by which the fundamental component of the induced grid current fails to lead the grid voltage by  $90^\circ$ . The angle  $\theta$  itself depends on the product of the frequency and transit time of the electron.

$$\sin \theta = \theta = k_2 f T \quad 54$$

Where:  $K_2$  is a constant  
 $T$  is the transit time

From equations 52, 53, and 54 the input conductance is given by:

$$G_g = k_3 g_m f^2 T^2 \quad 55$$

to a high degree of approximation.

Equation 55 shows that the grid input conductance increases as the square of the frequency for a given set of operating conditions. The input resistance encountered here is such that the driving power required for a given excitation increases as the square of the frequency.

The constant of equation 55 can be evaluated to include the effect of space charge.<sup>12</sup> The specific form of the grid <sup>conductance</sup>  $G_g$  is given by

$$G_g \approx \frac{4\pi^2}{180} g_m f^2 T_{gk}^2 \left[ 9 + 44 \frac{T_{gp}}{T_{gk}} + 45 \left( \frac{T_{gp}}{T_{gk}} \right)^2 - 2 \frac{T_{gp}}{T_{gk}} \right. \\ \left. \left( \frac{17 + 35 \frac{T_{gp}}{T_{gk}}}{1 + \frac{v_p}{v_g}} + 20 \left( \frac{T_{gp}}{T_{gk}} \right)^2 \right) \right] \quad 56$$

Where:  $T_{kg}$  is the cathode-grid transit time  
 $T_{gp}$  is the grid-plate transit time  
 $v_p$  is the electron velocity at the plate  
 $v_g$  is the mean electron velocity in the grid plane  
 $g_m$  is the grid mutual conductance

The actual equation of <sup>the</sup> input conductance is extremely complicated therefore we will confine ourselves to the derivations already mentioned. A more complete analysis can be found in reference 13.<sup>13</sup>

Now we may combine the effect of transit time and internal lead effects by using equations 56 and 45. The equivalent resistances that are due to cathode inductance feedback and electron transit time will be in parallel. The above equations for input admittances indicate only first order effects.

(12) North, D. O., Analysis of the Effect of Space Charge on Grid Impedance, Proc. IRE, Vol. 24, p. 108, Jan. 1936.

(13) Tube Admittances of Receiving Tubes, Tube Dept., Radio Corp. of America, New Jersey, November 1946,

Departures from simple theory indicated above are due to the following:

(1) The input capacity of a tube is nonlinear with transconductance. This is a low frequency effect due to space charge. *This* contributes to a nonlinearity between input conductance and tube trans-conductance.

(2) Partial resonance between lead inductance and inter-electrode capacity may change <sup>the</sup> apparent input capacitance.

(3) There may be a negative input conductance component due to screen lead inductance in pentodes and tetrodes.

(4) There are cold tube input conductance components due to lead resistance and dielectric losses that obscure lead inductance and electron transit time effects. The lead resistance yields an input conductance component that increases as the five-halves power of frequency as a result of skin effect. Dielectric losses yield a component of conductance that increases linearly with frequency.

Disregarding the departure from the simple theory we can include in the above derivations the external as well as the internal effects of the tube and the circuit of Figure No. 12 has to be modified slightly. The only difference between this <sup>modified</sup> equivalent circuit and that of Figure No. 12 will be an additional admittance component in parallel with the internal lead effects due to transit time phenomena. One will readily admit that the equivalent circuit becomes very complicated as the frequency goes up. Moreover as was pointed out above, many

assumptions have been made which will be no longer accurate at still higher frequencies.

As we shall see in the experimental determination of four pole admittances for the equivalent circuit of the vacuum tube all these methods for evaluation each effect separately and then recombining all the effects will be obsolete for the four pole admittances include all those effects.

SECTION II  
Electron Theories<sup>14</sup>

(A) Transit Time

Before starting the derivations of equivalent circuits based completely on electron stream theory, it is desirable to review some electron stream effects in vacuum tubes. The grid in a Class A triode is usually maintained negative. Theoretically then no grid current would flow. But experimental results by Irving Langmuir<sup>15</sup> shows that in many types of high vacuum tubes some electrons possess the ability to pass to an electrode having more negative potential than the cathode from which they originate. For example, an experiment on a cylindrical grid was made where the grid was biased 30 volts negative with respect to cathode and the electron current was observed to flow to this cylinder in spite of its negative potential. Experiment carried out shows that the current flow was very pronounced in cylindrical grid tubes. As we are concerned with parallel plane grid structures, we will neglect the above phenomena in our discussion which follows:

Let us now investigate the transit time phenomena on grid electron flow. As was mentioned above in Class A triode we may say that no grid current has to flow as long as the grid is maintained negative. With a little thought however,

- 
- (14) Linder, Ernest G., Excess Electron Motion in High Vacuum Tubes, Proc.IRE, Vol.26, p.346, 1938.  
(15) Langmuir, Irving, Scattering of Electrons in Ionized Mediums, Phys.Rev., Vol.26, p.585, Nov. 1925.

it can be seen that an electron approaching a negative grid will induce a current flowing from the negative grid to the positive cathode through the external grid circuit. The electron under this condition will supply energy to the grid circuit as it is decelerated. Likewise an electron moving away from the negative grid will induce a current in the reverse direction, or the electron will take energy from the grid as it is repelled by the negative grid charge. However, if a number of electrons are approaching a grid from one side and simultaneously an equal number of electrons are going away from the grid on the other side, the induced current effects cancel and the net energy interchange is zero. At ordinary audio frequencies and the lower radio frequencies the time of transit of a single electron between cathode and anode is usually very short with respect to time of a cycle of grid voltage. Thus for each incremental change in grid voltage during a cycle there is practically instantaneous readjustment of space charge and electron flow. At all times equal number of electrons are approaching and leaving the grid and no alternating current is induced in the grid circuit.

As operation enters the higher frequency regions, the time of transit of the electron is no longer short with respect to a cycle of grid voltage and the grid voltage may make a change of appreciable magnitude while some electrons are in flight from cathode to anode. As a result electrons may be leaving the cathode at an increased rate owing to a positive charge of grid voltage, whereon in the grid-anode space, the



electron density is lower owing to the preceding more negative value of the grid voltage. A net induced current then flows in the grid circuit and it can be seen that this current may have <sup>an</sup> arbitrary phase relation with respect to the a.c. grid voltage since its angle of lag depends on the relation of time of electron transit to time of <sup>the</sup> grid voltage cycle. However, in general the induced current may have a component in phase with the a.c. grid voltage. If a component of current is in phase with the grid voltage energy is supplied by the grid current to the electron stream. Flow of an in-phase component of alternating current in the grid circuit implies a conduction component in the grid admittance. Such a conductance is independent of, and in addition to, the normal grid conductance of this grid.

Since grid voltage sources are usually of high impedance the shunting of this high impedance by the transit time conduction results in lowering of the voltage applied to the grid and decreased amplification of the higher frequencies. Also since many grid sources are parallel resonant circuits, shunting them with a high conductance reduces the resonant impedance and broadens the resonant response curve thereby giving reduced selectivity.

Example of transit time effect phenomena:<sup>8</sup>

For a better understanding of transit time effect at higher frequencies it will be helpful to give an example of

---

(8) Thompson, op.cit.

this effect. A useful and satisfactory viewpoint is to consider the current flow <sup>lines</sup> between two parallel plate electrodes as shown in Figure No. 13.

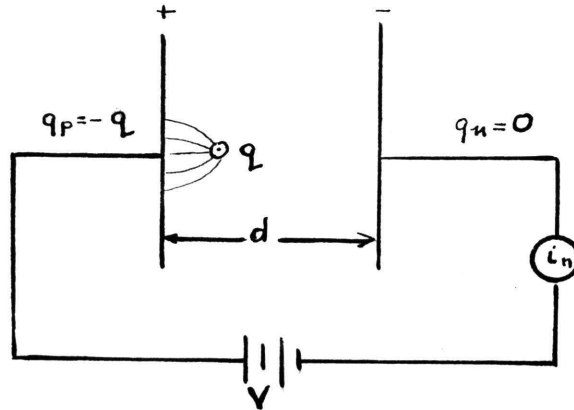


Figure No. 13  
A Charge Between Two Parallel Plates

The electric field between the electrodes is simply  $\frac{V}{d} = E$  where  $d$  is the distance between <sup>the</sup> electrodes. If a small positive electric charge  $q$  is placed between the plates very close to the positive plate, there will be an increase in the charge of the positive plate of amount  $q$  and no increase in the charge of the negative plate. There will be a force acting on the charge of magnitude  $F_q$  tending to move it toward the negative plate. If the charge is allowed to move, the work done on it by the field is equal to  $F_q x$  where  $x$  is the distance the charge has moved. The work done on the charge is supplied from the battery and is equal to the product of its voltage  $V$  and the change in charge induced on one of the plates. If  $q_n$  represents the charge induced on the negative plate we may write:

$$-Vq_n = Eqx$$

$$-Vq_n = \frac{Vqx}{d} \quad 58$$

$$q_n = -q \frac{x}{d} \quad 59$$

In other words, the charge induced on the negative plate is proportional to the charge in space and to the fraction of the total distance between plates which the charge has covered. Of course, the charge  $q_p$  induced on the positive plate is equal to the difference between the space charge and the charge induced on the negative plate, since the total charge induced on the two plates is always equal in magnitude and opposite in sign to the space charge. The current flowing to the negative plate as a result of the motion of the charge  $q$  is equal to the rate of change of the charge  $q_n$ . This is simply:

$$i_n = \frac{dq_n}{dt} = \frac{q}{d} \frac{dx}{dt} = -q \frac{v}{d} \quad 60$$

The important conclusion which we may draw from this simple analysis is that in a vacuum tube the current produced by the passage of an electron does not flow simply at the instant the electron reaches the electrode, but flows continuously in all adjacent electrodes while the electron is in motion. If the electron moves between parallel plates, the current flow does not depend on the position of the electron but only on its velocity. The total current flowing to an

electrode may be determined by adding up all the minute currents produced by the individual electrons, or more analytically by integrating the currents produced by infinitesimal strips of space current.

In a steady state condition, the current flow determined by such integration is exactly equal to the rate of arrival of electron at the electrodes. When the current is varying with time, as in the case of an amplifier tube with an alternating voltage applied to the grid, the rate of arrival of electrons at the electrode may be greater or less than the actual current flowing because of the finite transit time of the electrons. If the current is momentarily increasing, the rate of arrival of electrons may be less at any instant than the flow of electrons in the space between the parallel plates. These considerations show that the current flowing to an electrode may be different from the rate of arrival of electrons at the electrode. It is also possible to have a current flowing to an electrode at which no electrons arrive if the number or velocity of the electrons approaching the electrode is instantaneously different from the number or velocity of those receding from it.

(B) Space Charge<sup>16</sup>

---

(16) Fay, C.E., Samuel, A.L., Shockley, W., On the Theory of Space Charge Between Parallel Plane Electrodes, B.S.T.J., Vol. 17, p. 49, 1938

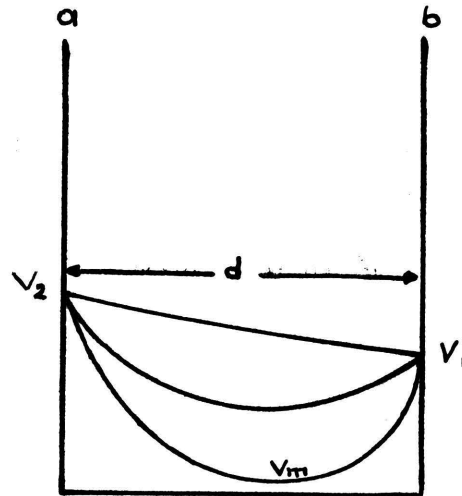


Figure No. 14

### Potential Distribution Between Two Planes of Positive Potentials

For a better understanding of the subsequent articles, a brief outline of space charge effects will be given.

Consider two planes, a and b, of fixed d. c. potentials,  $V_1$  and  $V_2$  ( $V_2$  is larger than  $V_1$ ) respectively, separated by a distance  $d$ . Let a uni-directional and uniform electron stream of  $J_0$  amp/cm<sup>2</sup> be injected into the space from the right plate and at right angles to the plane. If the injected current is extremely small the potential distribution does not differ very much from the free space one, represented by curve 1 on Figure No. 14. As the injected current is increased slightly the potential curve starts to sag, as in curve 2, and a further small increase causes a potential minimum to develop at the electrode of lower potential. Still greater increase in injected current makes the potential minimum  $V_m$  sink and move towards the electrode of higher potential. This state of affairs, with a continuously

decreasing potential minimum, continues until a critical value of injected current causes the potential minimum to sink abruptly to zero and a virtual cathode is formed (curve 3). This abrupt change is referred to as a Kipp.

(C) Plane-Electrode Space Charge Flow<sup>5</sup>

The relations between potential, distance, and current in the plane electrode case can be obtained from Poisson's equation, the energy equation, and the relation between current, charge and velocity. Poisson's equation in the one-dimensional case reduces to:

$$\frac{d^2V}{dx^2} = -\frac{\rho}{\epsilon_0} \quad 61$$

Where:  $V$  is the potential

$\rho$  is volumetric space charge density

$\epsilon_0$  is the dielectric constant of free space in mks units

The energy equation has the form:

$$\frac{1}{2} m v^2 = V e \quad 62$$

Where:  $m$  is the mass of the electron

$v$  is the velocity of the electron

$e$  is the charge of an electron

This equation assumes that the electron has started from rest at a point of zero potential. Also the current density is given by:

$$J_0 = \rho v \quad 63$$

Where:  $J_0$  is the convection current density

---

(5) Spangenberg, op.cit.

The three equations above suffice for a determination of all the relations involved in a parallel electrode space charge flow. By substituting of equations 62 and 63 into equation 61, we have:

$$\frac{d^2V}{dx^2} = \frac{J_0}{\epsilon_0} \sqrt{\frac{m}{2e}} V^{-1/2} \quad 64$$

A first integration is achieved by multiplying both sides of equation 64 by  $2 \frac{dV}{dx}$  and integrating:

$$\left(\frac{dV}{dx}\right)^2 = \frac{4J_0}{\epsilon_0} \sqrt{\frac{m}{2e}} V^{1/2} + C_1 \quad 65$$

Since  $\frac{dV}{dx} = 0$  when  $V$  is equal to zero so  $C_1$  is equal to zero. A second integration gives:

$$\frac{4V^{3/4}}{3} = \sqrt{\frac{4J_0}{\epsilon_0} \sqrt{\frac{m}{2e}} x} + C_2 \quad 66$$

where  $C_2$  is again zero.

Solving for  $J$  and substituting in the values for the constants, we have:

$$J_0 = \frac{2.335 \cdot 10^{-6} V^{3/2}}{x^2} \quad \text{amp/unit area} \quad 67$$

Equation 67 constitutes the Child-Langmuir<sup>17</sup> space charge law and has been verified experimentally. Solving for the potential gives equation 68.

$$V = 5,680 J_0^{2/3} x^{4/3} \quad \text{volts} \quad 68$$

---

(17) Langmuir, J., The Effect of Space Charge on Thermionic Currents in High Vacuum Tubes, Phys.Rev., Vol. 2, p.450, Dec.1913.

(D) Current Law for Plane Triodes

It is found experimentally that in triodes the total current released from the emitter is very nearly proportional to the three-halves power of the equivalent voltages,  $V_g + \frac{V_p}{\mu}$ . We can write, therefore,

$$J = J_p + J_g = K \left( V_g + \frac{V_p}{\mu} \right)^{3/2} \quad 69$$

Where:  $J_p$  is the plate current density

$J_g$  is the grid current density

in which  $k$  is a constant to be determined from experimental data.

(E) Effect of Space Charge upon Transit Time in Diodes<sup>5</sup>

The transit time in an electric field is given by the integral of the reciprocal of velocity with respect to distance.

$$T = \int_{x_1}^{x_2} \frac{dx}{v} \quad 70$$

For the plane-electrode diode the transit time with and without space charge is easily determined. Without space charge the potential profile is a straight line so that

$$V_x = \frac{x}{d_{kp}} V_p \quad 71$$

Where:  $V_x$  is the potential at any point between electrodes

$V_p$  is the plate potential

The velocity at any point, assuming zero initial velocity, is then given by:

$$v_x = \left( \frac{x}{d_{kp}} \right)^{1/2} v_p \quad 72$$

---

(5) Spongenberg, op.cit.



Where:  $v_x$  is the velocity at any point between two electrodes  
 $v_p$  is the velocity with which the electrons strike  
the plate.

therefore the transit time is:

$$T = \left( \frac{d_{cp}}{v_p} \right)^{1/2} \int_0^{d_{cp}} \frac{dx}{x^{1/2}} \quad 73$$

with the results that

$$T = \frac{2 d_{cp}}{v_p} \quad 74$$

When the space charge is present in the plane-electrode diode,  
then the potential follows a four-thirds law, so that

$$V_x = \left( \frac{x}{d_{cp}} \right)^{4/3} V_p \quad 75$$

The velocity at any point is given by

$$v_x = \left( \frac{x}{d_{cp}} \right)^{2/3} v_p \quad 76$$

So that the transit time is

$$T = \frac{d_{cp}}{v_p} \int_0^{d_{cp}} x^{-2/3} dx \quad 77$$

with the result that

$$T = \frac{3 d_{cp}}{v_p} \quad 78$$

This is seen to be of the same form as for the space charge  
free case, the only difference being that the time is 50  
percent greater.

Behavior SECTION III  
Vacuum Tube When Transit Time is Taken Into Account

(A) Derivation of Fundamental Equations<sup>18</sup>

At UHF the inclusion of the interelectrode components, lead effects and transit time in the equivalent circuit as discussed up to this point will still not be correct. A better approach to the exact result would be to analyze more rigorously the transit time effect.<sup>19</sup> From the analysis of transit time by many author's, Llewellyn's work seems to check with the Benham's theoretical work on vacuum tubes at high frequencies. In his development, Llewellyn takes two parallel planes of infinite extent, one of which is held at a positive potential  $V$  with respect to the others, and between the two, electrons are free to move under the influence of the existing fields.

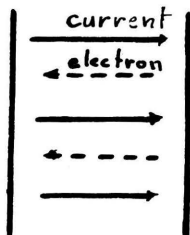


Figure No. 15  
Current Flow Between Two Parallel Planes

For the development of the fundamental relations existing between the two parallel planes,  $a$  and  $b$ , we may have the classical equation of the electromagnetic theory which may be set down as follows:

$$E = - \frac{\partial V}{\partial x}$$

79

- (18) Llewellyn, F.B., Vacuum Tube Electronics, Proc.IRE, Vol.21, p.1532, Nov. 1953.  
 (19) Bronwell, A.B., Electron Transit Time Effect in Time Varying Fields, Proc.IRE, Vol.33,p.752,Oct.1945.

$$\frac{\partial E}{\partial x} = \frac{\rho}{\epsilon} \quad 80$$

$$J = \rho v + \epsilon \frac{\partial E}{\partial t} \quad 81$$

Where: E is the electric intensity  
 V is the potential  
 ρ is the charge density  
 J is the total current density  
 v is the charge velocity

An electron located between two parallel plates will be acted upon by a force which determines its acceleration. The resulting velocity is a function of both the distance x, from the cathode and the time t. x is also a function of t in terms of partial derivatives. The equation expressing the relation between the force and acceleration can be written:

$$\frac{\partial v}{\partial t} + \frac{\partial v}{\partial x} \frac{dx}{dt} = \frac{e}{m} E \quad 82$$

or

$$\frac{\partial v}{\partial t} + \frac{\partial v}{\partial x} v = \frac{e}{m} E \quad 83$$

Substituting equation 80 into equation 81 we get:

$$J = \epsilon v \frac{\partial E}{\partial x} + \epsilon \frac{\partial E}{\partial t} \quad 84$$

$$\frac{J}{\epsilon} = v \frac{\partial E}{\partial x} + \frac{\partial E}{\partial t} \quad 85$$

Differentiating equation with respect to x and t respectively and substituting in 85 and rearranging we get:

$$\frac{e}{m} \frac{J}{\epsilon} = \left( \frac{\partial}{\partial t} + v \frac{\partial}{\partial x} \right)^2 v \quad 86$$

The advantage of this last equation as a starting point lies in the fact that the total density is not a function of  $x$ .

Now let us separate  $J$  into alternating and direct current components as

$$J = J_0 + J_1 + J_2 + \dots \quad 87$$

with corresponding

$$U = U_0 + U_1 + U_2 + \dots \quad 88$$

$$V = V_0 + V_1 + V_2 + \dots \quad 89$$

The quantities with the zero subscript are independent of time, that is, they are d.c. components; those with subscript 1 are dependent to first order upon time; those with subscript 2 are dependent to second upon time, and so forth. We will be concerned only with d.c. and fundamental components; that is we are going to neglect terms above first order

The concept of alternating current velocity component requires a few words of explanation. In the absence of any alternating current component, electrons leave a thermionic cathode with nearly zero velocity and move across the anode with continuously increasing velocity under the

well known classical laws. This velocity constitutes the direct current velocity component. When small alternating current components are introduced there will be a fluctuation of velocity superimposed on direct current value, and the alternating current component need not be zero at a virtual cathode or at the plane of a positive grid.

The first two equations of the system are as follows:

$$v_0 \frac{\partial}{\partial x} \left( v_0 \frac{\partial v_0}{\partial x} \right) = \frac{e}{m} \frac{J_0}{\epsilon} \quad 90$$

$$\left( \frac{\partial}{\partial t} + v_0 \frac{\partial}{\partial x} \right) \left( \frac{\partial v_1}{\partial t} + v_0 \frac{\partial v_1}{\partial x} + v_1 \frac{\partial v_0}{\partial x} \right) + v_1 \frac{\partial}{\partial x} \left( v_0 \frac{\partial v_0}{\partial x} \right) = \frac{e}{m} \frac{J_1}{\epsilon} \quad 91$$

In equation 90 the boundary conditions are restricted so that when  $x$  is zero, the velocity and acceleration both are zero. This restriction means that initial velocities are neglected, and that complete space charge is assumed. Thus the solution for  $v_0$  in equation 90 is as follows:

$$v_0 = \alpha x^{2/3}$$

$$\text{where } \alpha = \left( \frac{e}{m} \frac{J_0}{\epsilon} \frac{45}{10} \right)^{2/3} \quad 92$$

The solution of equation 91 is more complicated. Let us assign a particular value to  $J_1$ , namely  $J_1 = A \sin \omega t$ , and find the corresponding value of  $v_1$ . To solve for  $v_1$ , it is convenient to change the variable  $x$  to a new variable which will be called the transit angle. This new variable

is equal to the product of the angular frequency  $\omega$  and the time  $T$  which it would take an electron moving with velocity  $v_0$  to reach point  $x$  and is equal to

$$\theta = \omega T = \frac{3\omega}{\alpha} x^{1/3} \quad 93$$

Rewriting equation 86 with the new velocity component introduced we have:

$$\left( \frac{\partial}{\partial t} + \omega \frac{\partial}{\partial \theta} \right)^2 v_1 = \beta \sin \omega t \quad 94$$

$$\text{where } \beta = \frac{e}{m} \frac{A}{\epsilon} \quad 95$$

Equation 94 has the solution

$$v_1 = -\frac{\beta}{\omega^2} \left[ \sin \omega t + \frac{2}{\theta} \cos \omega t + F_1(\theta - \omega t) + \frac{1}{\theta} F_2(\theta - \omega t) \right] \quad 96$$

This equation contains two arbitrary functions of  $(\theta - \omega t)$  which must be evaluated from the boundary conditions selected for  $v_1$ . Thus the boundary conditions for the alternating current component make their first appearance.

From the form of equation 91 which is linear in  $v_1$ , it is evident that  $v_1$  must be a sinusoidal function of time having an angular frequency  $\omega$  in order to correspond with the form of  $J_1$ . It follows, then, that the most general form which can be assumed for the steady state functions  $F_1$  and  $F_2$  is as follows:

$$F_1(\theta - \omega t) = a \sin(\theta - \omega t) + b \cos(\theta - \omega t) \quad 97$$

$$F_2(\theta - \omega t) = c \sin(\theta - \omega t) + d \cos(\theta - \omega t) \quad 98$$

As pointed out, there is no mathematical necessity for boundary conditions imposed upon  $v_1$  to correspond with those which were imposed upon  $v_0$ . As on actual cathode consisting of an electron emitting surface, it would be appropriate to assume that the initial velocities are in no way dependent upon the current. In general we shall have to deal not only with actual cathodes, but also with virtual cathodes\* when the assumption of zero alternating current velocity and acceleration is unwarranted. The general equations for the alternating current will therefore apply when the origin is taken at the point of direct current potential minimum which forms the virtual cathode.

Since there are two arbitrary functions in equation 96, two boundary conditions will be needed. The first boundary condition is that the alternating current velocity is finite at the origin. For the other, a knowledge of the value of the alternating current velocity at any point between the two reference planes is sufficient. Thus, if at a particular value of  $\theta$ , say  $\theta_1$ , we know that  $v_1$  is equal to  $M\sin\omega t + N\cos\omega t$ , we then have enough information to calculate its value at all other points between the two parallel planes. In mathematical form the boundary conditions may be set forth as follows, when  $\theta=0$ ,  $v_1$  must be finite, and  $\theta=\theta_1$ ,  $v_1 = M\sin\omega t + N\cos\omega t$ . Substituting these boundary conditions into equations 96, 97, and 98, we have for the coefficients:  $c = 0$ ,  $d = -2$

$$a = \frac{\omega^2}{\beta} (M\cos\theta_1 - N\sin\theta_1) + \cos\theta_1 - \frac{2}{\theta_1} \sin\theta_1 \quad 99$$

$$b = \frac{2}{\theta_1} (1 - \cos\theta_1) - \sin\theta_1 - \frac{\omega^2}{\beta} (M\sin\theta_1 + N\cos\theta_1) \quad 100$$

---

\*See section on "Electron Effects" of this paper.

As a final result for equation 96 we have:

$$u_1 = (M + jN) (\cos \theta_1 + j \sin \theta_1) (\cos \theta_1 - j \sin \theta_1) \\ + \frac{\beta}{\omega^2} \left[ \left\{ \left( \cos \theta_1 - \frac{2}{\theta_1} \sin \theta_1 \right) - j \left( \frac{2}{\theta_1} - \frac{2}{\theta_1} \cos \theta_1 - \sin \theta_1 \right) \right\} \right. \\ \left. \left( \cos \theta_1 - j \sin \theta_1 \right) - \left( 1 - \frac{2}{\theta_1} \sin \theta_1 \right) - j \frac{2}{\theta_1} (1 - \cos \theta_1) \right] \quad 101$$

The next step is a determination of the potential corresponding to the velocities  $v_0$  and  $v_1$  respectively. Thus from equations 79 and 83, we get:

$$-\frac{e}{m} \frac{\partial V}{\partial x} = \frac{\partial v}{\partial t} + v \frac{\partial v}{\partial x} \quad 102$$

and then with the separation of components by equation 88 and 89, we have:

$$-\frac{e}{m} \frac{\partial V_0}{\partial x} = u_0 \frac{\partial u_0}{\partial x} \quad 103$$

$$-\frac{e}{m} \frac{\partial V_1}{\partial x} = \frac{\partial u_1}{\partial t} + \frac{\partial}{\partial x} (u_0 v_1) \quad 104$$

The solution of equation 103 is:

$$V_0 = -\frac{m}{2e} u_0^2 = -\frac{m}{2e} \alpha^2 x^{4/3} \quad 105$$

which is the well known classical relation between the potential, the current, and the position between two parallel planes where complete space charge exists.

The alternating current component of the potential is obtained by integration of equation 104 as follows:

$$-\frac{e}{m} V_1 = \frac{\partial}{\partial t} \int u_1 \partial x + u_0 v_1 + f(t) \quad 106$$



Solving for  $v_1$  we have

$$V_1 = -\frac{2m\alpha^3}{e9\omega^2} (M+jN) (\cos\theta_1 + j\sin\theta_1) \left[ (\theta\sin\theta + \cos\theta) + j(\theta\cos\theta - \sin\theta) \right] \\ - \frac{2m\alpha^3\beta}{e9\omega^4} \left[ \left( \cos\theta_1 - \frac{2}{\theta_1}\sin\theta_1 \right) - j \left( \frac{2}{\theta_1} - \frac{2}{\theta_1}\cos\theta_1 - \sin\theta_1 \right) \right] \\ \left\{ \left( \theta\sin\theta + \cos\theta \right) + j \left( \theta\cos\theta - \sin\theta \right) \right\} - \cos\theta - j \left( \theta + \frac{1}{6}\theta^3 - \sin\theta \right) \right] + C \quad 107$$

This equation is applicable between any two fictitious parallel planes where one plate is located at the origin where the boundary condition for  $V_0$  is satisfied, namely, that the direct current components of velocity at a point  $x_1$ , corresponding to the transit angle,  $\theta_1$ , is given by  $M + jN$ . Thus equation 107 gives the fundamental relation between the alternating current component  $J_1$  and the alternating current potential  $V_2$  in an idealized parallel plate diode.

#### (B) Application to Triodes with Negative Grid

In the application of the fundamental relations to triodes operating with <sup>the</sup> grid at a negative potential, the problem becomes more complicated, because of the different current paths which exist within the tube. Moreover the direct current potential distribution is disturbed in a radical way by the presence of the negative grid. In fact the negative grid triode in some respects offers greater theoretical difficulty than does the positive grid triode. 18,20,21

(18) Llewellyn, op.cit.

(20) Gill, E. W., A Space Charge Effect, Phil.Mag., vol.49, p. 933, 1925.

(21) Tonks, L., Space Charge as a Cause of Negative Resistance in a Triode and its Bearing on Short Wave Generator, Phys.Rev., Vol. 30, p. 501, Oct. 1929.

It will be assumed that the alternating velocity at a point  $x_1$ , located near the cathode is directly proportional to the alternating grid potential,  $V_g$ , so that we may write:

$$v_1 = (M + jN) = k V_g \quad 108$$

If the point  $x_1$  is very near the cathode we may assume  $\theta$  to be zero, so that equation 107 may be written as

$$V_p = \frac{12r_0 A}{\theta^4} \left[ (\theta \sin \theta + 2 \cos \theta - 2) + j \left( \theta + \frac{1}{6} \theta^3 - 2 \sin \theta + \theta \cos \theta \right) \right] \\ - (M + jN) \frac{\omega^2}{\beta} \left[ (\theta \sin \theta + \cos \theta - 1) - j (\sin \theta - \theta \cos \theta) \right] \quad 109$$

The equation may be written in condensed form with the aid of

$$V_p = J_1(r + jx) - V_g(\gamma + jy) \quad 110$$

where

$$r = -\frac{12r_0}{\theta^4} (\theta \sin \theta + 2 \cos \theta - 2) \quad 111$$

$$x = -j \frac{12r_0}{\theta^4} \left( \theta + \frac{1}{6} \theta^3 - 2 \sin \theta + \theta \cos \theta \right) \quad 112$$

$$\gamma = \frac{2\mu_0}{\theta^2} (\theta \sin \theta + \cos \theta - 1) \quad 113$$

$$y = j \frac{2\mu_0}{\theta^2} (\theta \cos \theta - \sin \theta) \quad 114$$

The significance of equation 110 is apparent when it is compared with the classical form of the equation representing the alternating current plate voltage, namely

$$V_p = I_p r_o - \mu V_g \quad 115$$

The plate resistance  $r_o$  has now become complex or likewise has the amplification factor  $\mu$ . Values of the internal plate impedance

$$Z_p = r + jx \quad 116$$

as a function of  $\theta$  are plotted in Figure 16 and 17. (See page 51 for these figures).

Values of the amplification factor

$$\sigma = \mu + j\nu \quad 117$$

are shown in Figures No. 18 and 19. (See page 52 for these figures).

The cathode to plate capacitance is included in the fundamental relations. At low frequencies, the equivalent circuit representation of equation 110 degenerates into that shown in Figure No. 20. Note that equation 109 has two real and two imaginary components, that is one minus and one plus for

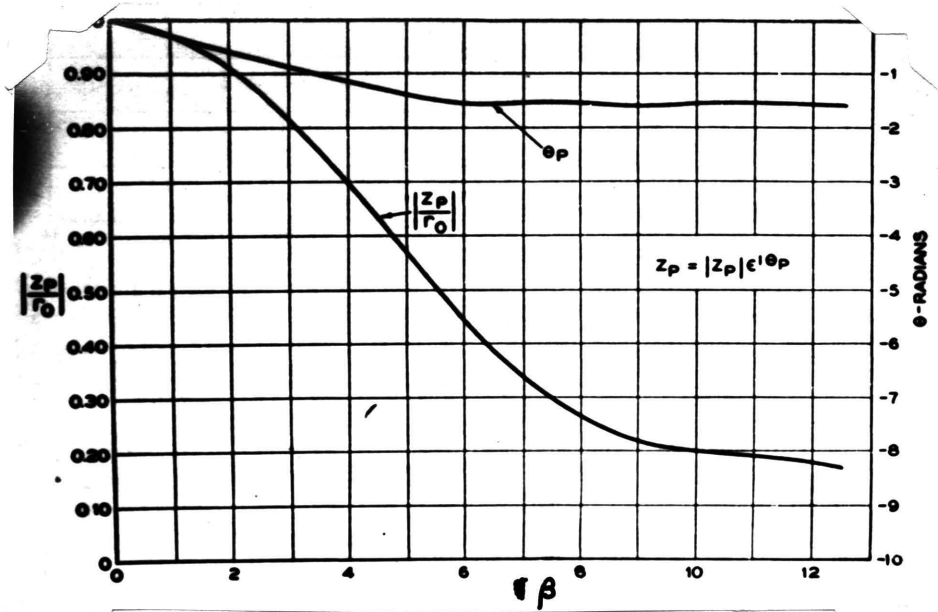


Figure No. 16  
Plot of Internal Plate Impedance Versus Frequency

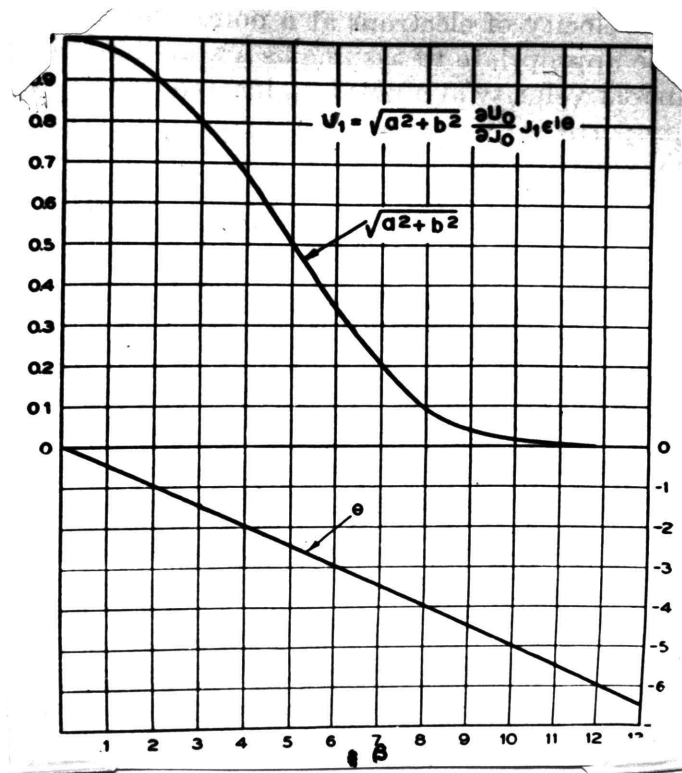


Figure No. 17  
Plot of Total Impedance Versus Frequency

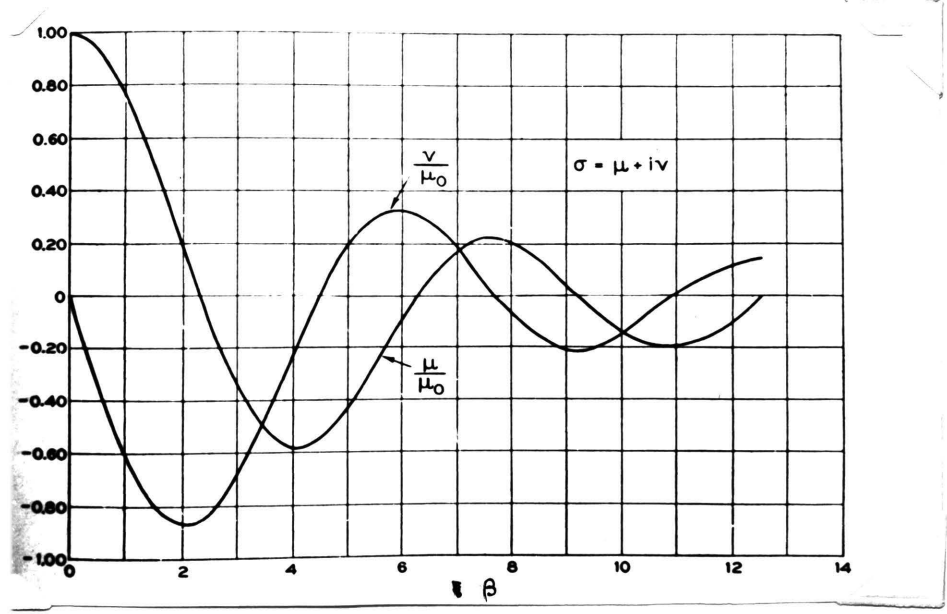


Figure No. 18  
Plot of Amplification Factor Versus Frequency

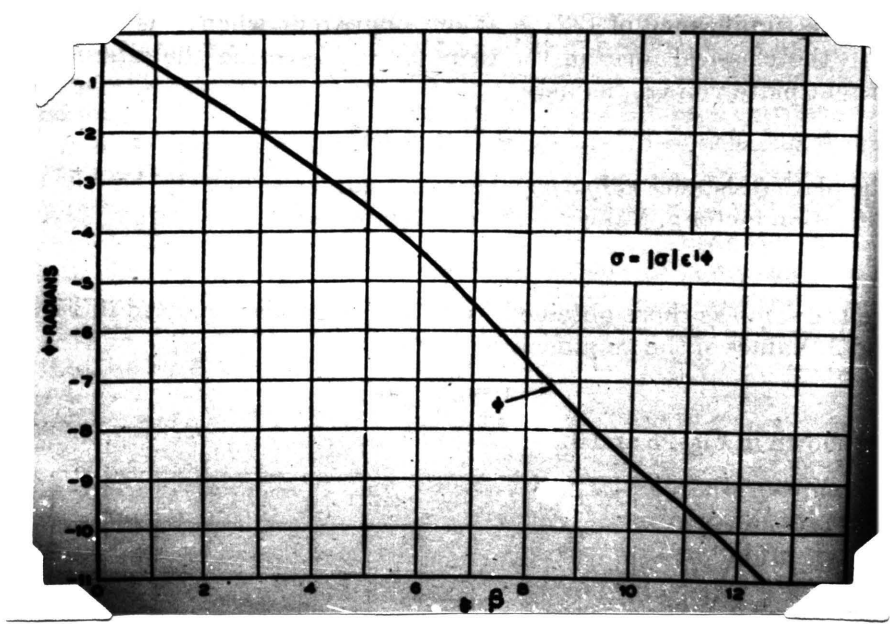


Figure No. 19  
Plot of Phase of Amplification Factor  
Versus Frequency

resistance and also one minus and one plus for reactance. So the equivalent circuit representation must be a parallel one with a series resistance in each branch.

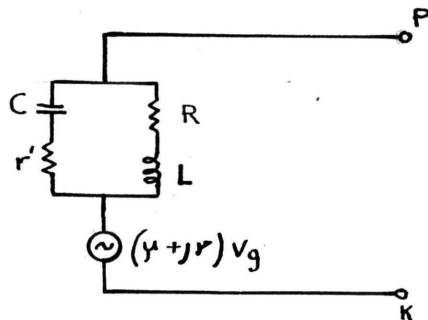


Figure No. 20  
Equivalent Circuit of Plate Cathode Path of Negative Grid Triode for Low Values of Transit Angle

Strictly speaking the equivalent circuit corresponding to equation 110 exists not between the plate and cathode but between plate and potential minimum near the cathode which is due to the facts explained in the electronic section of this paper. Practically, the difference is negligible except at very high frequencies. Since the impedance between cathode and potential minimum is small compared to <sup>the</sup> plate impedance, its effect is merely to add a loss to the system which increases with frequency, since the plate impedance approaches a capacity as the frequency approaches infinity. This can be seen from equations 111 and 112.

The force due to the grid acts on the high charge density region existing near the potential minimum. The impedance between cathode and grid, therefore, consists of two parts in

series, namely, capacity between grid and potential minimum and impedance between potential minimum and cathode, the latter part of this impedance being common both to plate and grid current paths.

If we were to connect the grid and cathode terminals of such a triode to a capacity bridge and measure the capacity existing there when the tube was cold and when the tube was heated, we would notice a slight increase in latter case. The reason for this increase may be best explained by noting that in the cold condition the electrostatic force from the grid is exerted on the cathode itself, whereas in the heated state, the force acts on the electrons near the potential minimum, thus resulting in an increased capacity in series with a resistive component.

Now let us consider the grid-plate path. First of all let us consider a low frequency case. In this case the electron stream passes through the spaces between <sup>the</sup> grid wires, afterward diverging as the plate is approached. Electrostatic force from the grid acts not only on the plate but also on the electrons in the space between. It is evident, then, that the path, which, when cathode was cold, constituted a pure capacity change into an effective capacity different from the original in combination with a resistive component. The losses would be expected to increase with frequency just as they did in the grid-cathode type. The change in grid-plate impedance is particularly noticeable when it is

attempted to adjust balanced or neutralized amplifier circuits with the filament cold, in which case the balance is disturbed when the cathode is heated.

It has been shown that both the cathode-grid path and the grid-plate path contain resistive components with corresponding losses which increase with increase of frequency. This loss may be used as a reason why triodes with negative grids cease to oscillate at the higher frequencies.

The electronics of the vacuum tube which was discussed in the preceding pages must be regarded as a starting point to the more rigorous solution of the problem.

Among the various assumptions which were made in the development of the theory, there are two which are of real importance and make the development far from being correct at Ultra High Frequencies. These two may be enumerated as follows:

- (1) Current flow in straight lines
- (2) No space charge effect.

We may now wonder why the results of this analysis is not combined in the internal and external lead effect as well as interelectrode capacitances to form a more accurate equivalent circuit of the vacuum tube. Of course this could be done but how accurate would be the overall equivalent circuit? It's answer depends merely on the range of frequencies, and the more the frequency goes up, the less accurate the circuit becomes. We must now look to some other approach which will give the overall behavior of



the electron stream within the vacuum tube.

This has been carried out by Benham and jointly by L. C. Peterson and Llewelyn. In the next section this new approach based on the consideration of electron stream within the vacuum tube must be analyzed. But unfortunately this approach disregards transit time effect at very high frequencies due to Maxwellian velocity distribution. The results from this new analysis can be considered as being reasonably correct up to  $10^{10}$  cycles/sec. The general steps in the new approach are the same as for the consideration of the transit time except for the addition of space charge effects, and slightly different boundary conditions.

## SECTION IV

## Electron Stream Theory as Applied to Vacuum Tubes

(A) Derivation of a General Impedance Formula<sup>22</sup>

This new analysis of vacuum tube starts with the work<sup>1</sup> of W. E. Benham who considers a special case comprising two parallel plane electrodes, a-b, one of which is an emitter and the other a collector.

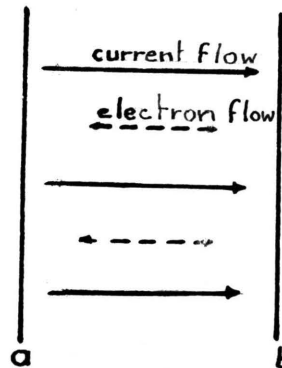


Figure No. 15  
Parallel Plane Electrodes

The conditions at the emitter are restricted by the assumption that the electrons are emitted with zero initial velocity and acceleration. The planes are of infinite extent.

Plane a is held at a positive potential  $V$  with respect to plane b. Between the two planes electrons are free to move under the influence of the existing field. The next step consists of separation of alternating and direct current components, not only of current and potential but also of electron velocity charge density and electric intensity. The

(22) Llewellyn, F.B. and Peterson, L.C., Vacuum Tube Networks, Proc. IRE, vol.32.p.199, 1944.

(1) Benham, op.cit.

analysis starts with one of the Maxwell equation giving the total current density in the space between the two parallel plates.

$$J = \rho v + \epsilon \frac{\partial E}{\partial t} \quad 81$$

The equation of motion of an electron is obtained by the equation

$$F = kma \quad 118$$

Where:  $k$  equals  $10^{-7}$

$F$  equals  $eE$

$$eE = kma \quad 119$$

Where  $e$  is the electron charge equal to  $1.59 \times 10^{-19}$  coulombs.

In this equation the effect of a magnetic field is disregarded\*.

This is thoroughly justified until electron velocities approach

that of light or the spacing between the two parallel planes

becomes comparable with the wave length of the alternating

field considered. The first fundamental equation used in

this development is:

$$\nabla \cdot \epsilon \vec{E} = \rho \quad 120$$

---

\*The force would be given by  $F = eE + ev \times \frac{H}{c}$  if the magnetic field is considered.

which for the parallel planes now considered, becomes

$$\epsilon \frac{\partial E}{\partial x} = \rho \quad 80$$

By substituting of this equation into equation 31 there results

$$J = \epsilon \left( \frac{\partial E}{\partial x} v + \frac{\partial E}{\partial t} \right) \quad 121$$

As  $E$  is a function both of  $t$  and of  $x$ , we can write:

$$\frac{dE}{dt} = \frac{\partial E}{\partial x} \frac{dx}{dt} + \frac{\partial E}{\partial t} \quad 122$$

Comparison of the right hand side of this equation with the equation for current density given above shows that as soon as the velocity  $v$  is identified with  $\frac{dx}{dt}$  we can write the current density in the form

$$J = \epsilon \frac{dE}{dt} \quad 123$$

where the total derivative indicates that we must imagine ourselves to be fixed to a certain electron and riding along with it in order to observe the variation in field intensity as time progresses. When  $E$  is replaced by the acceleration, as in equation 119 the current density may be written in the form

$$\frac{eJ}{kme} = \frac{da}{dt} \quad 124$$

in which the remarks made above in connection with E now apply to acceleration a.

The total current density J is not a function of x but it is only a function of t. This comes about because of the plane shape and parallel disposition of the electrodes as mentioned in the preceding section, and that the current always flows in closed path; that is, its divergence is zero. In order to integrate the equation, it will be found convenient to assume that

$$\frac{eJ}{kme} = J_0 + J_1 + J_2 + \dots \quad 125$$

in which  $J_0$  is a constant; all other J's are functions of time. Their exact definitions will develop in the course of the analysis, but at <sup>the</sup> present they may be considered as alternating current components of the current density. We may write also:

$$\frac{eJ}{kme} = k + \varphi'''(t) \quad 126$$

Where  $\varphi'''(t)$  is the sum of  $J_1 + J_2 + J_3 \dots$  and is the third derivative with respect to time of some time function while k is the constant component,  $J_0$ . With this understanding equations 124 and 125 can be written as:

$$\frac{da}{dt} = k + \varphi''(t) \quad 127$$

Integrating with respect to time gives

$$a = k(t - t_0) + \varphi'(t) - \varphi'(t_0) + a_0 + \psi(t_0) \quad 128$$

Where  $a_a + \alpha(t_a)$  is the acceleration; when  $t = t_a$ , that is, at the a-plane, and  $a_a$  is the independent of  $t_a$ , so that it is constant.

Another integration gives

$$v = \frac{1}{2} K (t-t_a)^2 + \phi'(t) - \phi'(t_a) - (t-t_a)\phi''(t_a)$$

$$+ (t-t_a)a_a + (t-t_a)\psi(t_a) + v_a + r(t_a)$$

129

Where  $v_a + r(t_a)$  is the velocity, where  $t = t_a$  and  $v_a$  is independent of  $t_a$ .

A third integration gives

$$x = \frac{1}{6} K (t-t_a)^3 + \phi(t) - \phi(t_a) - (t-t_a)\phi'(t_a) - \frac{1}{2}(t-t_a)^2\phi''(t_a)$$

$$+ \frac{1}{2}(t-t_a)^2 a_a + \frac{1}{2}(t-t_a)^2 \psi(t_a) + (t-t_a)v_a + (t-t_a)r(t_a)^{130}$$

Where:  $x$  equals 0

$t$  equals  $t_a$

In proceeding from this point onward, an important limitation must be kept in mind. In equation 81 from which 129 is derived, the velocity  $v$  is a single value function of  $x$  and  $t$ . Therefore in equation 129 initial conditions must never be assigned which cause any of the electrons to overtake one another at some point between the two planes considered, for that would imply electrons moving with different velocities across the same plane, so as to violate the single valued velocity condition. The required conditions must be satisfied as J. Muller<sup>23</sup> points out when:

$$\frac{\partial x}{\partial t_a} < 0$$

131

(23) Muller, J., Untersuchungen Über Elektronenstromungen Hochfreq. Tech.U.Elektrotechnik., Vol.41, May 1933.

because their electrons emitted at a certain time cannot overtake those previously emitted. By making the substitution:  $t - t_a = T + \delta$

Where  $t$  is the transit time if all fluctuating components were absent, and  $\delta$  is the variational transit time effect, and rearranging terms we get the expression:

$$0 = \frac{1}{6} K [3T^2\delta + 3T\delta^2 + \delta^3] + \phi(t) + \psi(t) + \gamma(t) + \dots \quad 132$$

where  $k$  is the constant current density component. This equation may be arranged in the form of a power series in  $\delta$ . It cannot at the present time be solved for  $\delta$ , but it has the advantage over equation 130 in that the variational time  $\delta$  is not involved in the functions  $\psi$ ,  $\phi$  and  $\gamma$  so that functions of  $\psi$ ,  $\phi$  and  $\gamma$  can be determined and then equation 131 can be solved for  $\delta$ .

Let  $\delta$ ,  $\phi$ ,  $\psi$  and  $\gamma$  each be split up into series as follows ;

$$\delta = \delta_1 + \delta_2 + \delta_3 + \dots$$

$$\phi = \phi_1 + \phi_2 + \phi_3 + \dots$$

$$\psi = \psi_1 + \psi_2 + \psi_3 + \dots$$

$$\gamma = \gamma_1 + \gamma_2 + \gamma_3 + \dots$$

133

As it is evident from the integration process,  $\phi$ ,  $\psi$ ,  $\gamma$  are integration constants which are functions of time, of acceleration, velocity, and space. These are then substituted into equation 132 and the resultant equation may be expressed as an infinite set of separate equations such that, in general, the sum of the subscripts of each term of the  $n^{\text{th}}$  equation is equal to  $n$ . For example, the first equation includes all linear terms which have the subscript 1, but no other terms; the second equation includes all linear terms having the subscript 2 and also all quadratic terms having the subscript

1; the third equation includes all linear terms having the subscript 3, cubic terms with subscript 1 and also products of quadratic terms with subscript 1. <sup>it has</sup> Also linear terms with subscript 1 as well as products of linear terms with subscript 2, and linear terms with subscript 1.

The first of these equations may be solved for  $\delta_1$  ; the second for  $\delta_2$  ; and the third for  $\delta_3$  , and so on. Let us express:

$$a = a_0 + a_1 + a_2 + \dots \quad 134$$

and evaluate each term by using equation 128. Also let us express:

$$v = v_0 + v_1 + v_2 + \dots \quad 135$$

and evaluate each term by means of equation 129. We then have the acceleration and velocity in terms of transit time  $t$ , and the initial velocity and acceleration. In circuit work, the potential difference between the two parallel planes,  $a$  and  $b$ , say is more often required than the electron acceleration. This may be found from the definition of the potential difference, namely:

$$V_b - V_a = \int_a^b E dx \quad 136$$



in which  $t$  remains constant during the integration. If all a.c. components were zero and  $t$  minus  $t_a$  equals  $T$ , where  $T$  is the transit time of all a.c. components were zero, then we would express equation 129 by

$$x = \frac{1}{6} k T^3 + \frac{1}{2} a_a T^2 + u_a T \quad 137$$

Differentiating we get:

$$dx = \left\{ \frac{1}{2} k T^2 + a_a T + u_a \right\} dT = v_a dT \quad 138$$

With the aid of this equation and equation 119 the potential difference is given by

$$W_b - W_a = \int_a^b a dx = \int_0^T a \left\{ \frac{1}{2} k T^2 + a_a T + u_a \right\} dT \quad 139$$

where  $W$  is used as an abbreviation for  $\frac{eV}{km}$ .

In the same way as the acceleration and velocity are divided into components, the potential difference may be split up into  $(W_a - W_b)_0$ ,  $(W_a - W_b)_1$ ,  $(W_a - W_b)_2$ , etc.

These components are defined as

$$\begin{aligned} (W_a - W_b)_0 &= \int_0^T a_0 v_0 dT \\ (W_a - W_b)_1 &= \int_0^T a_1 v_0 dT \\ (W_a - W_b)_2 &= \int_0^T a_2 v_0 dT \end{aligned} \quad 140$$

(B) Space Charge Factor Concept

Before the general equation for direct and alternating current are introduced it is necessary to introduce the space charge factor. In actual vacuum tubes there are usually many electrons present between the various planes of the tube at any given electron. The space charge factor  $\zeta$  is a measure of the effectiveness of that modification. In the treatment by C. E. Fay, A. L. Samuel and W. Shockley,<sup>16</sup> the solution of the fundamental equation for space charge problems are obtained in terms of parameters which are difficult to apply directly; therefore, it is easier to write the solutions in terms of direct current transit time as a parameter. Such a procedure allows the degree of space charge to be specified by defining a space charge factor, which we shall call  $\zeta$ .  $\zeta$  is zero when there is no space charge, as more and more electrons are injected through the a-plane and move across the b-plane, the density of space charge increases and  $\zeta$  increases likewise. However, it is a well known fact that the amount of electron current which may be injected through the a-plane and that will thereafter move across the b-plane is not unlimited, but has an upper value beyond which it is impossible to force more electrons into the space without having some of them turn around and move backwards toward the a-plane with a consequent reduction in the number crossing the b-plane.\*

---

\*See page 36.

The onset of this phenomena occurs very suddenly for a critical value of the injected current which we shall call  $I_m$ . When that value of injected current is exceeded the performance of the vacuum tube changes character very rapidly. Our present analysis is confined strictly to current values less than (or at most equal to) the limiting value of  $I_m$ . The space charge factor is defined in such a way that it varies from a value of zero for no space charge to a value of unity for complete space charge, the latter condition being that for which the injected current has its limiting value  $I_m$ . The relation between the actual current  $I_D$ , the limiting current  $I_m$  and this space charge factor  $\zeta$  may be written:

$$I_D/I_m = \left(\frac{9}{4}\right) \zeta (1 - \zeta/3)^2 \quad 141$$

A graph of this function is shown in Figure No. 22.  
(See Page 67 for Figure No. 21)

### (C) D. C. Equations

Using the first expression of equation 140 and substituting its values for  $a_0$  and  $v_0$ , integrating, and introducing the space charge factor  $\zeta$ , we obtain the following equation for the steady case.

$$\zeta = 3 \left(1 - \frac{T_0}{T}\right)$$

$$x = (1 - \zeta/3) (v_a + v_b) \frac{T}{2}$$

Where  $v_a$  is the velocity at plane a  
 $v_b$  is the velocity of plane b

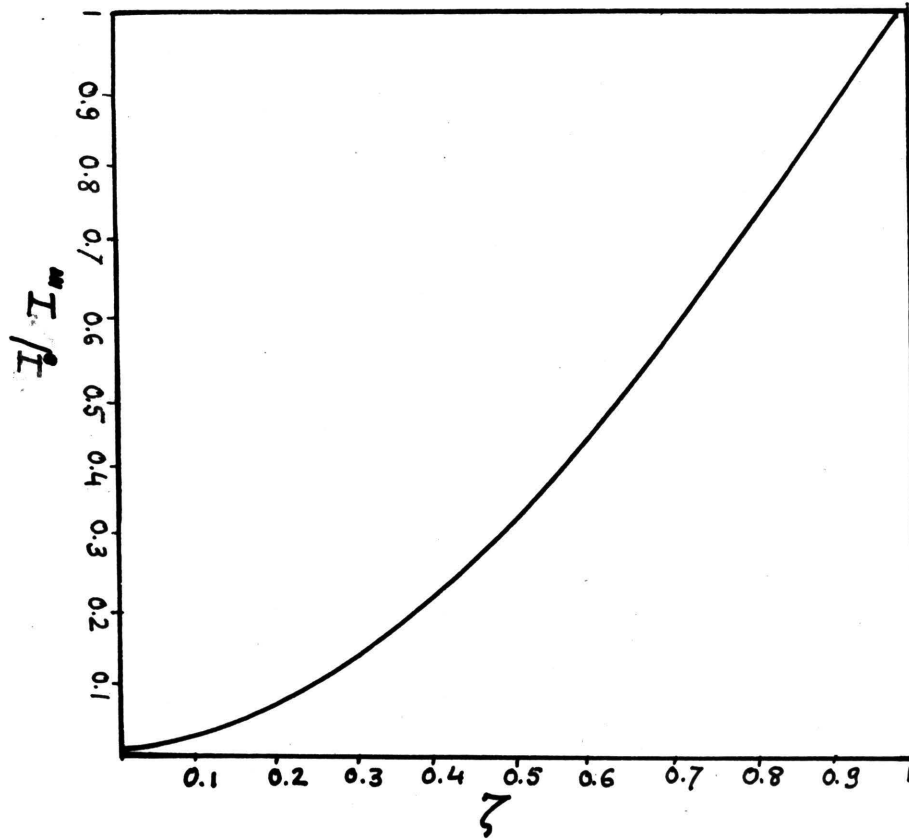


Figure No. 21  
 A plot of  $I_0/I_m$  Versus Space Charge Factor  $\zeta$

T is the time it takes for an electron to traverse the distance between a and b.

$T_0$  is the value which T would approach when  $\zeta$  approaches zero.

That is  $T_0$  is the transit time when there are no electrons present between the two planes besides the one under observation.

The formula for computing  $I_m$  may be obtained from equation 141 by setting  $\zeta$  equal to unity and eliminating T between equations 141 and 142.

$$\frac{10^7 e}{m \epsilon} J = \left[ \frac{2}{9} \left( \frac{v_a + v_b}{x^2} \right)^3 \right] \quad 143$$

In more convenient form the velocities  $v_a$  and  $v_b$  may be replaced by potentials.

$$J_m = \frac{2.33}{10^6} \left( \frac{\sqrt{W_a} + \sqrt{W_b}}{x^2} \right)^3 \quad 144$$

which is a somewhat extended form of Child's equation which applies only to the case where the a-plane coincides with a thermionic cathode, the potential  $W_a$  then becoming zero.

Using the second expression of equation 140 and substituting the values of  $a_1$  and  $v_0$  we can have the alternating current equations in terms of space charge factor again with the result that the different terms in the equations appear in such a form that their relative magnitudes may be directly compared. There are many possible choices for <sup>the</sup> space

charge factor. From actual tube operation it can be shown that reasonable good results can be obtained if a space charge factor is made equal to 1.0 for a region containing an emitting cathode or virtual cathode. Moreover, between any two grids of a vacuum tube, the value of  $\zeta$  is often extremely small and alternating current terms containing it as a factor may then be disregarded with little resulting error.

The alternating electronic equations are:

$$W_b - W_a = AJ + Bq_a + C v_a$$

$$q_b = DJ + E q_a + F v_a$$

$$v_b = GJ + H q_a + K v_a$$

145

The coefficients A through K are expressable in terms of direct current quantities already defined together with the frequency of the alternating current considered.

$q_b$  is the conduction current of plane b;  $v_b$  is the alternating electron velocity in centimeters per second;  $q_a$  is the conduction current density

A symbol  $\Theta$  will be used to represent the transit angle which is defined by the relations  $\Theta = \omega T$  and  $\beta = j \Theta$ .

The coefficient of equation 145 are given in Table I, II and III.

TABLE NO. I

Values of alternating-current Components

$$A = \frac{1}{\epsilon} (v_a + v_b) \frac{T^2}{2} \frac{1}{\beta^2} \left[ 1 - \frac{\zeta}{3} \left( 1 - \frac{12S}{\beta^3} \right) \right]$$

$$B = \frac{1}{\epsilon} \frac{T^2}{\beta^2} \left[ v_a (P - \beta Q) - v_b P + \zeta (v_a + v_b) P \right]$$

$$C = -\frac{1}{\eta} 2\zeta (v_a + v_b) \frac{P}{\beta^2}$$

$$D = 2\zeta \left( \frac{v_a + v_b}{v_b} \right) \frac{P}{\beta^2}$$

$$E = \frac{1}{v_b} \left[ v_b - \zeta (v_a + v_b) \right] e^{-\beta}$$

$$F = \frac{\epsilon}{\eta} \left[ \frac{2\zeta}{T^2} \left( \frac{v_a + v_b}{v_b} \right) \right] \beta e^{-\beta}$$

$$G = -\frac{\eta}{\epsilon} \frac{T^2}{\beta^3} \frac{1}{v_b} \left[ v_b (P - \beta Q) - v_a P + \zeta (v_a + v_b) P \right]$$

$$H = -\frac{\eta}{\epsilon} \frac{T^2}{2} \left( \frac{v_a + v_b}{v_b} \right) (1 - \zeta) \frac{e^{-\beta}}{\beta}$$

$$K = \frac{1}{v_b} \left[ v_a - \zeta (v_a + v_b) \right] e^{-\beta}$$

TABLE NO. II

Complete Space Charge  $\zeta=1$ 

$$A = \frac{1}{\epsilon} (v_a + v_b) \frac{I^2}{3\beta} \left( 1 - \frac{6S}{\beta^2} \right)$$

$$B = \frac{1}{\epsilon} \frac{I^2}{\beta^3} v_a (2P - \beta Q)$$

$$C = -\frac{2}{\eta} (v_a + v_b) \frac{P}{\beta^2}$$

$$D = 2 \left( \frac{v_a + v_b}{v_b} \right) \frac{P}{\beta^2}$$

$$E = -\frac{v_a}{v_b} e^{-\beta}$$

$$F = \frac{\epsilon}{\eta} \frac{2}{T^2} \left( \frac{v_a + v_b}{v_b} \right) \beta e^{-\beta}$$

$$G = -\frac{\eta}{\epsilon} \frac{I^2}{\beta^3} (2P - \beta Q)$$

$$H = 0$$

$$K = -e^{-\beta}$$



TABLE NO. III Space Charge  $\zeta = 0$ 

$$A = \frac{1}{\epsilon} (v_a + v_b) \frac{T^2}{2} \frac{1}{\beta}$$

$$B = \frac{1}{\epsilon} \frac{T^2}{\beta^2} [v_a(P - \beta Q) - v_b P]$$

$$C = 0$$

$$D = 0$$

$$E = e^{-\beta}$$

$$F = 0$$

$$G = -\frac{\eta}{\epsilon} \frac{T^2}{\beta^3} \frac{1}{v_b} [v_b(P - \beta Q) - v_a P]$$

$$H = -\frac{\eta}{\epsilon} \frac{T^2}{2} \left( \frac{v_a + v_b}{v_b} \right) \frac{e^{-\beta}}{\beta}$$

$$K = \frac{v_a}{v_b} e^{-\beta}$$

TABLE NO. IV

Symbols employed

$$\eta = 10^7 \frac{e}{m} = 1.77 \times 10^{15}$$

$$\epsilon = \frac{1}{36\pi \cdot 10^9} \frac{\eta}{\epsilon} = 2 \times 10^{28}$$

$$P = 1 - e^{-\beta} - \beta e^{-\beta} = \frac{\beta^2}{2} - \frac{\beta^3}{3} + \frac{\beta^4}{8}$$

$$Q = 1 - e^{-\beta} = \beta - \frac{\beta^2}{2} + \frac{\beta^3}{6} - \frac{\beta^4}{24} + \dots$$

$$S = 2 - 2e^{-\beta} - \beta - \beta e^{-\beta} = -\frac{\beta^3}{6} + \frac{\beta^4}{12} - \frac{\beta^5}{40} + \frac{\beta^6}{180} + \dots$$

As it is seen from the above equation, the expressions for the electron stream behavior are complex and lengthy. To attempt to have a second order solution will make the result even more complex. In our case the first order solution will give appreciably good results at moderately high frequencies. A second order solution is given in reference No. 1. The notations in equation 145 are slightly different from those given in "Electron Inertia Effects" by Llewellyn <sup>24</sup>. Llewellyn in his development neglects space charge effect and has its coefficients written in terms of velocities and transit time.

For a more complete treatment of the derivations of equation 145, see references 1, 19 and 24.

#### (D) Application to Diodes

As a first example of the application of the above development let us consider the case where no electrons are present between the a-plane and the b-plane of Figure No. 15.

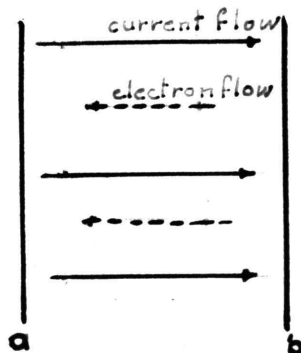


Figure No. 15  
Basic Picture of Electron Analysis

(24) Llewellyn, F.B., *Electron Inertia Effect*, Cambridge University Press, New York, N.Y., 1933

So the injected current  $q_a$  becomes zero and as the space charge is zero, consequently the first equation of 145 becomes

$$W_b - W_a = AI \quad 146$$

From the above equation it can be seen that  $A$  is the impedance per unit area of the two parallel planes. From Table No. II for zero space charge, the formula for  $A$  is:

$$A = \frac{1}{\epsilon} (U_a + U_b) \left( \frac{T_0^2}{2} \right) \left( \frac{1}{\beta} \right) \quad 147$$

However, from the second equation 142

$$x = (U_a + U_b) \frac{T_0}{2} \quad 148$$

Substituting this into the above expression for  $\alpha$  and remember that  $\beta = j\omega t$  we have:

$$A = \frac{x}{j\epsilon\omega} \quad 149$$

Now equation 149 is precisely the equation for the

impedance between two parallel plane conductors in vacuum and may be written:

$$A = \frac{1}{j\omega C} \quad , \quad C = \frac{\epsilon}{x} \quad 150$$

Which shows, that the capacitance per unit area between parallel planes is  $\frac{\epsilon}{x}$  farads.

As a second example let us investigate the characteristics of the general diode impedance with complete space charge condition. The equations needed are the expression for A taken from Table No. II and the expression for direct current potential  $(W_b - W_a)_0$  and the third equation of 142.

Thus we have for complete space charge

$$Z = A_{z,i} = \frac{1}{\epsilon} (U_a + U_b) \frac{T^2}{3} \left( \frac{1}{\beta} \right) \left[ 1 + \frac{6.5}{\beta^3} \right]$$

$$\eta \left( \sqrt{W_a} + \sqrt{W_b} \right)_0 = \frac{1}{2} (U_a + U_b) \quad 151$$

$$\left( \frac{\eta}{\epsilon} \right) I_D = (U_a + U_b) \frac{2}{T^2}$$

Where:  $\eta$  equals  $10^7 \frac{e}{m} = 1.77 \times 10^5$

By combining the above three equations we have:

$$Z = \frac{2}{3} \left( \frac{\sqrt{W_a} + \sqrt{W_b}}{I_D} \right)_0^2 \left[ \frac{2}{\beta} + \frac{12.5}{\beta^4} \right] \quad 152$$

The coefficient  $\frac{2(\sqrt{W_a} + \sqrt{W_b})^2}{3I_0}$  in this expression is of special interest. When the a-plane is a thermionic cathode,  $v_a$  may be taken as zero, corresponding to zero electron velocity of emission. Therefore the coefficient is merely  $\frac{2W_b}{3I_0}$ . This is the expression for the inverse slope of the static characteristic of a diode tube operating with complete space <sup>charge</sup> and hence may be represented by the symbol  $r_0$ , the zero frequency value of the diode resistance. In <sup>a</sup> more general case of Equation 151 where the electron velocities at the a-plane are not necessarily zero, but where the coefficient has the generalized form  $\frac{2(\sqrt{W_a} + \sqrt{W_b})^2}{3I_0}$ , we may still denote it by  $r_0$ , because for the low frequencies the bracketed factor in equation 152 reduces to unity as may be proved by using the series expression for S given in Table IV and allowing  $\beta$  to approach zero.

In general, then, for a diode with complete space charge we have

$$Z = r_0 \left[ \frac{2}{\beta} + \frac{12s}{\beta^4} \right] \quad 153$$

The graph of Figure No. 22 shows the diode resistance  $r$  and reactance  $x$  as a function of frequency in terms of the transit angle  $\theta$  given by  $\beta = j\theta = j\omega T$

(For Figure No. 22, see Page 77.)

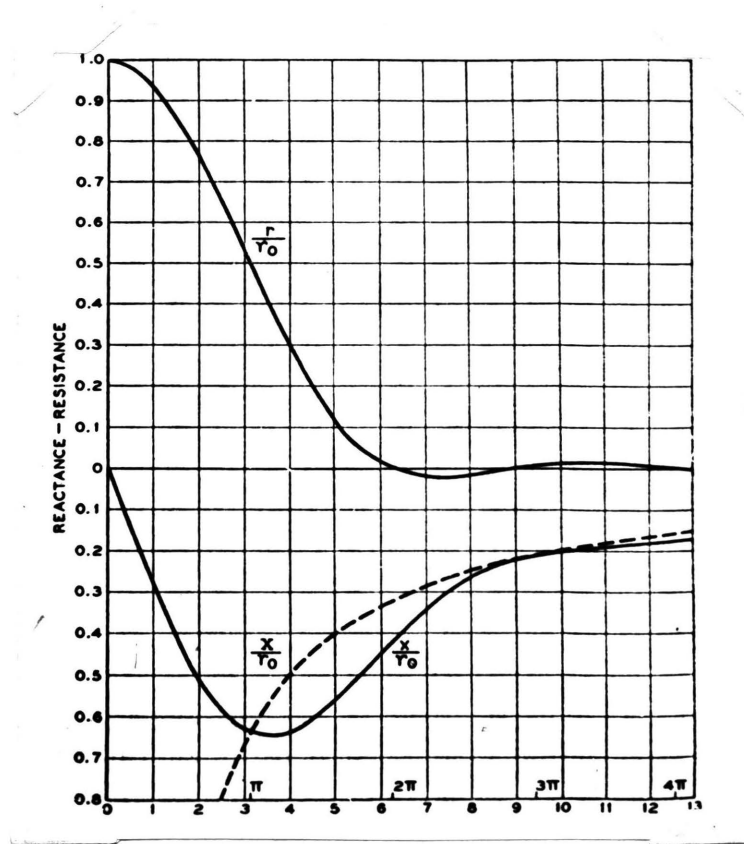


Figure No. 22  
 Plot of Diode Resistance and Reactance  
 Versus Transit Angle

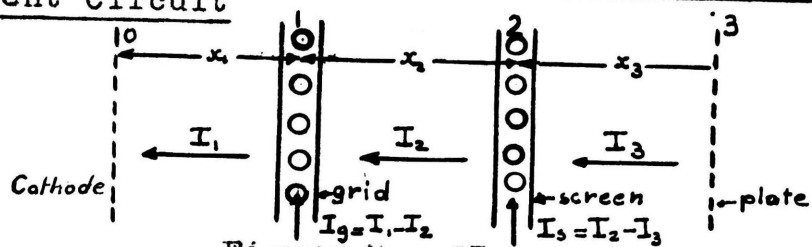
(E) Application to General Tubes and the Representation of Equivalent Circuit

Figure No. 23

## General Diagram of a Multielement Vacuum Tube

In the above figure is shown a planar tetrode. Between the cathode and grid, there exists conditions analogous to those shown in Fig. No. 15, when the proper values for boundary conditions at a and b are selected. Again, between the control grid and screen, another parallel plane diode may be envisioned with different boundary conditions and different values of space charge factor from these existing in the first region. A similar diode is located between the screen and the plate.

The grid wires themselves disturb the simple uniform relations of a parallel plane diode arrangement. We imagine the fictitious planes separating consecutive diodes to be located near the grid wires but not quite including them. However, the final plane for the region (1) in Fig. No. 23 and the initial plane for region (2) are both taken to be so close together that their potentials, both alternating and direct and alternating are the same. This potential is called the effective potential of the grid. Its value is determined in such a way, that currents and potential existing in the consecutive diodes are identical with those which occur if the grid were removed and substituting by a solid metallic plate having on its two surfaces these requisite boundary conditions, that is of conduction current

and electron velocity entering the one surface and leaving the other. The grid wires themselves are at different potential from this effective potential of the grid plane and the grid current is the difference between the total current flowing out of the left hand surface of the fictitious plane and that flowing into its right hand surface, illustrated by the difference between  $I_1$ , and  $I_2$ . In order to provide for the difference in potential between the grid wires and the grid plane, it is obviously necessary to establish the proper impedances and current sources to be connected between the grid wires and the fictitious solid solid plane at the effective potential of the grid.

No attention is to be confined to the main electron stream which originates at plane 0 of Figure No. 4. In region (2) between planes 0 and 1, therefore, the simple diode equations apply directly and the impedance is given by A.

For the region (2) the conditions are not quite so simple, because the electrons do not cross plane (1) and enter region (2) in a smooth continuous stream, but on the contrary they enter in groups or bunches moving at variable velocities having been acted on by the voltage between 0 and 1. However, equation 31 provides the means of calculating the initial conduction current and velocity of electrons injected into region (2) because the electrons enter region (2) with the same velocity with which they leave region (1) and the conduction current entering region (2) must also be the same as



that leaving region (1) whenever the grid at (1) is at a negative potential so that no electrons strike it and are thus prevented from moving into region (2). When this is not the case (that is, when the grid is positive) and therefore the wires collect some of the approaching electrons or when the transit time makes itself felt at higher frequencies.

The convection current per square centimeter injected into region (2) is less than that leaving region (1). The fraction  $\alpha$  may be used to represent this decrease in conduction current so that, if  $q$  is the convection current leaving region (1) then  $\alpha q$  is the convection current entering region (2). The fraction  $1 - \alpha$  is the differential capture fraction of the grid.

Denoting conditions at the right hand boundary of region (1) by the subscript (1), we have then, from equation 145:

$$W_a = 0 ; W_1 = A_1 I_1 ; q_1 = D_1 I_1 + E_1 q_0 ; v_1 = G_1 I_1$$

where the remaining terms in equation 145 has disappeared because of the initial conditions specified for region (1). Moreover, when plane 0 is a thermionic cathode with complete space charge  $E_1$  is zero because  $v_a$  is zero. When there is no space charge  $q_0$  is zero, so that  $E_1 \times q_0$  term above may be dropped in either case. It will be found convenient in later work to express these relations in terms of  $W_1$  in which case

they become

$$I_1 = \frac{W_1}{A_1} ; \quad q_1 = \frac{W_1 D_1}{A_1} ; \quad v_1 = \frac{W_1 G_1}{A_1}$$

Denoting conditions of the right hand end of region (2) by the subscript 2, we have for region (2) from equation 145

$$W_2 - W_1 = A_2 I_2 + B_2 \alpha_1 q_1 + C_2 v_1$$

$$q_2 = D_2 I_2 + E_2 \alpha_1 q_1 + F v_1$$

154

$$v_2 = G_2 I_2 + H_2 \alpha_1 q_1 + K_2 v_1$$

From equation 153 the  $q_1$  and  $v_1$  may be eliminated giving

$$I_2 = \frac{(W_2 - W_1)}{A_2} - \frac{W_1}{A_1 A_2} (B_2 \alpha_1 D_1 + C_2 G_1)$$

$$q_2 = \frac{(W_2 - W_1)}{A_2} + \frac{W_1}{A_1 A_2} \left[ A_2 (D_1 \alpha_1 E_2 + G_1 F_2) - D_2 (D_1 \alpha_1 B_2 + G_1 G_2) \right] \quad 155$$

$$v_2 = \frac{W_2 - W_1}{A_2} G_2 + \frac{W_1}{A_1 A_2} \left[ A_2 (D_1 \alpha_1 H_2 + G_1 K_2) - G_2 (D_1 \alpha_1 B_2 + G_1 C_2) \right]$$

For region 3, a similar procedure is followed and the results may be summarized by writing

$$I_1 = W_1 y_{11}$$

$$I_2 = (W_2 - W_1) y_{22} - W_1 y_{12}$$

156

$$I_3 = (W_3 - W_2) y_{33} - (W_2 - W_1) y_{22} - W_1 y_{13}$$

where the admittances are given by:

$$y_{11} = \frac{1}{A_1} \quad y_{22} = \frac{1}{A_2} \quad y_{33} = \frac{1}{A_3}$$

$$y_{12} = \frac{1}{A_1 A_2} (D_1 \alpha_1 B_2 + G_1 C_2)$$

$$y_{23} = \frac{1}{A_2 A_3} (D_2 \alpha_2 B_3 + G_2 C_3)$$

$$y_{13} = \frac{1}{A_1 A_2 A_3} \left[ A_2 \left\{ \alpha_2 B_3 (D_1 \alpha_1 E_2 + G_1 F_2) + C_3 (D_1 \alpha_1 H_2 + G_1 K_2) \right\} \right. \\ \left. - \left\{ \alpha_2 B_3 D_2 (D_1 \alpha_1 B_2 + G_1 C_2) + C_3 G_2 (D_1 \alpha_1 B_2 + G_1 C_2) \right\} \right] \quad 157$$

The formulation of equation 156 immediately suggests that any region, say the third, can be represented as shown in Figure No. 24. Here  $I_3$  is flowing in and out of the region.

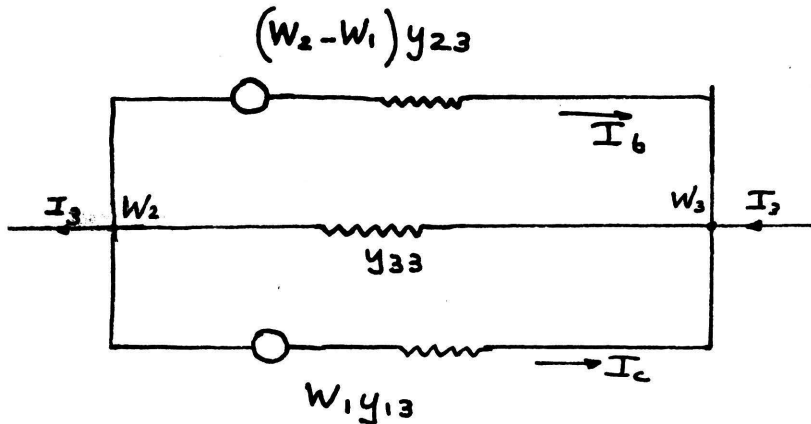


Figure No. 24  
Equivalent Circuit of the Third Region

The admittances  $y_{33}$  has two constant current sources connected across it, one for each preceding region in Figure No. 23. One current source impresses the current  $I_b$  through the admittance  $y_{33}$ , which is equal to  $(W_2 - W_1)y_{33}$ , while the other current source impresses through it a current  $W_1 y_{13}$ . The sum of the currents entering the

node at  $W_3$  thus gives  $I_3$  equals  $I_a$  minus  $I_b$  minus  $I_c$  which is in accord with equation 156 and demonstrates the correctness of the equivalent diagram of No. 24.

The equivalent diagram of the entire electron stream of Figure No. 23 is then shown in Figure No. 25.

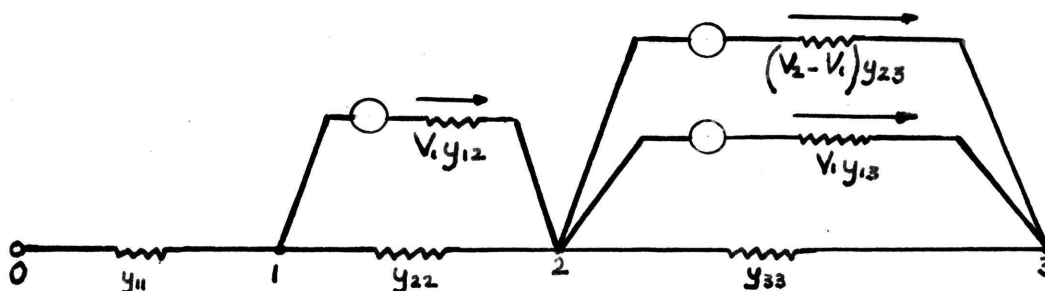


Figure No. 25  
Equivalent Network of Electron Stream of Figure No. 23

The constant current generators play a role analogous to that of constant voltage  $\mu$ -generators with which the older conventional vacuum tube network represents the control of the plate current by means of the grid voltage. In Figure No. 25 the controls on the various region are in terms of impressed currents rather than impressed voltages and the currents in turn are expressed in terms of voltages on the grid wires themselves. As soon as a relation between grid voltage and the voltage on the equivalent grid plane is found, then the admittances  $y_{12}$  and  $y_{13}$ , etc. may be multiplied by

the corresponding factor to give the transadmittance from the control grid to any other electrode. At low frequencies these transadmittances should degenerate into our usual transconductances.

**(E) Evaluation of Admittances**

The admittances  $y_{11}$ ,  $y_{12}$ ,  $y_{22}$ ,  $y_{23}$ , and  $y_{13}$  may be evaluated in terms of the parameters of the electron stream. Let us assume that the tube between cathode and grid operates with complete space charge and the plane 0 represents a thermionic cathode in Figure No. 23. In succeeding regions a very good approximation will be obtained if we assume that the space charge is negligible. Therefore from Table I it is seen that c, d and F are zero in all regions except the first. Moreover in region 1 where we have a complete space charge, H is zero and both B and E are small enough to be neglected because  $v_e$ , the electron velocity at the cathode, is only a small fraction of an equivalent volt. The result is that equation 156 takes the form

$$y_{11} = \frac{1}{A_1} \quad y_{22} = \frac{1}{A_2} \quad y_{33} = \frac{1}{A_3}$$

$$y_{12} = \frac{\alpha_1 D_1 B_2}{A_1 A_2}$$

$$y_{23} = 0$$

$$y_{13} = \frac{\alpha_1 \alpha_2 D_1 E_2 B_3}{A_1 A_3}$$

The coefficient  $y_{22}$  and  $y_{33}$  are the reciprocals of the  $\alpha$  values with no space charge and are shown by equation 151 to be equal to  $j\omega C$  where  $C$  is the free-space capacitance between the solid planes coinciding with the grids in question.

The coefficient  $y_{11}$  is given by equation 151. The transadmittances  $y_{12}$  and  $y_{13}$  in equation 159 are even more interesting. The fact that the factor  $\frac{1}{A_1}$  appears in both, shows that they are proportional to  $\frac{1}{r_0}$  as given by equation 153. Now, the reciprocal of  $r_0$  is  $\frac{3}{2} \frac{I_p}{W_0}$  for region 1 and may be conveniently written as  $g_0$ . In this form we recognize  $(-g_0)$  as the low frequency transconductance of the tube referred to the effective potential of the grid.

Expression for transadmittances are obtained by substituting from Table II into equation 158, giving

$$y_{12} = \alpha_1 \frac{2P_1}{\beta_1^2 A_1} \frac{(2/\beta_1^2)}{(v_1 + v_2)} \left[ v_1 (P_2 - \beta_2 Q_2) - v_2 P_2 \right] \quad 159$$

and

$$y_{13} = \alpha_1 \alpha_2 \frac{(2P_1)}{\beta_1^2 A_1} e^{-\beta_2} \frac{(2/\beta_2^2)}{(u_2 + u_3)} \left[ u_2 (P_3 - \beta_2 Q_3) - u_3 P_3 \right] \quad 160$$

where:  $\alpha_2$  is the grid capture factor of plane 2

P's and Q's are given in Table IV

The most significant thing to notice in equation 160 is that the transit time through region 2 appears only in the form  $e^{-j\theta_2} = e^{-\beta_2}$ . This means that the sole effect of that region upon regions following is to delay transmission to them.

It is useful to keep in mind the limiting values at very low and very high frequencies which are approached by the factors grouped within the several sets of parenthesis in equations 159 and 160. These limiting values are given in Table V.

TABLE V

	$\frac{2P_1}{\beta_1^2 A_1}$	$\frac{2}{\beta_n^2} \left[ \frac{u_{n-1} (P_n - \beta_n Q_n) - u_n P_n}{u_n + u_{n-1}} \right]$
$\beta=0$	$g_0$	$(-1)$
$\beta=\infty$	$-g_0 e^{-\beta_1}$	$-\frac{2}{\beta_n} \left( \frac{u_{n-1} - u_n e^{-\beta_n}}{u_{n-1} + u_n} \right)$

In between these limiting forms, the behavior of  $2P_i/\beta_i^2\alpha_i$  is especially important. Its phase varies widely but its magnitude remains within about 30 per cent of the low frequency magnitude  $g_0$ . Figure 26 shows the phase and magnitude of this factor in terms of the low frequency magnitude  $g_0$ . The low as well as the high frequency asymptotes of the phase are indicated by the dotted lines.

(For Figure No. 26, see Page 88)

The general admittances of equation 159 and 160 can be written as

$$y_{12} = -\alpha_1 g_0 \left[ 1 - j \left( \frac{11}{30} \theta_1 + \frac{1}{3} \theta_2 \frac{\sqrt{W_1} + 2\sqrt{W_2}}{\sqrt{W_1} + \sqrt{W_2}} \right) \right. \quad 161$$

$$- \left( \frac{11}{150} \theta_1^2 + \frac{11}{90} \theta_1 \theta_2 \frac{\sqrt{W_1} + 2\sqrt{W_2}}{\sqrt{W_1} + \sqrt{W_2}} + \frac{1}{2} \theta_2^2 \frac{\sqrt{W_1} + 3\sqrt{W_2}}{\sqrt{W_1} + \sqrt{W_2}} \right.$$

$$\left. \left. + \frac{1}{12} \theta_2^2 \frac{\sqrt{W_{01}} + 3\sqrt{W_{02}}}{\sqrt{W_{01}} + \sqrt{W_{02}}} + \dots \right) \right]$$

$$y_{13} = -\alpha_1 \alpha_2 g_0 \left[ 1 - j \left( \frac{11}{30} \theta_1 + \frac{1}{3} \theta_3 \frac{\sqrt{W_2} + 2\sqrt{W_3}}{\sqrt{W_2} + \sqrt{W_3}} + \theta_2 \right) \right. \quad 162$$

$$- \frac{11}{150} \theta_1^2 + \frac{11}{90} \theta_1 \theta_3 \frac{\sqrt{W_{02}} + 2\sqrt{W_{03}}}{\sqrt{W_{02}} + \sqrt{W_{03}}} + \frac{1}{12} \theta_3^2 \frac{\sqrt{W_{02}} + 3\sqrt{W_{03}}}{\sqrt{W_{02}} + \sqrt{W_{03}}} +$$

$$\left. \left. + \frac{11}{30} \theta_1 \theta_2 + \frac{1}{2} \theta_2^2 + \dots \right) \right]$$



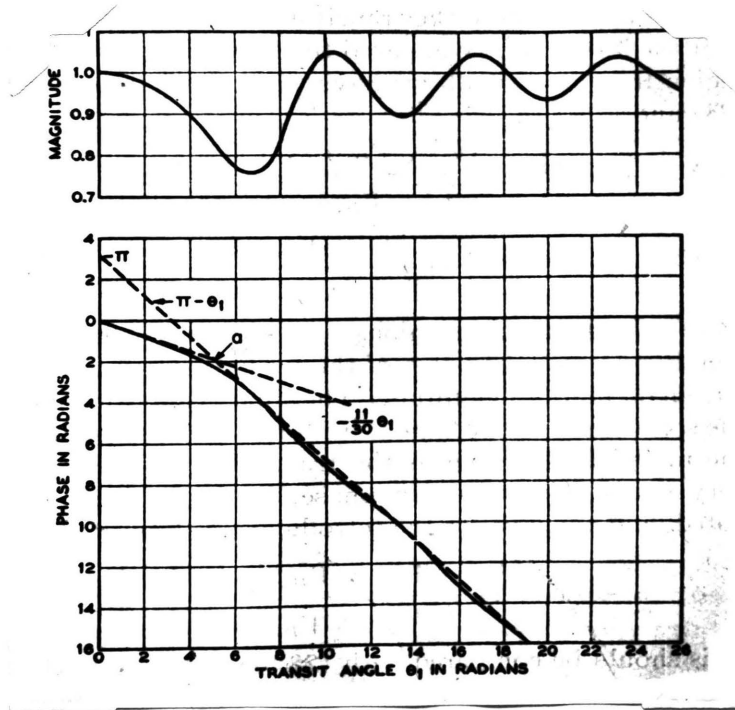


Figure No. 26  
 Plot of Magnitude and Phase of  $\frac{2P_1}{9-\beta_1^2 A_1}$  Versus

For the case where the transit angle in all regions except the last is very large compared to unity, we have the following forms of equations 159 and 160.

$$y_{12} = g_0 \alpha_1 e^{-j\theta_1} \left[ 1 - j \frac{\theta_2}{3} \frac{\sqrt{W_1} + 2\sqrt{W_2}}{\sqrt{W_1} + \sqrt{W_2}} \right] \quad 163$$

$$y_{13} = g_0 \alpha_1 \alpha_2 e^{-j(\theta_1 + \theta_2)} \left[ 1 - j \frac{\theta_3}{3} \frac{\sqrt{W_2} + 2\sqrt{W_3}}{\sqrt{W_2} + \sqrt{W_3}} \right] \quad 164$$

When we remove the restriction that the transit angle in the grid-plate region is small, namely; that the transit angle across all regions, including the input shall be large, then the trans-admittances for the triode and tetrode become from equations 160 and 161:

$$y_{12} = \alpha_1 g_0 e^{-j\theta_1} \frac{\sqrt{W_1} - \sqrt{W_2} e^{-j\theta_2}}{\frac{1}{2} j \theta_2 (\sqrt{W_1} + \sqrt{W_2})} \quad 165$$

$$y_{13} = \alpha_1 \alpha_2 g_0 e^{-j(\theta_1 + \theta_2)} \frac{\sqrt{W_2} - \sqrt{W_3} e^{-j\theta_3}}{\frac{1}{2} j \theta_3 (\sqrt{W_2} + \sqrt{W_3})} \quad 166$$

$\theta$  at any place between two planes can be determined by the formulas \*

$$\theta = \frac{9500x}{\lambda \sqrt{W}} = - \frac{126}{\lambda} \left( \frac{x}{I} \right)^{1/3} \text{ radians} \quad 167$$

Where:  $x$  is the distance between the two planes

$\lambda$  is the free-space wave length in centimeters of an alternating current of angular frequency  $\omega$   
or  $\theta_1, \theta_2$  can be given more specifically by the formulas

$$\theta_1 = \frac{2\omega C_1}{g_0} \quad 168$$

$$\theta_2 = \frac{\omega 2 x_2}{\sqrt{2\eta} (\sqrt{W_1} + \sqrt{W_2})} \quad 169$$

Where  $C_1$  is cold capacitance between anode and equivalent grid plane;  $x_2$  is grid anode distance in centimeters and  $\eta = 10^7 \frac{e}{m}$ .

In general the first grid is negative with respect to cathode, therefore,  $\alpha_1$  is one.  $\alpha_2$  in most practical cases is taken as  $0.7-0.8^4$ .

We therefore know every term in equation 165 and 166 and we can evaluate  $y_{12}$  as well as  $y_{13}, y_{11}$  and  $y_{22}$ .

#### (G) Extension to the Grid Wires of the Vacuum Tubes

The analysis so far would apply to actual tubes if the  $\mu$ 's of the individual grids were infinitely large. This is not the case, the existing relations between the potentials of the equivalent grid planes and those of the grid wires must be considered. Equation 144 furnishes the basis for analysis. The velocities of the electrons entering the differential region around the grid wires must be the same as those which pass through the grid. Also if the conduction current which passes through the grid is  $\alpha q$  then that moving toward the grid is  $(1-\alpha)q$ . For this region between grid plane and grid wires, the transit angle is extremely short and it is accordingly appropriate to use equation 144 as a formula for calculation with the transit angle allowed to approach zero. The result for any grid is therefore an equation of the form of equation 156. Thus for the control grid or first grid, the second equation of 156 gives the required form.

---

(4) Llewellyn and Peterson, op.cit.

$$I_g = (V_g - V_i) y_g - V_i y_{lg}$$

170

Where  $y_g$  is an admittance between the equivalent grid plane and the grid wires and  $y_{lg}$  is a transadmittance between region 1 and the region between the equivalent plane and the grid wires. The important thing is that, as part of the connecting network between the equivalent grid plane and the grid itself, there exists an admittance which comes out to be a simple capacitance if there is no space charge.

The electron stream causes a current to be impressed upon any region which it enters, and when the stream passes the screen, the conduction current splits into a fraction  $\alpha$ , which proceeds into the screen grid plate region and impresses on it a current which conforms to the characteristics of that region. The remaining factor  $(1-\alpha)$  moves towards the grid and impresses on the screen grid a current which conforms to the characteristics of the region between the equivalent plane of the screen grid and the screen grid wires. For the next grid or screen, we will have to follow the form of the third equation of equation 156 giving:

$$I_s = (V_s - V_2) y_s - (V_2 - V_i) y_{2s} - V_i y_{is}$$

171

When the screen is negative, no electrons can hit it and consequently the factor  $\alpha$ , is unity. Under this condition  $y_{lg}$  in equation 170 and  $y_{ls}$  in equation 171 are zero and the control grid is connected to the electron stream through a simple capacitance. From the results of this we can represent Figure No. 23 by

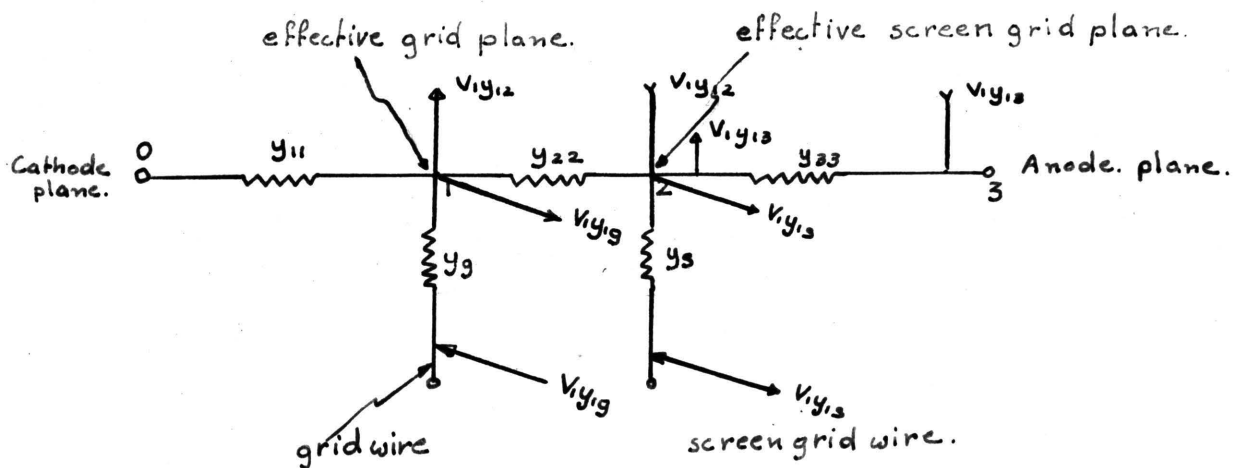


Figure No. 27  
Electron Stream Equivalent Circuit of a Tetrode

For a triode whose grid is negatively biased the circuit becomes as shown in Figure No. 28.

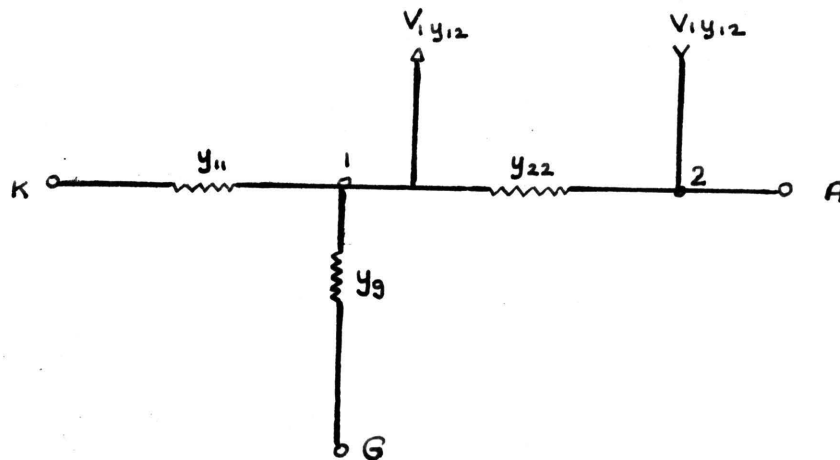


Figure No. 28  
Electron Stream Equivalent Circuit of a Negative Grid Triode

It can be shown that  $\frac{y_3}{y_{22}}$ <sup>4</sup> can be approximated by the general form for the amplification factor  $\mu$ . At this point we will depart from the representation of tube equivalent<sup>circuit</sup> by pure electron stream theory and try to apply them to four pole networks. The preceding method is useful from physical stand point of view. Usually consideration of electron stream theory for the representation<sup>of</sup> equivalent circuit causes some confusion. Moreover, it must be remembered that the important limitation of Llewellyn and Peterson's

---

(4) Llewellyn and Peterson, op.cit.

theory is the assumption of a single valued electron velocity<sup>4</sup> for all electrons crossing any plane parallel to the cathode surface; that is, electrons never pass each other in their transition from cathode to anode. This assumption leads to the d.c. potential and current being related by Child's Law. It neglects important properties of the potential minimum that usually exist in front of a cathode which ejects electrons with a Maxwellian velocity distribution. Only when the distance from cathode to the potential minimum is very small compared to cathode anode spacing in the two parallel planes (diodes) will Llewellyn's or any other solution based on single value electron velocity, gives reasonably correct answers. A very interesting paper by Kleymer<sup>25</sup> gives table for evaluation of the potential minimum distance.

Another very important point which has not been investigated by any author is that of electrons traveling in crossed magnetic and electric fields produced by multi-valued electron velocity and secondary emission. It can be shown that the electrons traveling in crossed electrical and magnetic fields follow cycloidal paths\*. These may have loops or curves or may be straight, depending upon the initial velocity. In this case

---

(4) Llewellyn and Peterson, op,cit.

(25) Kleymer, J.A., Extension of Langmuir's Tables for a Plane Diode with a Maxwellian Velocity Distribution, Phillips Res. Rep., Vol. 1, p. 81, January 1936.

(\* ) See Appendix III.



even the consideration of double stream electron velocity<sup>26</sup> won't be effective. Robertson claims<sup>\*</sup> that consideration of Maxwellian velocity distribution would solve the problem of<sup>the</sup> equivalent circuit. But how to apply Maxwell's velocity distribution theory to the electron stream is another problem. It is evident from the discussion in Appendix III that every crossing of electron streams with each other changes the intensity of field. As Maxwellian velocity distribution assumes that electrons are scattered in x, y and z direction it would be difficult to give or calculate any value for the field intensity between two electrodes. It can readily be seen that the evaluation of the circuit parameters for the electron stream equivalent circuit will become quite complex and even impossible.

Nevertheless, in order to indicate the complexity and lengthiness of the electron stream equivalent circuit parameters even at moderately high frequencies, we will apply them to a negative grid triode.

---

(\*) See Appendix III

(26) Brillouin, Influence of Space Charge on the Bunching of Electron Beams, Phys.Review, vol. 70, p. 187, 1946.

SECTION V  
Four Terminal Networks in General

(A) Definition

Any network of circuit elements, no matter how complex, as long as it has linear circuit elements, two input and two output terminals, and contains no energy sources, can be regarded as a linear, passive four terminal or a passive four pole network. The simplest type of four terminal networks are the T and  $\Pi$ , which are often used in circuit theory work.

If the network contains sources, the network is considered to be an active four terminal network.

At this point a distinction will be pointed out between two types of active networks given below.

(1) Sources in the system are functions of input or output voltages.

(2) Sources in the system are not functions of input or output voltages.

The first type of active network can be handled as a passive one, that is, the circuit parameters can be determined from simple current to voltage ratios as will be explained later.

When the network contains sources which are independent of input or output voltages the analysis becomes quite complex. In such a case the four pole parameters cannot be determined from simple current to voltage ratios. For further information on this type of analysis, see referenc 27.

---

(27) E.N.T. Elektrische Nachrichten Technik, 1929.

(B) Fundamental Relations

For the simplest passive circuit shows in the figure below,

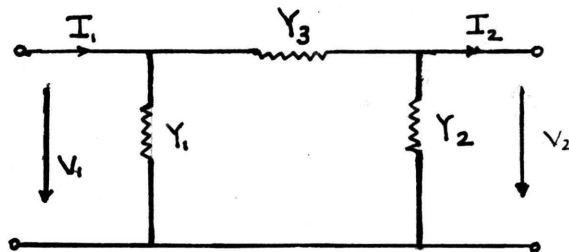


Figure No. 29  
General Four Pole Equivalent Circuit

the nodal equation of the system are as follows:

$$I_1 = V_1 Y_1 + (V_1 - V_2) Y_3 \quad 172(a)$$

$$I_2 = -V_2 Y_2 + (V_1 - V_2) Y_3 \quad 172(b)$$

These equations can be rewritten in the form:

$$I_1 = V_1 (Y_1 + Y_3) - V_2 Y_3 \quad 173$$

$$I_2 = -V_2 (Y_2 + Y_3) + V_1 Y_3 \quad 174$$

Let

$$Y_1 + Y_3 = \beta_{11} \quad Y_3 = -\beta_{12}$$

$$-(Y_2 + Y_3) = \beta_{22}$$

Therefore equations 173 and 174 become:

$$I_1 = \beta_{11} V_1 + \beta_{12} V_2 \quad 175$$

$$I_2 = \beta_{22} V_2 - \beta_{12} V_1 \quad 176$$

The last two equations are the general equations of a four pole network. The admittances  $\beta_{11}$ ,  $\beta_{12}$ ,  $\beta_{22}$  are called four pole admittances. If the circuit was not bilateral the admittances  $\beta_{12}$  in both equations would not be equal. It will be shown later that the vacuum tubes are not bilateral but by adding and subtracting the current source in the general four pole vacuum tube equivalent circuit and rearranging the general four pole equations we can represent the four pole vacuum tube equivalent circuit as a bilateral one.

A circuit satisfying equation 175 and 176 is shown below:

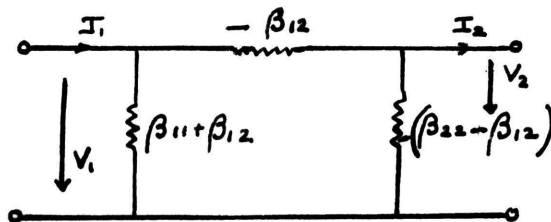


Figure No. 30  
General Four Pole Network

79638

Now let us investigate the physical meaning of the admittances  $\beta_{11}, \beta_{12}, \beta_{22}$ . If the terminals of Figure No. 30 are shorted, it can be seen from equation 175 that

$$I_1 = \beta_{11} V_1$$

and or  $\beta_{11} = \frac{I_1}{V_1}$

$$\beta_{12} = -\frac{I_2}{V_1}$$

Similarly if the input terminals are shorted, the output admittances is given by

$$\beta_{22} = \frac{I_2}{V_2}$$

and the feedback admittance becomes:

$$\beta_{21} = \frac{I_1}{V_2}$$

The admittances  $\beta_{11}, \beta_{22}$  are called the four pole driving point admittances and  $\beta_{12}$  the four pole transfer admittance. If the  $\beta$ 's were not equal in both cases, that is  $\frac{I_2}{V_1}$  were not equal to  $\frac{I_1}{V_2}$ , then we would have  $\beta_{12} \neq \beta_{21}$ ;  $\beta_{12}$  and  $\beta_{21}$  are then called transfer and feedback admittances respectively.

Before applying these admittances to the vacuum tube equivalent circuits, the reasons for the adoption of the four pole network to vacuum tubes will be discussed.

The basic analysis involving the four pole admittances for a particular vacuum tube has to be performed only once. That is, if we have once the plot of impedance versus frequency

and phase versus frequency we can apply them to the vacuum tube in consideration under any operating condition and under any load.

Also by using four pole equivalent circuits we have a much simpler circuit with a minimum number of parameters. It means that we have an equivalent circuit having simple relationships to quantities which can be measured directly. This last point will be clearer when we take up the evaluation of four pole parameters by the use of the results obtained from experimental measurements.

SECTION VI  
Application of Four Pole Terminal  
Admittances to Vacuum Tubes

(A) Application to Vacuum Tubes Operated at Low Frequencies

As already pointed out in the section on four pole terminal networks in general, a system can be handled as passive as long as the internal sources are functions of input or output sources. In Llewellyn's and Peterson's equivalent circuit for vacuum tubes<sup>4</sup>, the current sources established due to the passage of electron stream through various grid elements are functions of input voltages, therefore usual methods for <sup>the</sup> transformation of that circuit to four pole networks are valid.

Let us now represent even the simplest vacuum tube circuits as <sup>a</sup> four terminal networks. Take for example the equivalent circuit of Figure No. 6 and the equation 29. Rewriting equation 29:

$$I_1 = \frac{1}{r_g} V_1 - \frac{\mu_g}{r_g} V_2 \quad 177$$

$$I_2 = -\frac{\mu_p}{r_p} V_1 - \frac{1}{r_p} V_2 \quad 178$$

They are of the general form of four pole network representation:

$$I_1 = \beta_{11} V_1 + \beta_{12} V_2 \quad 179$$

---

(4) Llewellyn and Peterson, op.cit.

$$I_2 = \frac{Y}{r_p} - \frac{1}{r_p} V_2$$

180

where:

$$\begin{aligned} \beta_{11} &= \frac{1}{r_g} \beta_{12} & \beta_{12} &= -\frac{Y_g}{r_g} \\ \beta_{21} &= -\frac{Y}{r_p} & \beta_{22} &= -\frac{1}{r_p} \end{aligned}$$

It is seen that even at low frequencies the general idea of four terminal networks is applicable. It is to be pointed out that the equivalent circuit is not bilateral, so care must be taken in using                      and                      .

#### (B) Extension to Higher Frequencies

Let us extend our point of view on four pole networks to higher frequencies. Let us take the circuit of Figure No. 6 and resolve it into its conduction parts and displacement currents. We then have the same equations for the conduction part as we had in equations 177 and 178. For the displacement current portion we have (See Figure No. 7):

$$I_1' = j\omega(C_{gK} + C_{gP}) V_1 - j\omega C_{gP} V_2 \quad 181$$

$$I_2' = j\omega C_{gP} V_1 - j\omega(C_{PK} + C_{gP}) V_2 \quad 182$$



Where:

$$\beta_{11}' = j\omega(C_{gk} + C_{gp})$$

$$\beta_{12}' = -j\omega C_{gp}$$

$$\beta_{22}' = -j\omega(C_{gk} + C_{gp})$$

Taking  $I_t$  as the thotal current, i.e., displacement plus conduction, we have:

$$I_{1T} = \left[ \frac{1}{r_g} + j\omega(C_{gk} + C_{gp}) \right] V_1 - \left[ \frac{\mu_g}{r_g} + j\omega C_{gp} \right] V_2 \quad 183$$

$$I_{2T} = \left[ -\frac{\mu_g}{r_g} + j\omega C_{gp} \right] V_1 - \left[ \frac{1}{r_p} + j\omega(C_{pk} + C_{gp}) \right] V_2 \quad 184$$

Equations 183 and 184 can be represented by the general four pole equation.

$$I_1 = \beta_{11} V_1 + \beta_{12} V_2$$

$$I_2 = \beta_{21} V_1 + \beta_{22} V_2$$

Where:

$$\beta_{11T} = \frac{1}{r_g} + j\omega(C_{gk} + C_{gp})$$

$$\beta_{12T} = - \left[ \frac{\mu_g}{r_g} + j\omega C_{gp} \right]$$

$$\beta_{21T} = - \frac{\mu_g}{r_p} + j\omega C_{gp}$$

$$\beta_{22T} = - \left[ \frac{1}{r_p} + j\omega(C_{pk} + C_{gp}) \right]$$

From the above expression we see that the vacuum tube is not bilateral, that is  $\beta_{12}$  is not equal to  $\beta_{21}$ , but we can make the equivalent four pole representation bilateral by simple mathematical manipulations. Starting with the familiar four pole equations we have equation 185:

$$I_1 = \beta_{11} V_1 + \beta_{12} V_2$$

$$I_2 = \beta_{21} V_1 + \beta_{22} V_2 \quad 185$$

As already pointed out the various parameters are:

- $\beta_{11}$  is the input admittance with output shorted
- $\beta_{22}$  is the output admittance with the input shorted
- $\beta_{12}$  is the feedback admittance with input shorted
- $\beta_{21}$  is the transfer admittance with output shorted

To make the system bilateral, add and subtract in the second equation of equation 175.

Therefore:

$$I_1 = \beta_{11} V_1 + \beta_{12} V_2$$

$$I_2 = \beta_{21} V_1 + \beta_{22} V_2 + \beta_{12} V_1 - \beta_{12} V_1 \quad 186$$

Rearranging as:

$$I_1 = \beta_{11} V_1 + \beta_{12} V_2$$

$$I_2 = -\beta_{12} V_1 + \beta_{22} V_2 + (\beta_{12} + \beta_{21}) V_1 \quad 187$$

The last two equations of the system can be represented as a bilateral network with a current source at the output (See figure below).

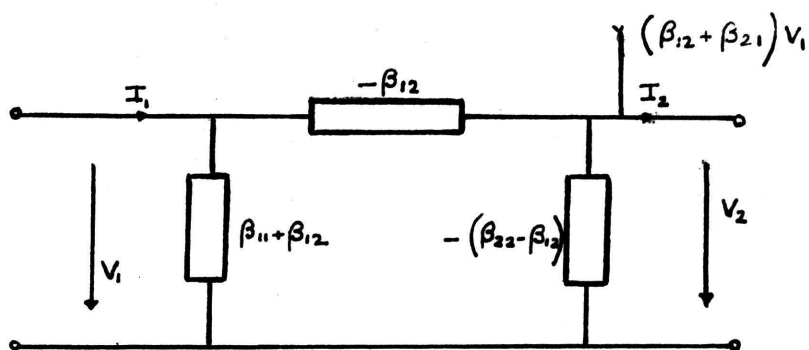


Figure No. 31  
Representation of the Bilateral Equivalent Vacuum Tube Circuit

Let us apply the system to a positive grid triode with various capacitances included. We already pointed out the various four pole parameters.

They are:

$$\beta_{11} = \frac{1}{r_g} + j\omega(C_{gk} + C_{gp})$$

$$\beta_{12} = -\left[\frac{\mu_g}{r_g} + j\omega C_{gp}\right]$$

$$\beta_{21} = \frac{-\mu}{r_p} + j\omega C_{gp}$$

$$\beta_{22} = -\left[\frac{j}{r_p} + j\omega(C_{pk} + C_{gp})\right]$$

Applying to Figure No. 31 we have:

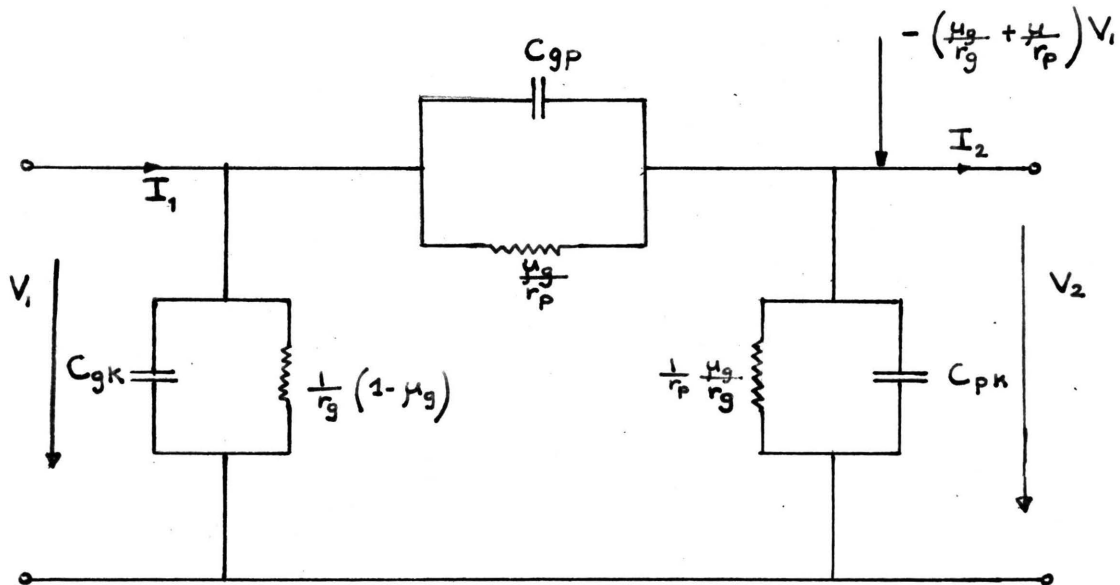


Figure No. 32

#### Equivalent Circuit of Positive Grid Triode At Moderately Low Frequencies

Comparing this representation with the one shown in Figure No. 6, we see that while in Figure No. 6 the source and source free constituents are intermingled, this is not the case in Figure No. 32. On the contrary, a clear demarcation is presented between such constituents. In regard to the general network of Figure No. 31 it may be noted that the network is composed of two parts. One obeys the reciprocal law and is represented by a  $\pi$  network and consequently<sup>is</sup> specified by three elements. The other is merely an impressed current controlled by the input potential  $v_1$ . We therefore have a four terminal network with input and output voltage applied to it.

It should be noted also that the network representation holds for all frequencies. The effect of frequency will be that the admittances in the network change with frequency and in changing they will, for example, reflect effects due to parasitic elements and electron transit time.

It is obvious of course that the equivalent four pole network can be represented also as T-type and also the impressed source can be applied to the input. But the above representation is the most convenient one.

(C) Application of the Electron Stream Equivalent Circuit to Four Pole Networks

We will now apply to Llewelyn's and Peterson's equivalent circuit derived by using electron stream theory the four terminal admittances ideas. With a given set of available terminals the first step in obtaining the network consists of calculating the four pole parameters with respect to these terminals. It will be assumed that the lead effects can be disregarded so that the available terminals actually coincide with anode, grid, and cathode. This set of available terminals brings us to the electron stream.

Now let us take the circuit in Figure No. 28. It will be recalled that we assumed that the grid was negatively biased; so by this assumption we eliminate one current source across  $Y_g$ . It should be emphasized also that the derivations are for planar rather than cylindrical structures. Another restriction on the derivations was that the electron stream was of single valued velocity. The second restriction is not

as serious as there is a tendency toward planar structures in high frequency tube design so as to produce as uniform a stream as possible.

Redrawing the equivalent circuit shown in Figure No. 28 we have for a negative grid triode:

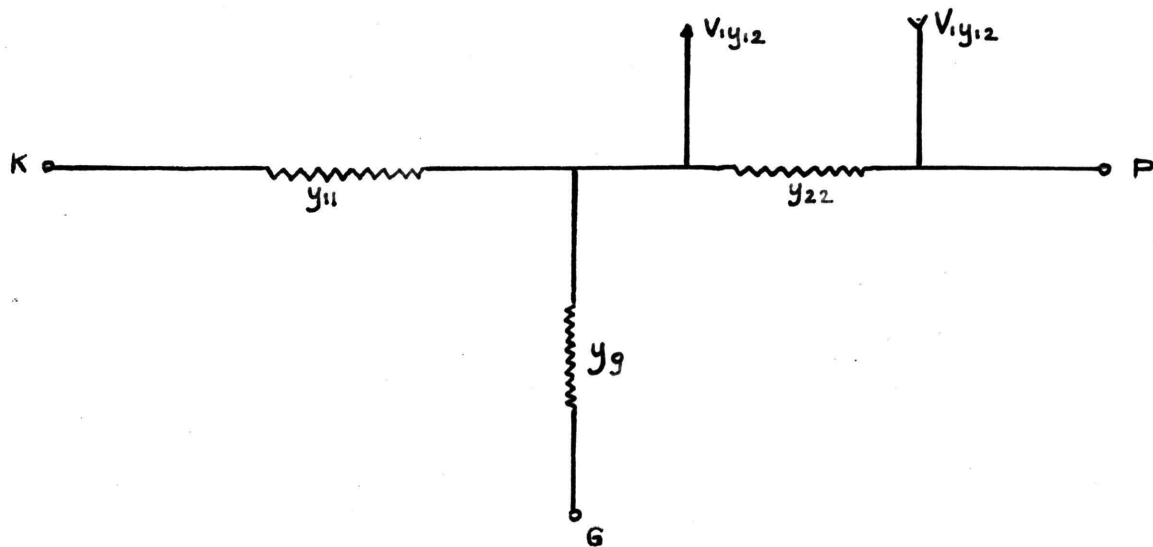


Figure No. 33  
Electron Stream Equivalent Circuit of a Triode With Negative Grid

Redrawing Figure 33 in a somewhat different form we have:

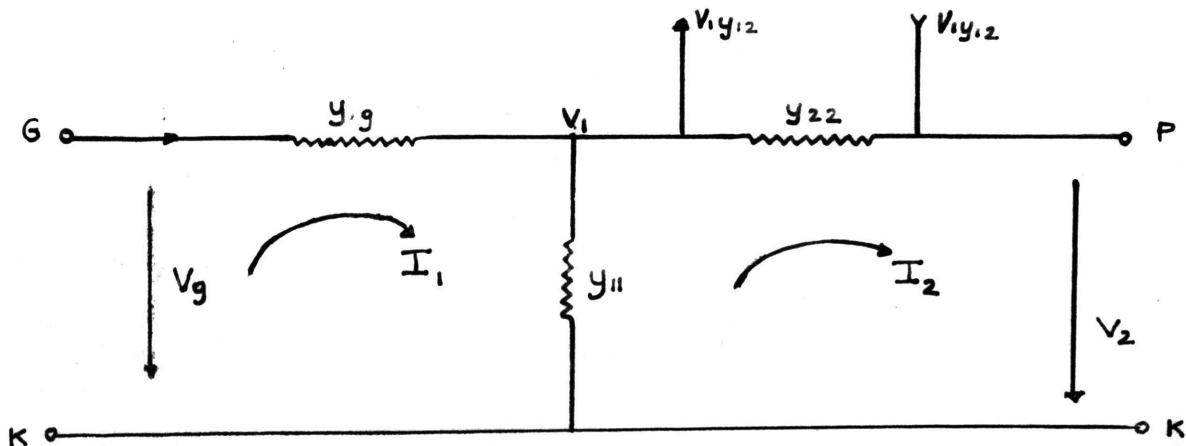


Figure No. 34  
A Different Representation of Figure No. 33

By transforming current source to voltage source, we have:

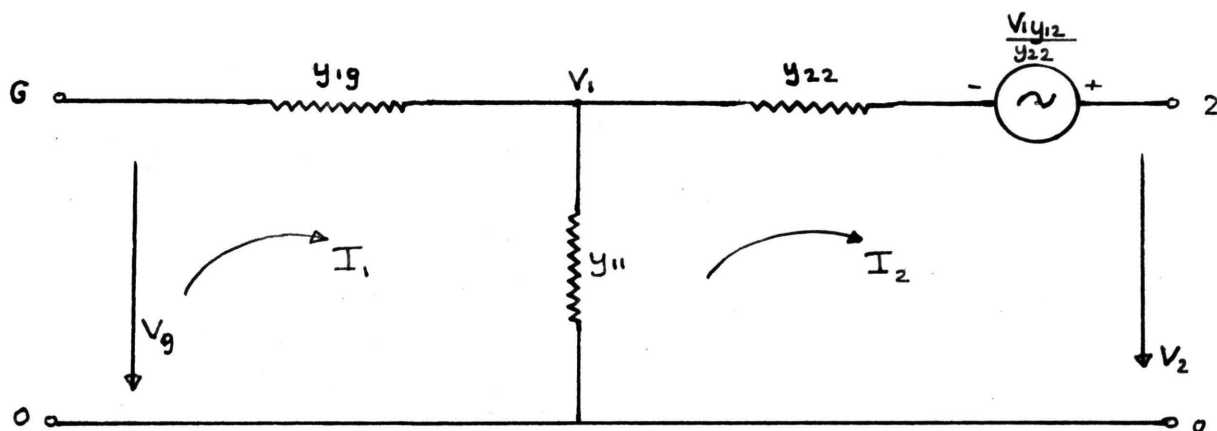


Figure No. 35  
Transformation of Current Source to Voltage Source of Fig.No. 34

Writing the loop equations of the last circuit, we have:

$$V_g = \frac{I_1}{Y_{11}} - \frac{I_2}{Y_{12}} \quad 188$$

$$V_2 = \frac{I_2}{Y_{22}} - \frac{I_1}{Y_{21}} + \frac{V_1 y_{12}}{y_{22}} \quad 189$$

$$I_1 = (V_g - V_1) y_{1g} \quad 190$$

where

$$\frac{1}{Y_{11}} = \frac{1}{y_{1g}} + \frac{1}{y_{11}} \quad \frac{1}{Y_{22}} = \frac{1}{y_{22}} + \frac{1}{y_{21}}$$

$$\frac{1}{Y_{12}} = \frac{1}{y_{11}}$$

$$\frac{1}{Y_{21}} = \frac{1}{y_{11}}$$

Rearranging and substituting 190 and 191 we get

$$V_g = \frac{I_1}{Y_{11}} - \frac{I_2}{Y_{12}} \quad 191$$

$$V_2 = \frac{V_1 y_{12}}{y_{22}} = -\frac{I_1}{Y_{21}} + \frac{I_2}{Y_{22}} \quad 192$$

Using the determinants for the solution we have:

$$I_1 = \frac{1}{D} \begin{vmatrix} V_g & -\frac{1}{Y_{12}} \\ -(V_2 - \frac{V_1 y_{12}}{y_{22}}) & \frac{1}{Y_{22}} \end{vmatrix}$$

where

$$D = \begin{vmatrix} \frac{1}{Y_{11}} & -\frac{1}{Y_2} \\ \frac{1}{Y_{21}} & \frac{1}{Y_{22}} \end{vmatrix}$$

Solution of the above determinants yields

$$I_1 = y_{22} \mu \frac{[V_g y_{11} + V_g y_{22} - V_2 y_{22} + V_g y_{12}]}{y_{11} + y_{22} + y_{12} + \mu y_{22}} \quad 193$$

where

$$\beta_{11} = \frac{y_{22} \mu (y_{11} + y_{22} + y_{12})}{y_{11} + y_{22} + y_{12} + \mu y_{22}} \quad 194$$



$$\beta_{12} = \frac{\overline{y_{22}^2} \mu_1}{y_{11} + y_{22} + y_{12} + \mu_1 y_{22}}$$

195

Likewise:

$$I_2 = \frac{1}{D} \begin{matrix} \frac{1}{y_{11}} & -V_g \\ -\frac{1}{y_{21}} & (V_2 - \frac{V_1 y_{12}}{y_{22}}) \end{matrix}$$

$$I_2 = \frac{\frac{1}{y_{11}} (V_2 - \frac{V_1 y_{12}}{y_{22}}) - \frac{V_g}{y_{21}}}{D}$$

196

We can write  $V_1$  in terms of  $V_2$  and  $I_2$  by using the relationship:

$$V_2 - V_1 - \frac{V_1 y_{12}}{y_{22}} = \frac{I_2}{y_{22}}$$

197

which gives

$$V_1 = \frac{V_2 y_{22} - I_2}{y_{22} + y_{12}}$$

198

Substituting the last equation into equation 196 and solving for  $I_2$  we have

$$I_2 = \frac{V_2 y_{22} (y_{11} + y_g) - V_g (y_g y_{22} + y_g y_{12})}{y_{11} + y_{22} + y_g + y_{12}} \quad 199$$

where

$$\beta_{22} = \frac{y_{22} (y_{11} + y_g)}{y_{11} + y_{22} + y_g + y_{12}} = \frac{y_{22} (y_{11} + \mu y_{22})}{y_{11} + y_{12} + y_{22} + \mu y_{22}} \quad 200$$

and

$$\beta_{21} = \frac{-\mu y_{22} (y_{22} + y_{12})}{y_{11} + y_{22} + y_{12} + y_{22} \mu} \quad 201$$

After the evaluation of the four pole parameters the circuit in Figure No. 31 can be represented as:

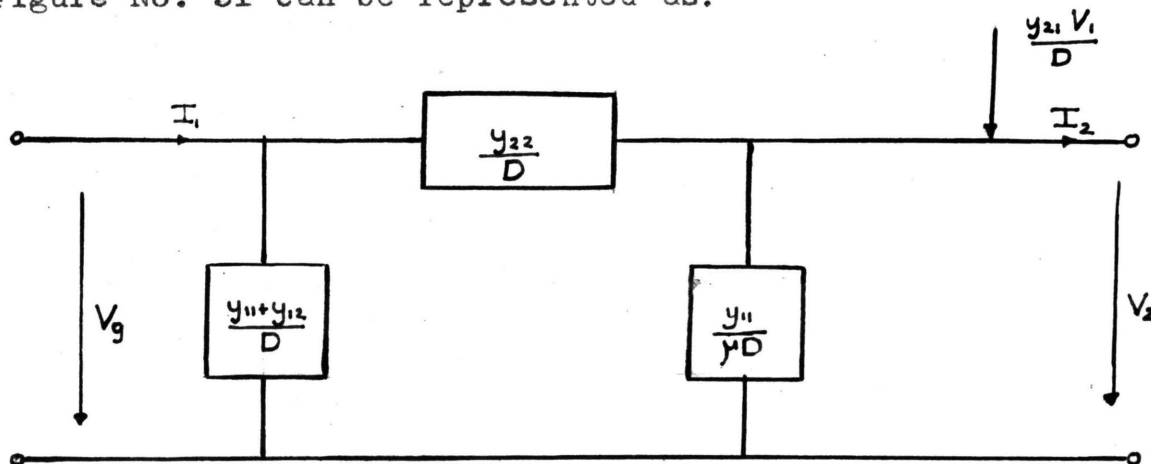


Figure No. 36  
Representation of Electron Stream Equivalent Circuit by Four Pole Terminal Network

Since the above circuit is derived from parameters upon which no restrictions are made, either frequency or space charge, the network itself is not restricted. In passive systems one is accustomed to the use of only the three basic elements of resistance, inductance, and capacitance. For the network now under consideration other quantities also need to be included. However under normal operation there is usually complete space charge in the grid plate region. Under such circumstances the admittance  $y_{22}$  is a real simple capacitance and the amplification factor  $\mu$  is a real number. The admittances  $y_{11}, y_{21}$  on the other hand do not allow simple circuit interpretation to be made, except in the range of moderately low frequencies when electron transit time is taken into account only to first order of approximation. It is believed that, in general, these admittances should be considered complete by themselves as new admittance elements.<sup>4</sup>

#### (D) Triode Networks at Moderately High Frequencies<sup>4</sup>

The entire cumbersome derivation starting from the basic principals of electronics and ending up with four pole networks would be limited to vacuum tubes in which appreciable interaction between input and output terminals is present. From a practical stand point this means that their usefulness would be mainly found in connection with triodes. Let us analyse a triode at moderately high frequencies. The operating conditions are assumed to be the usual ones with complete space charge in the cathode grid region and negligible space

(4) Llewellyn and Peterson, op, cit.

charge in the grid-plate region. Also it will be assumed that the grid is <sup>at</sup> a negative d.c. potential with respect to the cathode.

By taking Llewellyn's derivations for impedances and making various assumptions, Peterson comes out with the value given below. As a detailed computation is lengthy only the final results will be given.

The circuit will be represented by:

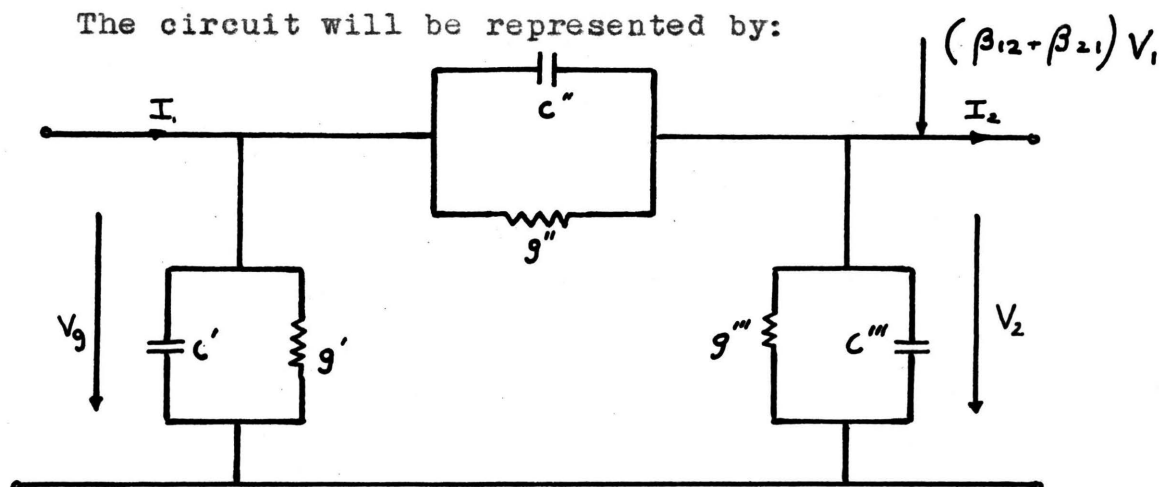


Figure No. 37

Representation of Electron Stream Equivalent Circuit by Four Terminal Networks at Moderately High Frequencies

The results are:

$$\beta_{11} = \frac{1}{5} \frac{(\omega C_1)^2}{g_0} \frac{F}{\left[1 + \frac{1}{\mu} \left(1 + \frac{4}{3} \frac{x_2}{x_1} f\right)\right]^2} + j\omega \frac{\left(\frac{4}{3} C_1 f + C_2\right)}{1 + \frac{1}{\mu} \left(1 + \frac{4}{3} \frac{x_2}{x_1} f\right)} \quad 202$$

$$\beta_{12} = - \left[ \frac{-(\omega C_1)^2}{g_0} \frac{1}{5\mu} \frac{F}{\left[1 + \frac{1}{\mu} \left(1 + \frac{4}{3} \frac{x_2}{x_1} f\right)\right]^2} + j\omega \frac{C_2}{1 + \mu \left(1 + \frac{4}{3} \frac{x_2}{x_1} f\right)} \right] \quad 203$$

$$\beta_{22} = - \left[ \frac{g_0}{\mu} \frac{1}{1 + \frac{1}{\mu} \left(1 + \frac{4}{3} \frac{x_2}{x_1} f\right)} + j\omega \frac{C_2 + \frac{6}{10\mu} C_1}{1 + \frac{1}{\mu} \left(1 + \frac{4}{3} \frac{x_2}{x_1} f\right)} \right] \quad 204$$

$$\beta_{12} + \beta_{21} = - \frac{g_0}{1 + \frac{1}{\mu} \left(1 + \frac{4}{3} \frac{x_2}{x_1} f\right)} \left[ 1 - j \frac{11}{30} \theta_1 \left(1 - \frac{3}{11\mu} \frac{\frac{x_2}{x_1} F}{1 + \frac{1}{\mu} \left(1 + \frac{4}{3} \frac{x_2}{x_1} f\right)}\right) - j \frac{1}{3} \theta_2 \right] \quad 205$$

Where:

$$\theta_1 = \frac{2\omega C_1}{g_0}$$

$$\theta_2 = \frac{\omega^2 x_2}{\sqrt{2\eta}(\sqrt{W_1} + \sqrt{W_2})}$$

$$\eta = 10^7 \frac{e}{m} = 1.76 \times 10^5$$

$W_1$  is equivalent to d-c grid potential

$W_2$  is anode d-c potential

$$F = 1 + \frac{22}{9} \frac{\theta_2}{\theta_1} \frac{\sqrt{W_1} + 2\sqrt{W_2}}{\sqrt{W_1} + \sqrt{W_2}} + \frac{5}{3} \left(\frac{\theta_2}{\theta_1}\right)^2 \frac{\sqrt{W_1} + 3\sqrt{W_2}}{\sqrt{W_1} + \sqrt{W_2}}$$

$$f = 1 + \frac{1}{2} \frac{\theta_2}{\theta_1} \frac{\sqrt{W_1} + 2\sqrt{W_2}}{\sqrt{W_1} + \sqrt{W_2}}$$

$$k = \frac{\sqrt{W_1} + 2\sqrt{W_2}}{\sqrt{W_1} + \sqrt{W_2}}$$

Representing the various circuit elements as shown in Figure No. 37, we have:

$$g' = -\frac{(\omega C_1)^2}{5g_0} \frac{F}{\left[1 + \frac{1}{\mu} \left(1 + \frac{4}{3} \frac{x_2}{x_1} f\right)\right]^2}$$

$$C' = \frac{4}{3} C_1 \frac{f}{1 + \frac{1}{\mu} \left(1 + \frac{4}{3} \frac{x_2}{x_1} f\right)}$$

$$g'' = -\frac{(\omega C_1)^2}{5g_0} \frac{1}{\mu} \frac{F}{\left[1 + \frac{1}{\mu} \left(1 + \frac{4}{3} \frac{x_2}{x_1} f\right)\right]^2}$$

$$C'' = C_2 \frac{1}{1 + \frac{1}{\mu} \left(1 + \frac{4}{3} \frac{x_2}{x_1} f\right)}$$

$$g''' = \frac{g_0}{\mu} \frac{1}{1 + \frac{1}{\mu} \left(1 + \frac{4}{3} \frac{x_2}{x_1} f\right)}$$

$$C''' = \frac{C_2 + \frac{6}{10\mu} C_1}{1 + \frac{1}{\mu} \left(1 + \frac{4}{3} \frac{x_2}{x_1} f\right)}$$

As may be seen the network comes out to be of resistance capacitance type. It may be noted that, in some branches, negative conductance appears. However, as seen from the external tube terminals, they are overcome by corresponding positive elements.

The reader will admit that even at moderately high frequencies the circuit parameters become complex. It must be remembered that these derivations are based on the following assumptions.

- (1) Planar structure of tubes
- (2) Full space charge between cathode grid and negligible space charge between grid plate
- (3) Very small distance between virtual cathode and cathode structure
- (4) No secondary emission from any structure
- (5) Single electron velocity
- (6) No magnetic field effect on moving electrons
- (7) Zero velocity of electrons emitted from cathode
- (8) No self inductance of the tube elements within the tube

As <sup>it</sup> is evident the electron stream theory doesn't apply to outside effects and this would be another drawback of the general consideration. Under these circumstances one would look for an easier and more accurate method for the evaluation of circuit parameters and ~~and~~ <sup>therefore</sup> in the next part we are going to introduce methods for the measurement of four pole parameters.

## SECTION VII

28

## Admittance Measurement of Vacuum Tubes

(A) Comparison of Llewellyn's Impedance Formulas With Experimental Results

Before going into the explanation of admittance measurements it will be helpful to repeat the most effective<sup>ive</sup> restrictions put in Llewellyn's and Peterson's work concerning the electron stream analysis in the vacuum tube.

If only a relatively few electrons are available at the cathode, the potential distribution between electrodes will be approximately equal to the space charge free distribution indicated by curve a.

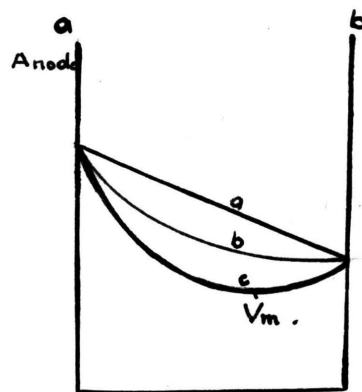


Figure No. 38  
Potential Distributions in a Diode

If an ample supply of electrons is provided by the cathode with zero initial velocity, then the space charge is complete in accordance with Child's law, and the potential distribution follows curve b. If, on the other hand, the cathode is capable of supplying an ample supply of electrons, the electrons being emitted with a Maxwellian initial velocity distribution, the potential distribution will be represented by curve c. The cases shown by curves a and b can be treated by Llewellyn analysis.

Let us consider curve c in greater detail. The fact that electrons are emitted with a Maxwellian velocity as in Child's law or complete space charge case, means that more electrons are introduced in the space between the electrodes than can flow in the anode in accordance with Child's law.

The surplus electrons depress the potential near to the cathode at a value below that of the cathode as  $v_m$  in the Figure No. 38. Electrons which have sufficient energy to cross this barrier return to the cathode.

It is observed that in the space between potential minimum and the anode the electrons travel with an unidirectional velocity but not with a single velocity. With close spacings and higher frequencies the distance between the cathode and the potential minimum may be an appreciable part of the total cathode anode spacing, so that electrons



returning to the cathode may absorb a substantial amount of power from the high frequency field.

With wide spacings and at low frequencies the admittances obtained with distribution of the c type may be approximated by the results obtained by analysis of distribution of the b-type. But with tubes of close spacings the theoretical analysis of Llewellyn doesn't hold any more as it was proven in the Bell Laboratories for the 1553 triode<sup>28</sup>.

---

(28) Robertson, op. cit.

(B) Measurements for Diodes

In the measurement of the diode admittances, as in every kind of vacuum tube measurement, the problem is to learn how to relate admittances measured with a standing wave detector located in the wave guide supply line to the equivalent two terminal admittance located at the cathode anode space of the diode itself. In other words we have to know the transformation ratio between the admittances of the cathode anode space of the diode and the admittance of the wave guide measured at the terminals of the wave guide.

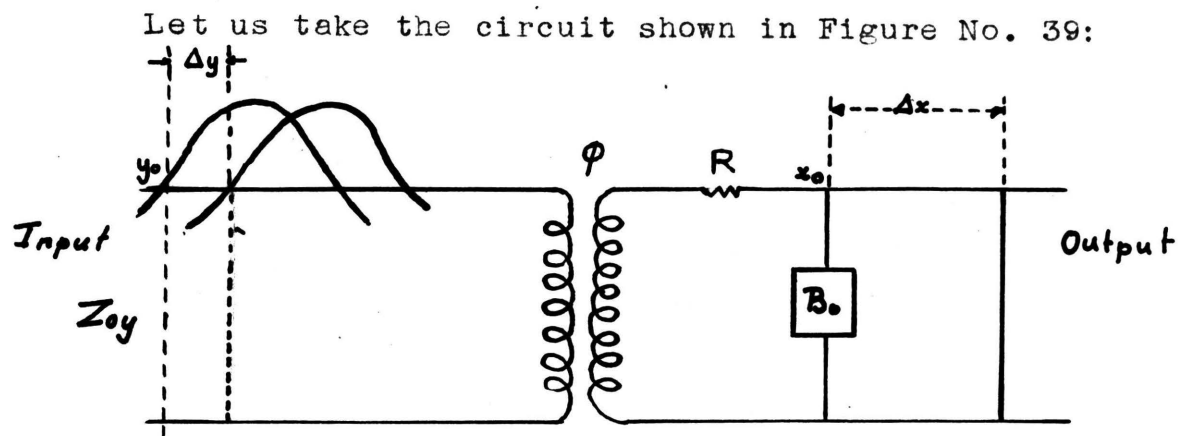


Figure No. 39

## Equivalent Circuit of a Diode Measuring Equipment

The circuit may either be a transmission line or a wave guide having a characteristic impedance  $Z_{0y}$ , connected through an ideal transformer to an output line having a characteristic impedance  $Z_{0x}$ . The output line having a

connection to the transformer is at point  $X_0$ . The diode whose admittance is to be measured is placed between  $X_0$  points. First let us short the output line at a point  $X_0$ . If we inject power into the input line then a standing wave will be established on the line which will have a minimum point say at  $Y_0$ . If we move the short circuit a distance  $\Delta x$  on the right hand transmission line, then the standing wave on the left hand transmission line will move a certain distance  $\Delta y$ . We can assume the part to the right of the point  $X_0$  as a total impedance connected at point  $X_0$ . Then the shift of the minimum point on the transmission line at the input will be a function of the connected load at <sup>the</sup>  $X_0$  points. We can express the relationships as:

$$\frac{1}{Z_{0y}} \cot \frac{2\pi\Delta y}{\lambda y} = \frac{\phi}{Z_{0x}} \cot \frac{2\pi\Delta x}{\lambda x} - \phi B_0 \quad 206$$

It is not necessary that the two lines be identical. For example one might be a coaxial and the other <sup>a</sup> wave guide.

$\phi$  is the transformation ratio of the ideal transformer and  $B_0$  is the effective leakage susceptance of the tube and transformer referred to the terminals at  $X_0$ .

If we plot  $\frac{2\pi\Delta y}{\lambda y}$  as a function of  $\frac{2\pi\Delta x}{\lambda x}$  on cot-cot coordinate paper, a straight line is obtained whose slope  $m$  is:

$$m = \phi \frac{Z_{0y}}{Z_{0x}} \quad 207$$

and whose ordinate intercept  $Z$  is:

$$Z = -\rho B_0 Z_0 y$$

208

Suppose now the transmission line to the right hand is removed and the diode gap is connected at the transformer terminals  $X_0$ . Let  $Y_{wg}$  denote the impedance seen at the terminals  $Y_0$  referred to the point  $X_0$  and  $Y_n$  the unknown diode admittance.  $Y_n$  is then given by the following relation:

$$Y_x = \frac{1}{Z_{ox} m} [Y_{wg} + jZ]$$

209

After the determination of  $Y_0$  point, it remains to measure the slope  $m$  and the intercept  $Z$  on the cot-cot curve. Of course the characteristic impedance is already known as we used it in the drawing of the cot-cot curve.

If no losses were associated with the transformer or the parts of the diode external to the actual cathode-anode region, such as the metal vacuum envelop, the above measurements would give complete information regarding the tube. On the other hand there are certain losses associated with the transformer and tube. The equivalent series resistance is given by the relation:

$$R = \frac{\rho Z_0 y}{\rho}$$

210

which can be written as:

$$R = \frac{Z_{0ym}}{\rho}$$

211

where  $\rho$  is the standing wave ratio and  $m$  the slope of cot-cot curve.

### (C) Results of the Measurements

Electron stream measurements were made by S. D. Robertson at a frequency of 4060 megacycles with a number of diodes over a wide range of anode and heater voltages. In making these measurements the radio frequency power was kept at a relatively low level (0.2 milliwatt) in order that the measured admittances would be independent of the radio frequency voltage. In computing the admittance of the electron stream, it was necessary to allow for the circuit and tube losses previously discussed. The equivalent series resistance  $R$  of the diode circuit was determined by biasing the tube negatively to the point where a further increase in bias failed to produce a perceptible change in the wave guide standing wave ratio. Under such condition the electrons experienced a large retarding field at the cathode and did not emerge an appreciable distance into the cathode-anode region. Any resistance measured at this time was due to the series loss and was not produced electronically.

We shall choose a diode with a very high  $g_0$  and compare the experimental results with Llewellyn's derivations. The curves for  $\frac{126 \times \sqrt[3]{J_0}}{J_0^{7/3}}$  versus  $\frac{\text{high frequency admittance}}{\text{low frequency conduction}}$  are <sup>given</sup> in Figure No. 40 (For Figure No. 40, see page 125).

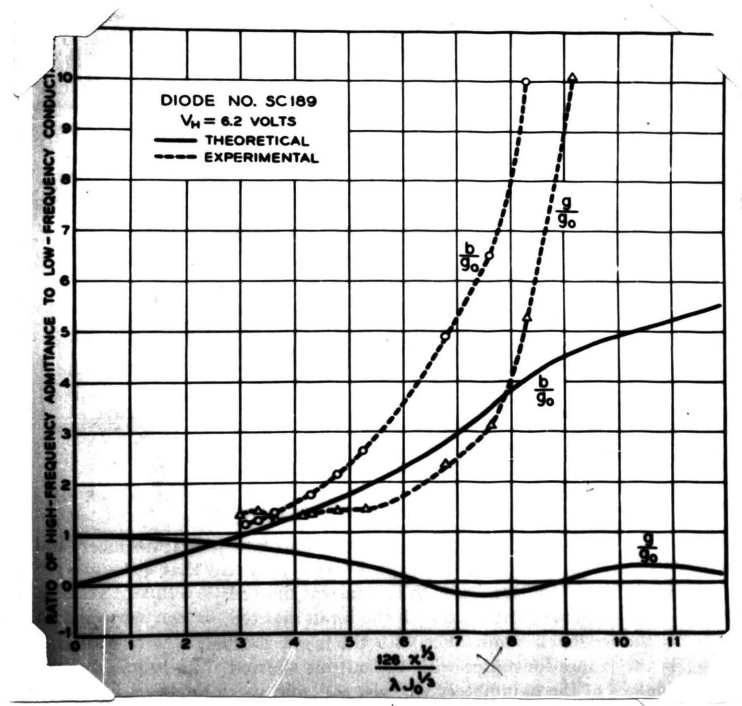


Figure No. 40  
 Plot of Experimental and Theoretical  
 Values of  $\frac{b}{g_0}$  Versus  
 $\frac{a}{g_0}$   
 High Frequency Admittance  
 Low Frequency Conductance

(dashed lines give experimental results)  
 (solid lines give theoretical results)

The curves give a very good comparison between single valued electron velocity and Maxwellian velocity distribution as found in experimental results. Several diodes have been measure and the results can be combined as follows:<sup>4</sup>

The microwave conductance of a diode is greater than the low frequency value. The ratio  $\frac{g}{g_0}$  appears to increase as the spacing decreases. This increase will probably continue until the portion of the potential minimum approaches the anode plane. The susceptance decreases with the increasing current and appears to level off at high current densities. For a given current density, the ratio  $\frac{g}{g_0}$  does not appear to vary appreciably as the cathode temperature is changed.

An attempt has been made by L. C. Peterson to study the available diodes at 10,000 megacycles. It is found that the value of R was so high at this frequency and that variations in the tube conductance were so small in comparison with R that accurate results could not be obtained.

#### (D) Four Pole Admittances of a Triode

Recalling the equivalent four pole representation of a triode we have:

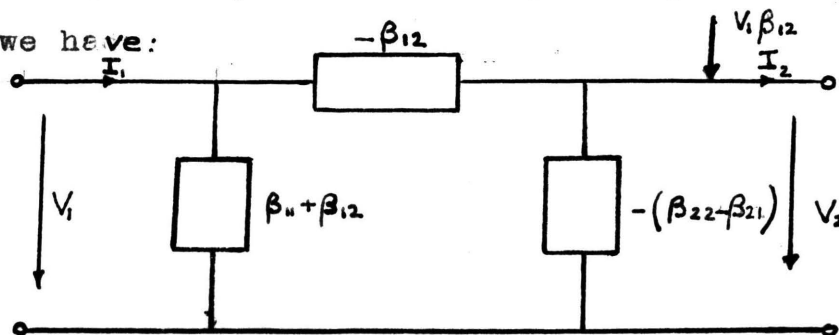


Figure No. 41

Four Pole Representation of a Negative Grid Triode

(4) Llewellyn and Peterson, op.cit.

Where:  $+\beta_{11}$  is the input admittance with output shorted  
 $+\beta_{22}$  is the output admittance with input shorted  
 $+\beta_{12}$  is the feedback admittance with input shorted  
 $+\beta_{21}$  is the transadmittance with output shorted

In order to measure the four pole parameters, the triode is mounted in a coaxial circuit of the type shown in Figure No. 42.

(For Figure No. 42, see page 128)

The grid-anode output circuit of the tube is connected directly with the coaxial output line. The input circuit requires a more careful design. Due to the size of the base of the tube it is necessary to taper the input coaxial as shown. In the early stages of this work, difficulty was experienced with higher order modes in the large diameter section of the input coaxial. It is believed that these modes were generated by the action of the parallel wire grid which lacked the radial symmetry required in coaxial transmission. This difficulty was overcome by constricting the outer diameter of the coaxial line in the immediate vicinity of the grid tube, thus inhibiting generation of the higher order mode.

Before measurements can be made, it is necessary to calibrate the input and output and output circuit. As one might expect, the value of the cot-cot slope of the output circuit must be close to unity (See section on diode measurement). Experimentally it is found to be 0.9 for the coaxial circuit of the type shown in Figure No. 42. In the



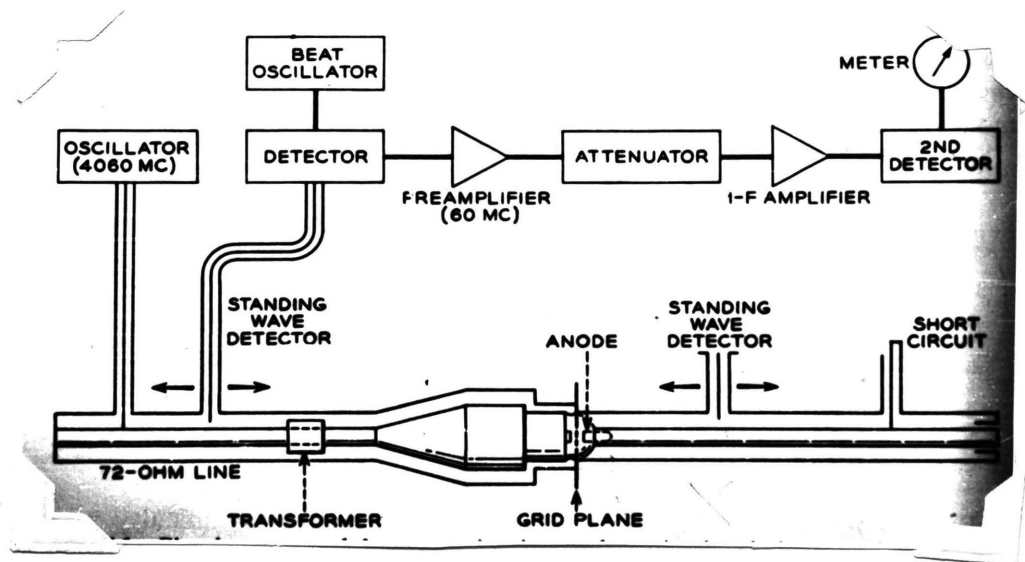


Figure No. 42  
 Schematic Diagram of a Coaxial Circuit and Its Associated  
 Instruments for the Measurements of the Triode Admittances

circuit the slope might be greater than one , therefore it is necessary to introduce a transformer in the coaxial input circuit to permit tuning.

In order to measure  $\beta_{11}$  , the output coaxial line is short circuited at a point an integral number of half wave lengths from the grid anode terminal of the tube. The admittance measured in the input line could then be used in computing  $\beta_{11}$  . To measure  $\beta_{22}$  , the procedure is reversed, that is, the input line is shorted and the corresponding admittance is measured in the output line.

(E) Procedure in the Measurement of  $\beta_{12}$  and  $\beta_{21}$

The transfer admittances are measured by the circuit shown in Figure No. 43. This method is based upon the principal of homodyne detection. Hybrid coils, which are the basic tool in these measurements, are fully explained in the appendix.

(For Figure No. 43, see Page 129)

Radio frequency power from the oscillator is applied to the H-plane branch of a hybrid <sup>29</sup> junction where it divides and emerges in equal portions from the two lateral branches. The portion of the signal applied to the calibrated variable phase shifter at the top of the figure becomes the homodyne carrier. The remaining portion is applied to a balanced crystal modulator <sup>30</sup> through a second variable phase shifter which need not be calibrated. This variable phase shifter

is used in order that the phase of any modulated power  
 (29) Tyrell, W.A. Hybrid Circuits for Microwaves, Proc.IRE, Vol. 35, No. 11, pp.1294-1306, Nov. 1947.  
 (30) Hund, Frequency Modulation, p.159.

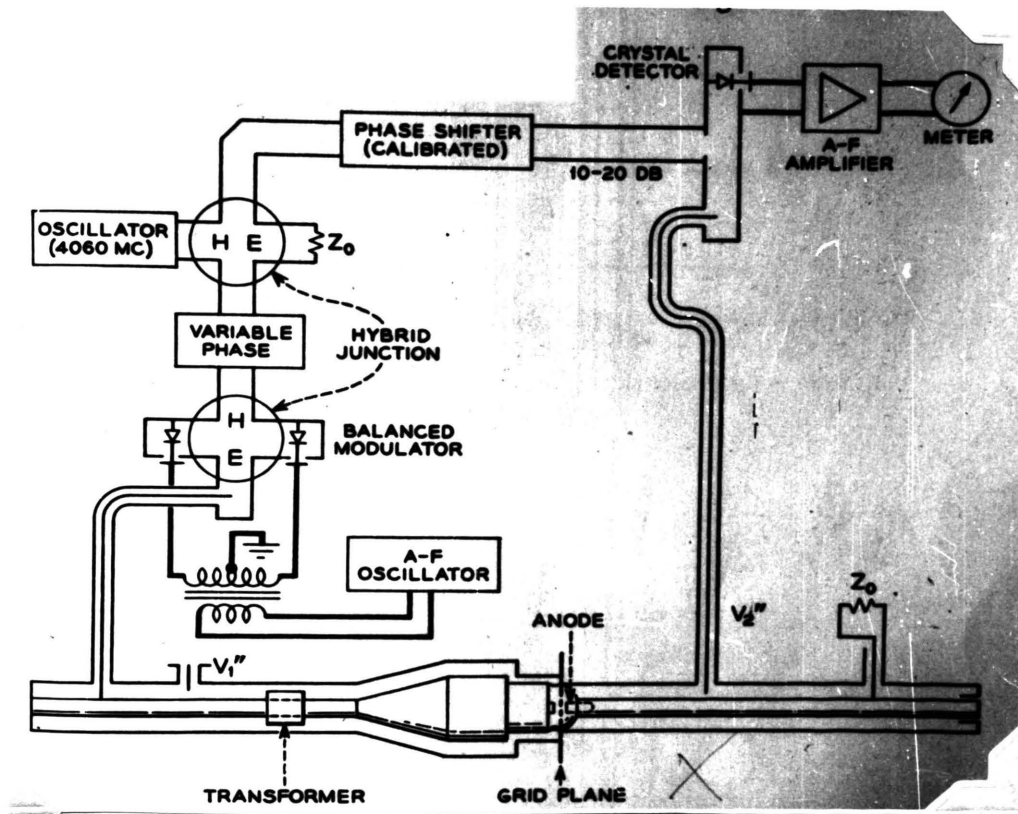


Figure No. 43  
Schematic Diagram of a System for Phase Angle and  
Transfer Impedance Measurements

reflected due to an imperfect balance in the modulator could be shifted in quadrature with the homodyne carrier and therefore not produce an audible signal in the detector.

The portion of the power which enters the modulator is modulated by a signal derived from an audio frequency oscillator. The suppressed carrier, double side band signal, leaves the modulator and is applied to the input of device for sampling the signals.

The homodyne carrier emerging from the calibrated phase shifter is attenuated to a level of about one milliwatt and is applied to the crystal detector. The output of the detector is connected to an audio frequency amplifier terminated by a pair of headphones or an output meter. An attenuator may be placed between the amplifier and the detector as an aid in measuring the magnitude of the transfer impedance

The procedure for adjusting the apparatus and measuring phase is as follows:

With both sampling probes disconnected from the detector the variable phase shifter between the oscillator and modulator is adjusted until the output of the detector is zero. This balances out the effect of any signal reflected by the modulator. The input probe is then connected to the detector and the calibrated phase shifter is adjusted until the signal disappears in the audio output. When this occurs, the homodyne carrier is in quadrature with the signal side-

bands, and the resultant signal applied to the detector is equivalent to a phase modulated wave having a low modulation index, and consequently is not demodulated by a detector of the type used here.

The input probe is then disconnected from the detector and is replaced by the output probe. The phase shifter is again adjusted for a null in the audio output. The difference in phase between the two adjustments of the phase shifter is equal to the phase shift between the input and output of the device.

In measuring transfer impedances it is desirable to know the ratio of the magnitudes of the output and input voltage as well as their phase differences. The equipment described can be used for measuring amplitudes of  $V_1''$  and  $V_2''$  by adjusting the phase shifter for a maximum signal in the audio output in each case. Maximum signal levels can then be compared with the aid of an audio frequency attenuator and output meter connected as shown in Figure No. 43.

The measuring procedure described above has been tested experimentally at 4000 m.c. with very satisfactory results. It is possible to measure phase differences with an accuracy of better than half a degree with this type of equipment.

From the measurements discussed in the preceding section the four pole parameters can be evaluated by using equations 202, 203, 204, and 205. Figure No. 44 gives the equivalent circuit of a triode and associated measuring equipment.

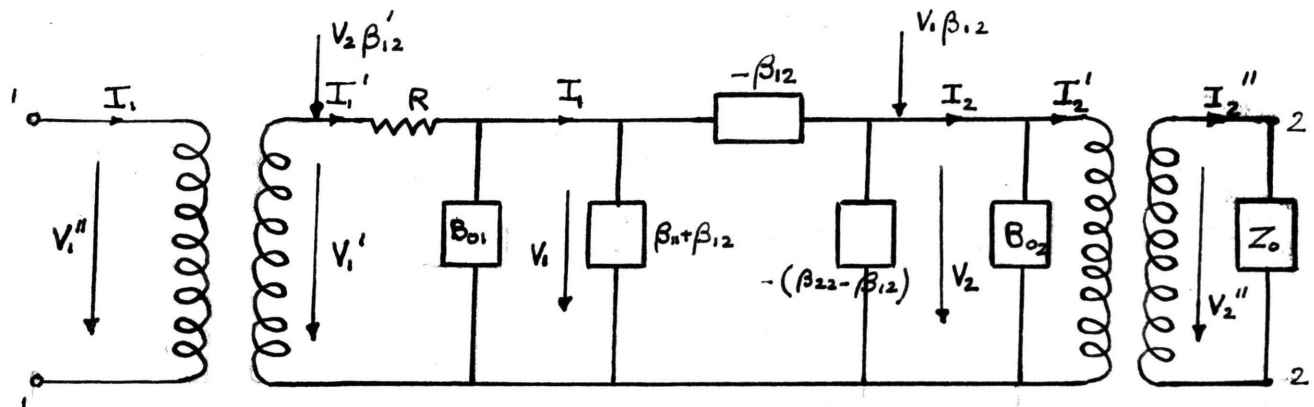


Figure No. 44  
Equivalent Circuit of a Triode and its Associated  
Measuring Equipment

The various symbols used in Figure No. 44 and obtained from measurement discussed in preceding section are:

$Y_1$  is the admittance measured at 1-1 with 2-2 shorted.

$Y_2$  is the admittance measured at 2-2 with 1-1 shorted  
 $\frac{V_1''}{V_2''}$  is  $\gamma_{21}$  measured without output line terminated in  $Z_0$ .

In calibrating the circuit we will use the following parameters which were fully explained in the section for diode measurements.

$Z_1$  is the ordinate intercept of input cot-cot curve

$Z_2$  is the ordinate intercept of output cot-cot curve

$m_1$  is the slope of input cot-cot curve

$m_2$  is the slope of output cot-cot curve

$$B_{o1} = -\frac{Z_1}{Z_o'm_1}$$

$$B_{o2} = -\frac{Z_2}{Z_o'm_2}$$

$Z_o$  is the characteristic impedance of input and output coaxial;  $R$  which represents the losses in the circuit is measured by shorting the output line and measuring the admittance of the input line with a large negative bias on the tube. Therefore:

$$R = Z_o'm_1 R_e(Y_1)$$

212

Where the  $Z_o'$  represents the characteristic impedance of the coaxial line used in calibrating the input circuit and corresponds to  $Z_{ox}$  in equation 206.

Fortunately the series resistance in the output circuit came out to be very small in the experiments carried out with the system of Figure No. 44 and can be neglected.

The computations of the four pole parameters by using the values obtained by measurement are as follows:

$$\beta_{11}' = \frac{Y_1}{Z_o'm_1} \quad \beta_{22} = \frac{Y_2}{Z_o'm_2}$$

213

$$\beta_{11} = \frac{Y_1}{Z_o'm_1 - Y_1 R} + \frac{jZ_1}{Z_o'm_1}$$

214

$$\beta_{22} = \frac{1}{Z_{om_2}} [\gamma_2 + jZ_2] \quad 215$$

In order to compute  $\beta_{21}$ , the following four pole equations are used.

$$V_1' = \frac{I_1'}{\beta_{11}'} + \frac{V_2 \beta_{12}'}{\beta_{11}'} \quad 216$$

$$V_1 = \frac{I_1}{\beta_{11}} + \frac{V_2 \beta_{12}}{\beta_{11}} \quad 217$$

$$V_2 = \frac{I_2}{\beta_{22}} + \frac{V_1 \beta_{21}}{\beta_{22}} \equiv \frac{I_2}{\beta_{22}} + \frac{V_1' \beta_{21}'}{\beta_{22}} \quad 218$$

It follows that:

$$V_1 \beta_{21} \equiv V_1' \beta_{21}' \quad 219$$

$$\beta_{21} \equiv \beta_{21}' + \frac{V_1'}{V_1} \quad 220$$

Referring to Figure 44 we may write:

$$V_1 = V_1' - (I_1' + V_2 \beta_{12}') R_s \quad 221$$



Combining equations 212 and 217 we have

$$\frac{V_1'}{V_1} = \frac{1}{1 - \beta_{11}' R_s} \quad 222$$

and  $\beta'_{21}$  can be evaluated by making use of the relation

$$V_2 \approx \frac{I_2'}{\beta_{22}'} + \frac{V_1' \beta_{21}}{\beta_{22}} \quad 223$$

Dividing equation 223 by  $V_2$  and rearranging terms we have:

$$\beta_{21}' \approx \frac{\beta_{22}'}{\left(\frac{V_1'}{V_2}\right)} \left[ 1 - \frac{I_2'}{V_2 \beta_{22}'} \right] \quad 224$$

where  $\frac{I_2'}{V_2}$  can be expressed by:

$$\frac{I_2'}{V_2} = \frac{1}{Z_0' m_2 Z_0} = \frac{1}{Z_0' m_2} \quad 225$$

Where  $Z_0 = 1$ ,  $\frac{V_1'}{V_2}$  can be expressed in terms of  $\gamma_{21}$ ,  $m_1$  and  $m_2$  by using the relations

$$\frac{V_1'}{V_1''} = \sqrt{\frac{Z_0' m_1}{Z_0}} \quad 226$$

$$\frac{V_2}{V_2''} = \sqrt{\frac{Z_0' m_2}{Z_0}}$$

227

Solving equations 226 and 227 for  $\frac{V_1'}{V_2}$  and remembering that  $\frac{V_1''}{V_2''} = \gamma_{21}$  :

$$\frac{V_1'}{V_2} = \gamma_{21} \sqrt{\frac{m_1}{m_2}}$$

228

If equations 228 and 225 are substituted in equation 224, one finds

$$\beta_{21}' \cong \frac{\beta_{22}'}{\gamma_{21}} \sqrt{\frac{m_2}{m_1}} \left[ 1 + \frac{1}{Z_0' m_2 \beta_{22}'} \right]$$

229

By using equations 220 and 222,  $\beta_{21}$  can then be written as:

$$\beta_{21} \cong \frac{\beta_{22}'}{\gamma_{21}} \sqrt{\frac{m_2}{m_1}} \left[ 1 + \frac{1}{Z_0' m_2 \beta_{22}'} \right] \left[ \frac{1}{1 - \beta_{11}' R} \right]$$

230

#### (F) Discussion of Results

In Bell Laboratories experiments were carried out on several 1553 triodes. The equivalent circuit of a 1553 H.F. triode at 4060 m.c. come out to be as shown in Figure No. 45.

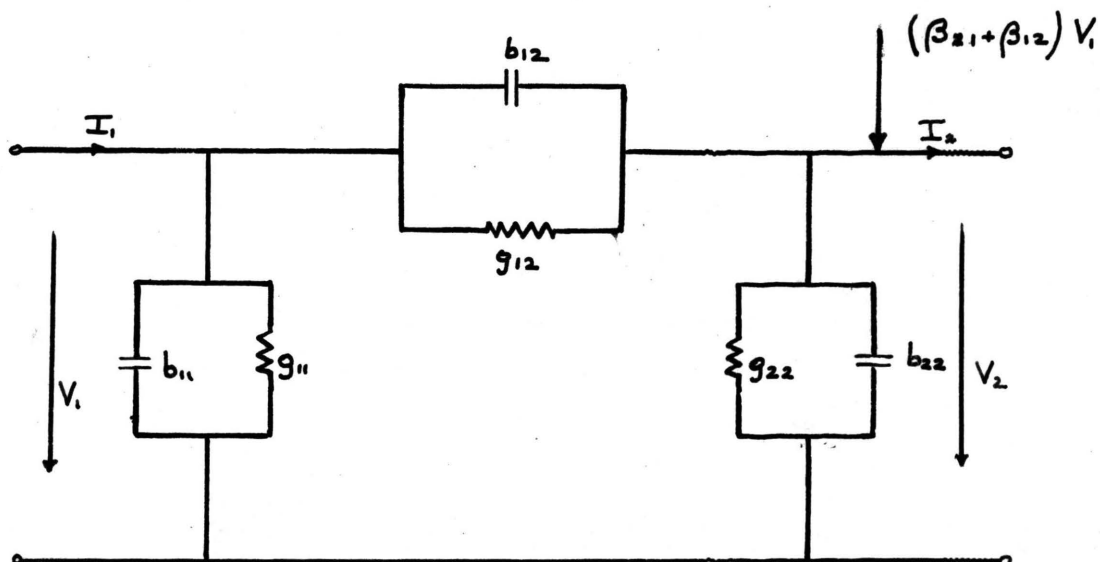


Figure No. 45

## Equivalent Circuit of a Triode Based on Experimental Results

There are a number of interesting things about Figure No. 45, as with the diode,  $b_{11}$  for a large negative bias approaches the "cold" value computed from the capacitance. However, as anode current is drawn,  $b_{11}$  drops rapidly to a much lower value as was suggested by Behnam<sup>31</sup>. The conduction  $g_{11}$  behaves somewhat like  $g$  for the diode.

$b_{22}$  is equal to the value computed from the grid anode capacitance and is not appreciably influenced by the electron stream.  $g_{22}$  was very low with a magnitude of slightly less than 1000  $\mu\text{mhos}$  at a maximum anode current. The transadmittance

$\beta_{21}$  is worth considering when the bias is several volts negative,  $\beta_{21}$  has a value of about 9000 micromhos. This

(31) Behnam, Tube and Amplifier Theory, Proc. IRE, vol. 26, p. 1105, 1938.

is about 50 times as high as one would expect from a consideration of the electrostatic capacitance between the cathode and anode of the tube.

This effect has been discussed in greater detail in the subsequent pages. As the tube starts to draw plate current, it rises and reaches a maximum value of about 40,000 micromhos. It is also observed that the high frequency admittance is only slightly lower than  $g_m$  (transconductance at lower frequency). This is in agreement with theories by Llewellyn. The agreement appears reasonable when one remembers that in the theoretical analysis, the magnitude of the ratio  $\beta_{21}$  is relatively independent of the transit time in the input space.

It was also found that with high negative bias the feedback admittance  $\beta_{12}$  is substantially equal to  $\beta_{21}$  but as the current density increased,  $\beta_{12}$  decreased.

Figure No. 46 shows the variations of the phase of the transadmittance  $\beta_{21}$  for a 1553 triode and also the theoretical curve of the Llewellyn analysis for purposes of comparison.

(For Figure No. 46, see Page 139)

The behavior of  $b_{11}$  for a triode is not as expected. It is thought that as the grid voltage is varied, so that the input space changed from a condition of zero space to one of maximum space charge,  $b_{11}$  would vary from its initial cold value to a value approaching 60 per cent of the cold value. Experimentally it is found out to drop much lower than 60%.

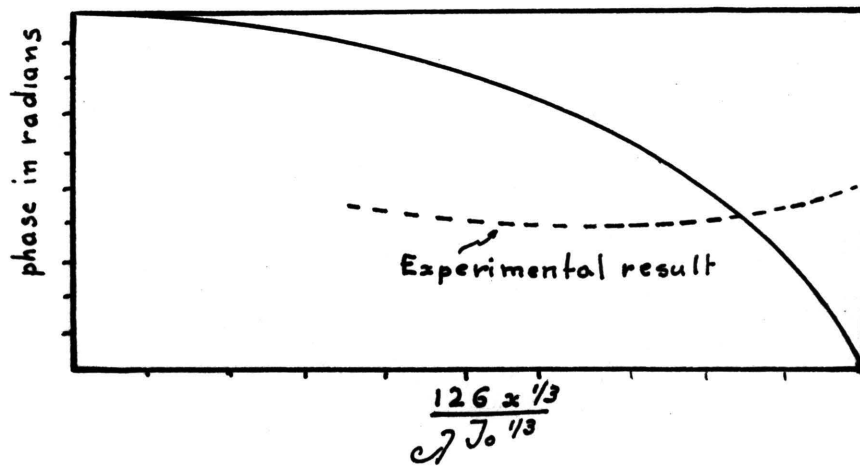


Figure No. 46  
 A Plot of the Experimental and Theoretical Values of  
 the Phase of the Transadmittance for a 1553 Triode  
 Versus  $\frac{126x^{1/3}}{\omega J_0^{1/3}}$

This effect has not been explained from the theoretical point of view. It is probable that the variation in  $b_{11}$  is a space charge effect. A clue to this effect might be discovered by making measurements on structures with different cathode grid spacings.

Experiments carried out to determine the effect of plate voltage on the input admittance of the triode of Figure No. 44 showed that the input admittance did not vary greater with plate voltage changed from 250 volts to 40 volts. The experiment carried out in this case suggest that for a given geometry, the value of  $b_{11}$  is primarily a function of the total current density in the input circuit.

#### (G) Substitution Method for the Measurement of Admittances <sup>32</sup>

In this method unknown admittance is connected across a parallel resonant circuit, the capacitance of which is adjusted until the circuit is in resonance with the frequency of the driving oscillator. The resonance reading is indicated by a vacuum tube voltmeter. A resistance is then substituted for the unknown admittance. The resistance is adjusted and the capacitance simultaneously varied to obtain resonance until the same reading is obtained on the vacuum tube voltmeter as before. The unknown admittance is then given by the value of the substituted resistance, the frequency, and the change in capacitance required to re-establish resonance. The

(32) Miller, J.; Solzberg, B., Measurement of Admittance at UHF, Vol. III, No. 4, p.486, Apr. 1939.

substitution resistance in the actual setup consists of a fixed resistor connected across a low-loss transmission line which constitutes the inductance of the parallel resonance circuit. The transmission line is short circuited at one end and attached to a variable capacitor at the other, or sending end. The fixed resistor is arranged so that it can be readily connected across the line at any point. When the fixed resistor is connected across the line at its short circuited end, the admittance of the line at its sending end terminals is equal to that obtained in its unloaded state, i.e., with the fixed resistor removed. On the other hand, when the fixed resistor is connected across the line at its open end, the sending end admittance is equal to the sum of the admittances of the resistor and the sending end admittance of the line in its unloaded state. When the fixed resistor is connected across the line at some intermediate point, the value of the sending end admittance lies between these two limiting end values. The transmission line may thus be regarded as an auto-transformer which steps down the admittance of the fixed resistor. The effective admittance is a function of the resistance, reactance, and position of the resistor on the line and the parameters of the line. To determine the quantitative relationship between these factors we proceed as follows:

Consider a transmission line short circuited at its distant end, and bridged by an admittance  $Y$  at a point  $x$  centimeters from the distant end. The line length is  $l$  centimeter.

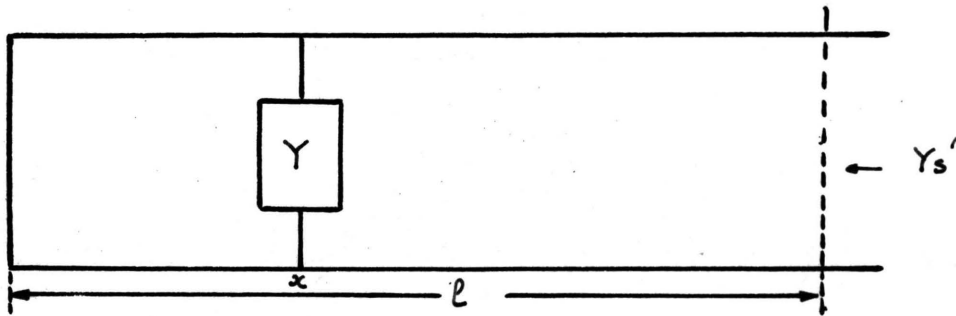


Figure No. 47  
A Short Circuited Transmission Line

The admittance at  $x$  of the portion line to the left of the bridging admittance is:

$$Y_{s,x} = Y_0 \coth \gamma x$$

231

where  $Y_0$  is the characteristic admittance of the line

$\gamma$  is the propagation constant of the line

The vector sum of this admittance and the bridging admittance must be regarded as representing a receiving end admittance for the rest of the line, extending from  $x$  to  $l$ . The value of this receiving end admittance is:

$$Y_r = Y + Y_0 \coth \gamma x$$

232



The sending end admittance at  $l$ , is:

$$Y_s' = Y_0 \frac{Y_r + Y_0 \tanh y(l-x)}{Y_0 + Y_r \tanh y(l-x)} \quad 233$$

Substituting equation 233 into 232 and leaving only tanh terms we have:

$$Y_s' = Y_0 \frac{Y \tanh yx + Y_0 [1 + \tanh yx \tanh y(l-x)]}{Y \tanh yx + \tanh y(l-x) + Y_0 [\tanh yx + \tanh y(l-x)]} \quad 234$$

When the bridging admittance is removed, the sending end admittance is simply:

$$Y_s = Y_0 \coth y l \quad 235$$

With the unknown  $Y_u$  connected across the sending end of the line, the bridging admittance removed, and the tuning capacitance adjusted to obtain resonance, the total admittance at the sending end terminals of the line is:

$$Y_s + Y_u + j b_c = g_s + g_u \quad 236$$

Since resonance requires that the total susceptance be zero, i.e., ( $b_c$  plus  $b_s$  plus  $b_u$ ) equal 0. In the above equation, therefore:

$$b_c + b_s + b_u = 0$$

237

$Y_s$  equals  $g_s$  plus  $jb_s$  and is the sending end admittance of the line when the bridging admittance is removed.  $Y_u$  equals  $g_u$  plus  $jb_u$  and is the unknown admittance.  $b$  equals susceptance of the tuning capacitance required for resonance, when the unknown is connected.

Now when the unknown admittance is removed and the bridging admittance is moved along the line until the same reading is obtained at resonance, as before, the total admittance at the sending end terminals of the line is:

$$Y_s' + jb_c' = g_s + g_u$$

238

Resonance now requires that:

$$b_c' + b_s' = 0$$

239

The new quantities are:

$Y_s' = g_s' + j b_s'$  is the sending end admittance of the line when the bridging admittance is connected.

$b_c'$  is the susceptance of the tuning capacitance required for resonance when the unknown admittance is removed.

Equations 237 and 235 gives us an expression for the unknown admittance in terms of the total substitution admittances:

$$Y_u = (Y_s' - Y_s) + j(b_c' - b_c) = \Delta Y_s + j \Delta b_c \quad 240$$

The components of the unknown admittances are accordingly:

$$g_u = g_s' - g_s = \Delta g_s \quad 241$$

$$b_u = (b_s' - b_s) + (b_c' - b_c) = \Delta b_s + \Delta b_c \quad 242$$

If the bridging admittance is merely a conductance, the first term of the right hand member of equation 242 vanishes, and we have:

$$b_u = \Delta b_c \quad 243$$

This quantity is given directly by the change in tuning capacitance required to re-establish resonance, and by the operating frequency.

The quantity  $\Delta Y_s$  in equation 240 is the one we are looking for. It may be resolved by subtracting 235 from 232, thus:

$$\Delta Y_s = Y_s' - Y_s = \frac{Y \tanh yx + Y_0 [1 + \tanh yx \tanh y(l-x)]}{Y \tanh yx \tanh y(l-x) + Y_0 [\tanh yx + \tanh y(l-x)]} \quad 244$$

By means of a straight forward manipulation, this can be written as:

$$\Delta Y_s = Y \left( \frac{\sinh yx}{\sinh yl} \right)^2 \frac{1}{1 + \left( \frac{Y}{Y_0} \right) \frac{\sinh yx}{\sinh yl} \sinh y(l-x)} \quad 245$$

Now, in equation 245,  $\Delta Y_s$ ,  $Y$ ,  $Y_0$  and  $y$  are in general, complex quantities of the form  $(\Delta g_s + j \Delta b)$ ,  $(g + jb)$  respectively. We notice, however, that if:

$$\left( \frac{\sinh yx}{\sinh yl} \right)^2 \approx \left( \frac{\sin \beta x}{\sin \beta l} \right)^2$$

and

$$\left| \frac{Y}{Y_0} \frac{\sinh yx}{\sinh yl} \sinh y(l-x) \right| \ll 1$$

then equation 244 can be written as:

$$\Delta Y_s = Y \left( \frac{\sin \beta x}{\sin \beta l} \right)^2 \quad 246$$

If in addition,  $\sin \beta l \cong \beta l$ , then a further simplification results:

$$\Delta Y_s = Y \left( \frac{x}{l} \right)^2 \quad 247$$

In the case of comparison of two resistors,  $R_1$  and  $R_2$ , which are located at two intermediate points on the line,  $x_1$  and  $x_2$ , such that the deflection of the vacuum tube is the same, each resistor can be considered the equivalent of the same admittance  $\Delta Y_s$  at the sending end.

Hence from equation 245, we get:

$$Y_s = \frac{1}{R_1} \left( \frac{\sin \beta x_1}{\sin \beta l} \right)^2 = \frac{1}{R_2} \left( \frac{\sin \beta x_2}{\sin \beta l} \right)^2 \quad 248$$

or

$$\frac{R_1}{R_2} = \left( \frac{\sin \beta x_1}{\sin \beta x_2} \right)^2 \quad 249$$

and in the case of a short line:

$$\frac{R_1}{R_2} = \left( \frac{x_1}{x_2} \right)^2 \quad 250$$

(H) Measurement of Input and Output Admittance of Vacuum Tube  
By Substitution Method

The input impedance of a vacuum tube can be measured by connecting the grid of the tube by means of a short lead to the high potential end of the line through a by-pass capacitor. The other desired bias voltages are applied to the tube electrodes and the vacuum tube voltmeter is read (See Figure No. 47). The grid connection is then opened, or the tube biased to cut-off as desired. Resonance is re-established by the terminal capacitor, and a standard resistance is placed on the line at a point which gives the same deflection of the vacuum tube voltmeter. The voltage calibrations of the line then gives the resistive part of the impedance of the tubes, as described above, and the change in the terminal capacitor gives the capacitive component. Difficulties are found in obtaining resistors having negligible reactance at frequencies of the order of  $10^8$  cycles per second or higher. Wire-wound resistors are not usable at such frequencies. The most satisfactory types are the metalized-glass or ceramic rod resistors of relatively small physical size, having low-inductance terminals and very little distributed capacitance. A further difficulty arises from the fact that such resistors are obtainable only in discreet values of resistance. It would not be practicable to obtain the very large number of resistors needed to match the resistance of any electron tube circuit. Hence it is necessary to utilize a transformation property of the admittance measuring equipment in order to match any

arbitrary admittance with one of the available standard resistors.

A more practical method is the susceptance variation method, which will be explained in the next paragraph.

### (I) Susceptance Variation Method <sup>33</sup>

This method is a form of the well known reactance variation widely used for the measurement of two terminal admittances. It is adopted to the termination of the transfer admittances, as well as to the driving point admittances. Figure No. 48 gives a semi-schematic diagram of the test equipment.

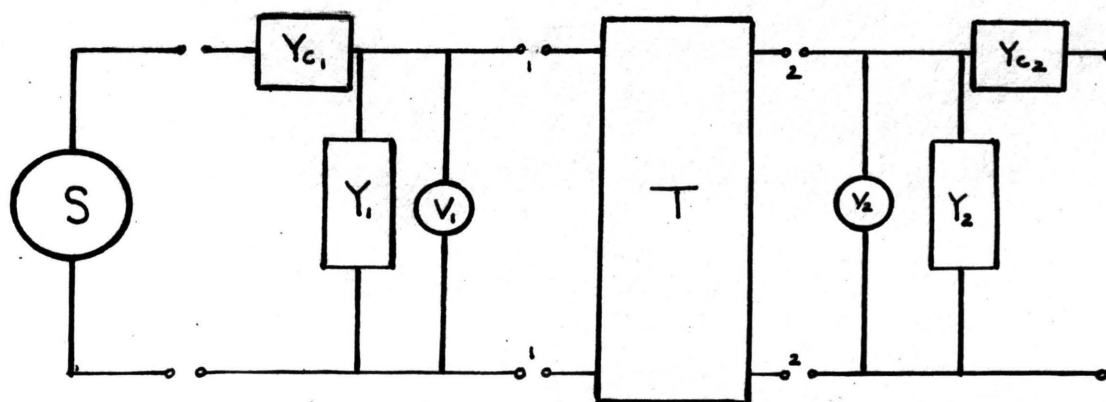


Figure No. 48  
Semi-Schematic Diagram for Susceptance Variation Method

In this figure, T is the active or passive transducer to be measured and  $Y_1$  and  $Y_2$  are calibrated variable admittance elements, which may be of various forms, such as coils, and capacitors, or adjustable length lines. Signal measuring devices  $V_1$  and  $V_2$  are placed across the input and output terminals of the system, these may be simply crystal or diode voltmeters or heterodyne receivers.

Variable admittances  $Y_{c1}$  and  $Y_{c2}$  are used for coupling the input or output circuits to the signal oscillators. The sequence of measurements is as follows:

1. Measurement of  $\beta_{11}$

- a. Short circuit the output terminals 2-2. This may be done either by detuning  $Y_2$  sufficiently or by placing a suitable by-pass capacitor directly across terminals 2-2.
- b. Excite the input circuit by coupling the signal oscillator loosely through  $Y_{c1}$  and  $Y_1$
- c. Adjust  $Y_1$  for resonance as indicated by a maximum reading of  $V_1$ . In order to insure that the coupling to the oscillator is sufficiently small, reduce the coupling until further reduction does not change the setting of  $Y_1$  for resonance. Record the calibrated values of  $G_1$  and  $B_1$  for this setting, where  $B_1$  is the input susceptance and  $G_1$  is the input conductance.
- d. Vary  $Y_1$  on either side of resonance until the voltage  $V_1$  is reduced by a factor  $\frac{1}{\sqrt{2}}$ .



Record the calibrated values of this total variation of  $Y_1$  between half power points at  $\Delta G_1$  and  $\Delta B_1$ . In order to insure that the oscillator and detector are not loading the circuit, reduce the coupling until further reduction does not change the susceptance variation  $\Delta B_1$ . The short circuit input susceptance is then given by the relation:

$$B_{11} = -B_1 \quad 251$$

and the short circuit input conductance by the relation:

$$\beta_{11} = \frac{\Delta B_1}{2} \left[ \left( (1 + 2\eta^2)^{\frac{1}{2}} + \eta \right) \right] + G_1 \quad 252$$

where  $\eta$  is given by  $\frac{\Delta G_1}{\Delta B_1}$ .

In most systems the inequality

$$\eta^2 = \left( \frac{\Delta G_1}{\Delta B_1} \right)^2 \ll 1 \quad 253$$

holds; thus we may write equation 246 as:

$$\beta_{11} = \frac{\Delta B_1}{2} [1 + \eta + \eta^2] - G_1 \quad 254$$

or even further by the relation:

$$\beta_{11} = \frac{\Delta B_1}{2} - G_1 \quad 255$$

if  $\eta$  is negligible.

## 2. Measurement of the Magnitude $\beta_{12}$

- a. With the input termination still set at the value required for resonance obtained in step c above, excite the output circuit through  $Y_{c2}$ .
- b. Record the voltmeter reading  $V_1$  and  $V_2$ . The magnitude of the feedback admittance is then given by the relation:

$$\beta_{12} = \frac{V_1}{V_2} \frac{\Delta B_1}{2} \left[ (1 + 2\eta^2)^{1/2} + \eta \right] \quad 256$$

and if

$$\eta^2 = \left( \frac{\Delta G_1}{\Delta B_1} \right)^2 \ll 1 \quad 257$$

Equation 251 may be simplified as:

$$|\beta_{12}| = \frac{|V_1|}{|V_2|} \frac{\Delta B_1}{2} [1 + \eta + \eta^2] \quad 258$$

or

$$|\beta_{12}| = \frac{\Delta B_1}{2} \frac{|V_1|}{|V_2|} \quad 259$$

### 3. Measurement of $\beta_{22}$

The **short** circuit output admittance may be measured by following the procedure outlined for the input coefficient, the signal being coupled through  $Y_{c2}$ . If the subscripts are interchanged, all of the above formulas concerning  $\beta_{11}$  may be used to relate  $\beta_{22}$  to the measured data.

### 4. Measurement of $\beta_{21}$

The magnitude of the transfer admittance may be measured by following the procedure outlined previously for the measurement of the magnitude of  $\beta_{12}$ . If the subscripts 1 and 2 are interchanged all of the formulas concerning  $\beta_{12}$  may be used to relate  $\beta_{21}$  to the measured data.

For further details on higher frequency impedance measurements see the articles given in references, 32, 33, and 34.

---

(32) Miller, Solzberg, op,cit.

(33) Nergaard, L.S., Survey of UHF Measurements, RCA, Rev.,p.156, July 1938.

(34) Chipman, R.A. A Resonance Curve Method for the Absolute Measurement of Impedance at Frequencies of the Order of 300 m.c., Journal of Applied Physics, vol.10, p. 27, 1939.

## CONCLUSIONS

The vacuum tube equivalent circuit found its first application shortly after the first appearance of the vacuum tube in 1918. From this time on it underwent various developments and in the year 1949, it obtained its final and most practical form.

It would be of interest to go briefly through every stage of development of the vacuum tube equivalent circuit and point out the various advantages and disadvantages. The most simplest equivalent circuit, namely, the one used at low frequencies, was derived by assuming that  $i_p$  was a function of  $e_g$  and  $e_p$ . As long as the signal applied to the tube was of small magnitude and low frequency, this equivalent circuit gave reasonable results. But as the frequencies increased, the results obtained from this equivalent circuit deviated an amount depending upon the range of the frequency used. The reason for this deviation was that in addition to convection current there was a displacement current between tube electrodes which had to be taken into account at higher frequencies. Therefore, a displacement current equivalent circuit was added to the simple classical vacuum tube equivalent circuit. As long as the frequencies used stayed in the range of a few m.c., the equivalent circuit gave satisfactory results. But as the frequencies further increased, the equivalent circuit ceased to be satisfactory again and this was thought to be due to

vacuum tube lead effects. This consideration was an improvement in the vacuum tube equivalent circuit but still the results were not correct. The addition of transit time effect in the equivalent circuit brought us closer to the correct equivalent circuit, but this produced <sup>1</sup>such a complicated circuit and was found to be of little practical value. The mathematical evaluation of each parameter would be very tedious and lengthy. Besides this, the equivalent circuit was not absolutely correct, as it was a combination of several effects being considered separately and then added together.

The development of the equivalent circuit through the use of the electron stream theory brought about an entirely new approach in this field of equivalent vacuum tube circuits. From physical point of view it was an interesting problem but from the point of practical usefulness, it was discouraging, as the results were lengthy and complex. Besides this, the results were not absolutely correct for the following assumptions were made.

- (1) Single velocity electron stream
- (2) No secondary emission from any structure
- (3) Zero velocity of electrons emitted from cathode
- (4) No self inductance of the tube leads within the tube

The effects of the above assumptions were not pronounced at low frequencies, and the electron stream equivalent circuit gave correct results. But even in this case the equivalent circuit was far from being of any practical use.

An improvement in the representation of the equivalent circuit was the application of the four pole terminal networks to electron stream equivalent circuit. This had the advantage of reducing the circuit elements to a minimum number. Still, the four pole parameters had to be determined from the expressions derived by the use of the electron stream theory.

The four pole equivalent circuit brought about a new idea in the evaluation of the four pole impedances, namely, the experimental determination of the four pole parameters. In this case the correctness of the results depends upon the accuracy of the instruments used and the technique of measurements.

Experiments carried out by S. D. Robertson give reasonable comparison with the theoretical results of Llewellyn and Peterson. Theoretical results were found to differ considerably from the experimental results especially at high frequencies. This is claimed to be due to Maxwellian's electron velocity distribution.

At the present time the application of four pole vacuum tube equivalent circuit is rather restricted. This is due to the lack of measurements carried out for the plot of impedance and phase versus frequency for various types of tubes. But its wide and extensive use is expected in the coming years even at low frequencies.

## APPENDIX NO. 1

(A) Hybrid Circuits for Microwaves<sup>29</sup>

The hybrid coil has been used in telephone practice for a long time in order to secure preferential isolation of circuits. The word "hybrid" has been selected to describe the equipment that performs at high frequency the same function as a hybrid coil. In the high frequency equipment physical similarity with the conventional hybrid coil is found.

A hybrid device is represented schematically in Figure No. 49:

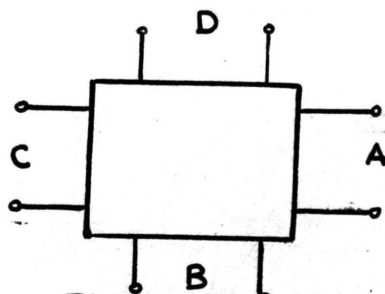


Figure No. 49  
A Hybrid Device

When a source of alternating electromotive force is connected across the terminals A, no signal appear at the terminals C, but transmission takes place freely between A and B and between A and D, with the input power thus divided between loads placed at B and D. If the generator is transferred from A to C, no voltage appears at A, from reciprocity considerations, and again the input power is divided in some fashion between loads B and D. It is generally desirable that the terminals B and D be balanced with respect to each other, so that a generator applied at either of these points delivers power

---

(29) Tyrrell, op.cit.

only to loads at A and C. In most cases, the circuit is so proportioned as to bring about equal power division between the driven loads. Usually the loads or generators, which are connected to these lines, terminate each arm in its characteristic impedance. If matching is not obtained at the terminals, reflection from the loads will tend to upset the balance of the load distribution.

### (B) Hybrid junctions

In addition to hybrid coils<sup>29</sup> there are hybrid junctions which are those used in Figure No. 49 for high frequency impedance measurements. One form of such a junction is shown in Figure No. 50 as a cross section of the electric field plane.

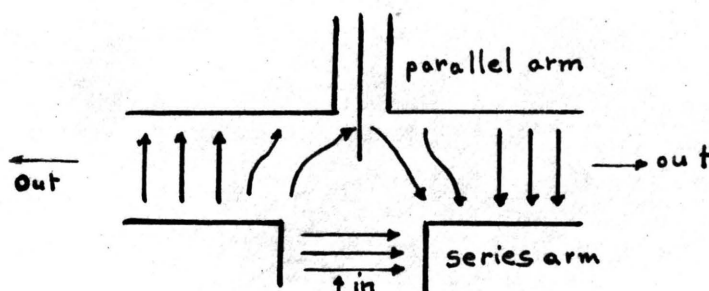


Figure No. 50  
Spreading of a Wave Front into a Compound Junction  
from the Series Arm

In the electric field plane wave guide junction the side arm is effectively connected in series with the main guide. We will make this point clearer in the subsequent pages. When power is sent toward the junction from the series, two sets of waves are set up in the main guide, traveling in opposite directions away from the junctions. These two sets of waves are

---

(29) Tyrrell, op,cit.



180 degrees out of phase with respect to each other, that is, their polarities are reversed. If the two ends of the main guide are terminated in characteristic impedance, the power will divide equally between the two loads, and no power will appear in the coaxial line, as the voltage induced in the coaxial line cancel each other.\*

In order to make clear the meaning of series arm connection, let us consider Figure No. 51 shown below:

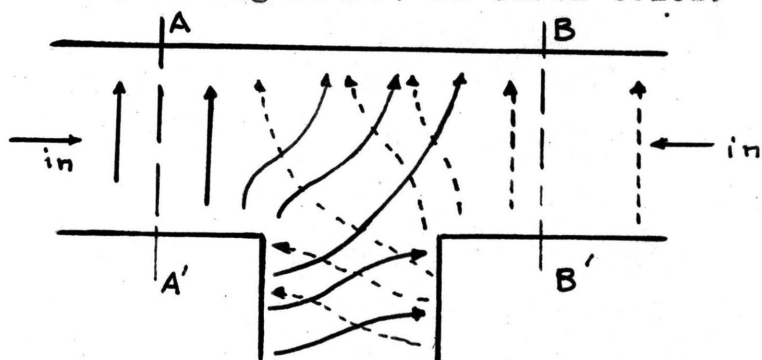


Figure No. 51  
T-Junction in a Wave Guide in the E Plane

Figure No. 51 show a T-junction with solid lines representing electric intensity in successive positions of the same wave front for waves arriving from the left, and with broken lines for waves from the right, in the main guide. If the waves are in phase at AA' and BB' the side arm receives two waves which are 180° out of phase. If the amplitudes of the incoming waves are equal, the waves in the side arm cancel completely, and this branch receives no power. Such sets of waves of equal amplitude traveling in opposite directions create pure standing waves in the main guide with a voltage maximum at the junction. In such a case no electric field appears in the side arm

\*This will not be true if the coaxial is large enough to support freely the first higher order transmission mode.

connection. Conversely, the side arm of an electric plane T junction receives maximum power when a pure standing wave exists in the main guide with a voltage minimum (current maximum) at the junction. This is the behavior exhibited by a load which has a series connection to a transmission line. From the point of view of phase relationships, therefore, the side arm of the electric field plane T may be regarded as connected in series with the main guide.

The same junction as in Figure No. 50 is shown in Figure No. 52, but here the power is introduced from the parallel arm, i.e., from the coaxial line. When power is sent from the parallel arm the two arms of the main guide receive equal intensities of power in phase and no net voltages appear across the series branch.\*

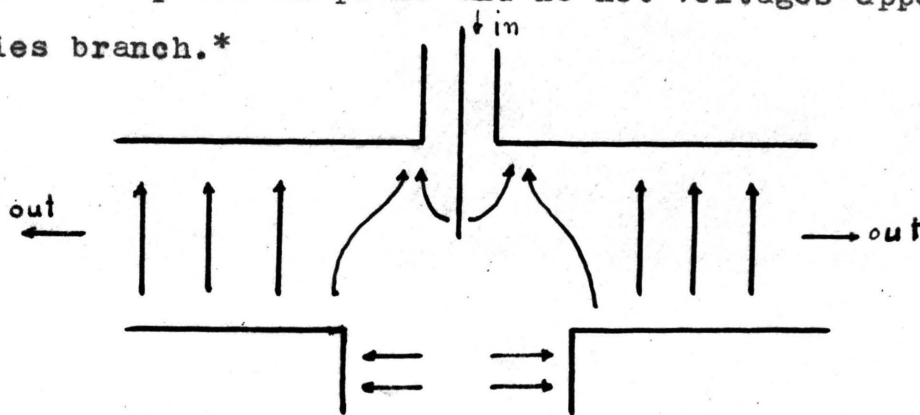


Figure No. 52  
Spreading of a Wave Front Into a Compound Junction from the Parallel Arm

In order to make clear the meaning of parallel arm connection, consider Figure No. 53. In magnetic plane wave guide junction or parallel arm connection the electric intensity is perpendicular to the plane of Figure No. 53. In Figure No. 53,

\* This will not be true if the series arm is large enough to support freely the TM, (coaxial line) transmission mode.

there the electric field intensities are in phase at both ends of the wave guide. If waves of equal amplitude are sent toward the junction from the left and right so as to be in phase at the junction, the side arm receives two sets of waves in phase and therefore maximum power. From the point of view of phase relationships, then, the side arm magnetic plane T is connected in parallel across the main guide.

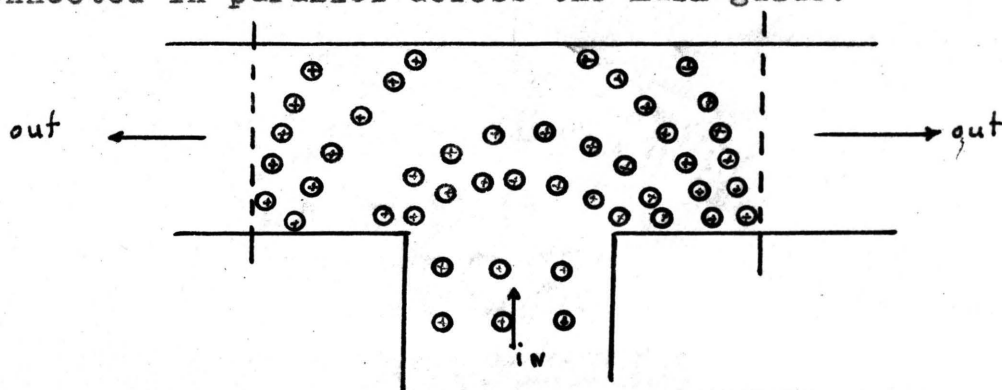


Figure No. 53  
A T Junction in the Wave Guide in the H Plane.

A clearer view of the compound junction where the parallel connection is established by means of magnetic plane wave guide junction, instead of coaxial line, is given in Figure No. 54.

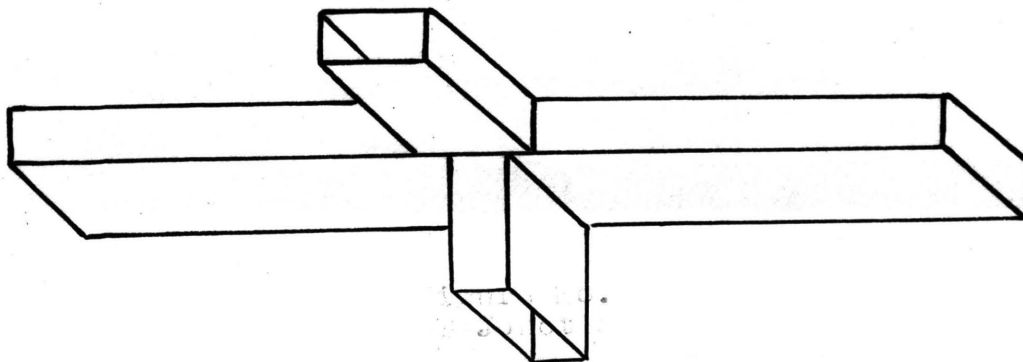


Figure No. 54  
Compound T Junction of a Wave Guide

## APPENDIX NO. 2

(A) Discussion of Single Stream and Double Stream Electron Velocity Theory

One of the questions which arises in Sections III and IV of this thesis concerns with the nature of electron trajectories. When trajectories do not cross, the motion retains the "single velocity stream" behavior, as was assumed, where at each point in space only one velocity vector is found for the moving electrons. Crossing of trajectories causes "bunching", and a change to "double velocity stream" motion, where two different electron velocities are obtained at some points in space.

To prove that the double velocity stream causes a change in electric field at the point of crossing, we shall start with single stream electron velocity, assuming a plane structure, where all quantities (field, space charge) depend only upon  $x$  and  $t$  but not upon  $y$  or  $z$ . We shall also define the total current density (convection plus displacement) by  $J_x$ .

From Maxwell's equations we have:

$$\nabla \cdot J = \frac{\partial I_x}{\partial x} = 0 \quad 260$$

Hence  $J_x$  is a function of  $t$  only, but not of  $x$ ;  $J_x$  is also equal to:

$$J_x(t) = -\rho v - \epsilon_0 \left( \frac{\partial E}{\partial t} \right)_x \quad 261$$

Where:  $\rho$  is the charge density  
 $v = \frac{dx}{dt}$  is the velocity of the electron.

From Poisson's relation we have

$$\epsilon_0 \left( \frac{\partial E}{\partial t} \right) = \rho \quad 262$$

From equations 256 and 257 we can show that:

$$\frac{dE}{dt} = \frac{\partial E}{\partial t} + \frac{dx}{dt} \frac{\partial E}{\partial x} = - \frac{J_x}{\epsilon_0} \quad 263$$

This is the point where the "single velocity stream" assumption is introduced implicitly through the assumption of single direction of current flow. In a double stream motion, the space charge density  $\rho$  would split into two parts,  $\rho_1$ , moving with  $\frac{dx_1}{dt}$  and  $\rho_2$  moving with  $\frac{dx_2}{dt}$ . Hence, equation 256 should consequently be modified and equation 258 would not be correct.

Let  $E_0(t)$  be the field on the cathode. An electron leaving the cathode at time  $t_0$  reaches a certain distance  $x(t_0, t)$  at time  $t$  and the electric field acting upon it at any time  $t$  is:

$$\begin{aligned} E(t_0, t) &= E_0(t_0) + \int_{t_0}^t \frac{dE}{dt} dt. \\ &= E_0(t_0) + \frac{1}{\epsilon_0} \int_{t_0}^t J_x(t) dt \end{aligned} \quad 264$$

The integration of the second term yields  $Q$ , the space charge density. Therefore, integrating equation 259, we have:

$$\epsilon_0 [E(t_0, t) - E_0(t_0)] = Q$$

265

The physical content of this formula is explained in Figure No. 55 which shows the plot of the electron trajectories versus  $x$  and  $t$  for two different electrons emitted from the cathode.

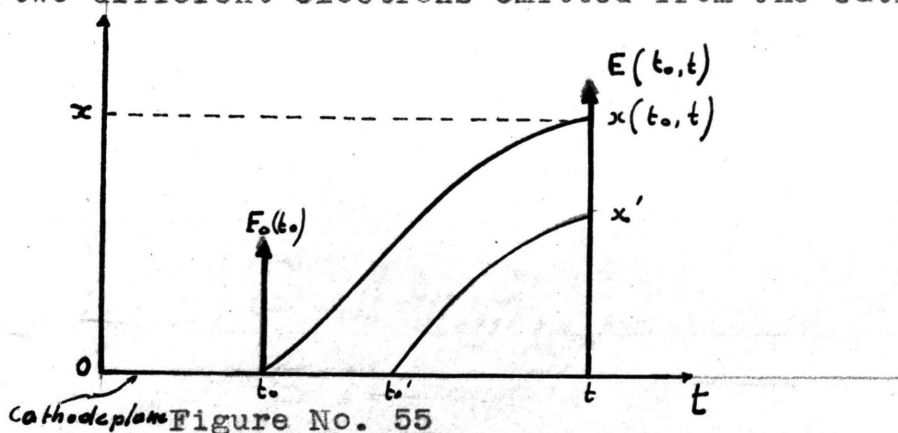


Figure No. 55  
Plot of Electron Trajectories Versus  $x$  and  $t$

At time  $t$ , the total charge density between the plates at any point  $x$ , is equal to  $Q$  and expressed by equation 265.

Next we note that, between time  $t_0$  and  $t$ , there has been an increase of the surface charge density equal to  $Q$  on the cathode and can be expressed by:

$$\epsilon_0 [E(t) - E_0(t_0)] = q$$

266

Therefore the total charge density is given by:

$$q + Q = - \int_{t_0}^t J_x(t) dt$$

267

In the above equations we see that we can express charge density in terms of electric field.

Next let us see what happens to an electric field if a crossing of the trajectories take place. Figure No. 56 gives a physical picture of the condition that exists when electrons cross each other.

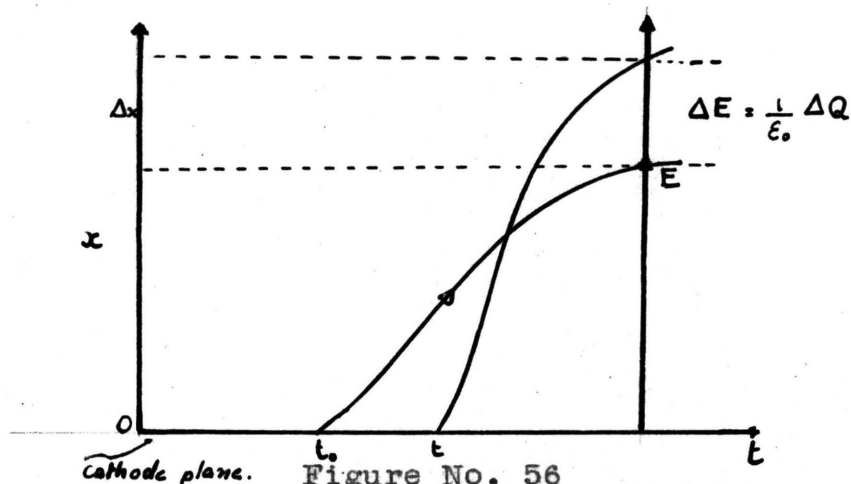


Figure No. 56  
Plot of Electron Trajectories Versus  $t$  and  $x$  When  
Two Electrons Cross

We can see from the above figure that electron crossing brings about a change of charge  $Q$  in front of the trajectory due to the change in electric field  $\Delta E$  in the neighborhood of the point  $x$ . It decreases the field  $E(t, t)$  by an amount  $\frac{1}{\epsilon_0} \Delta Q$  and is given by:

$$E(t, t) = E_0(t_0) - \frac{1}{\epsilon} \int_{t_0}^t J_x dt - \frac{1}{\epsilon_0} \Delta Q. \quad 268$$

The amount of charge  $\Delta Q$  which is due to intercrossing can be evaluated and hence the field correction required for Llewellyn's work can be obtained. From the above explanation

we can conclude that whenever there is intercrossing of electron streams there is a change of electric field intensity.

A full discussion of the evaluation of field corrections are given in reference relative to Kleyner. This discussion has been carried out for a parallel plane diode, for a diode wherein electrons are injected with a given velocity and also for several other types of tubes. But again there are some restrictions to these derivations. Two of them are:

- (1) Electron trajectories should not intercross prior to the instant of time when the motion is investigated.
- (2) The flow of electrons from the cathode must be uninterrupted. Suppose that the current is negative at a certain time near the cathode and if at this time new electrons are emitted from the cathode then overlapping of electron streams will occur. This will interrupt the usual flow of electrons near the cathode.

Very little error is introduced when these restrictions are neglected and the derivations, in the 26th reference, can be considered as improvement on Llewellyn's and Peterson's work on electron stream theory.





## APPENDIX NO. 3

(A) Maxwellian Velocity Distribution<sup>5</sup>

The heat energy that a body of gas contains exists in the kinetic energy of motion of the gas molecules. As the temperature is increased, the heat energy increases and the velocity of the molecules increases. The molecules will have velocities in all directions and with all magnitudes but most of them will have velocities grouped around a most probable velocity. Maxwell has shown from application of the theory of probability that the distribution of velocities of molecules in a gas is given by:

$$y = \frac{4}{\sqrt{\pi}} x^2 e^{-x^2}$$

269

Where  $x$  is the ratio of velocity to the most probable velocity and  $y$  is the corresponding probability that a molecule will have a velocity  $x$ .

The most probable velocity increases with the square root of the absolute temperature.

$$v_p = 12.900 \sqrt{\frac{T}{M}}$$

270

Where  $T$  is the absolute temperature and  $M$  is the molecular weight of the gas.

(5) Spangenberg, op.cit.

## BIBLIOGRAPHY

1. Books:

Glasgow, Principles of radio engineering. First edition, fifteenth impression. MacGraw Hill Book Co., 1936. p.132.

Hund, Frequency modulation. First edition, eighth printing, MacGraw Hill Book Co., 1942, p.153.

Spangenberg, Vacuum Tubes. First edition. McGraw Hill Book Co., 1948, Chapt.16, p.425.

2. Foreign Publications:

Muller, J., Untersuchungen Uber Elektronenstromungen Hochfreq. Tech. U. Elektrotechnik, Vol. 41, May 1933.

E.N.T., Elektrische Nachrichten Technik, 1929.

3. Periodicals:

Benham, W. E., Theory of Internal Action of Thermionic Systems at Moderately High Frequencies, Phil. Mag., Vol. 11, p. 457, Feb. 1931.

Benham, W. E., Tubes and Amplifier Theory, Proc. IRE, Vol. 26, p. 1105, 1938.

Brillouin, Influence of Space Charge on the Bunching of Electron Beams, Phys. Rev., Vol. 70, p. 187, 1946.

Bronwell, A. B., Electron Transit Time Effect in Time Varying Fields, Proc. IRE, Vol. 33, p.752, Oct. 1945.

Chaffee, E. L., Equivalent Circuits for an Electron Triode and the Equivalent Input and Output Admittances, Proc. IRE, Vol. 12, p.1633, Sept. 1929.

Chapman, R.A., A Resonance Curve Method for Absolute Measurement of Impedance at Frequencies of the Order of 300 m.c., Journal of Applied Physics, Vol. 10, p. 27, 1939.

Fay, C.E., Samuel, A.L., Shockley, W., On the Theory of Space Charge Between Parallel Plane Electrodes, B.S.T.J., Vol. 17, p. 49, 1938.

Ferris, W. R., Input Resistance of Vacuum Tubes at UHF Amplifiers, Proc. IRE, Vol. 24, p.82, Jan.1936.

Gill, E. W., A Space Charge Effect, Phil. Mag., Vol. 49, p.933, 1925.

Kleymer, J.A., Extension of Langmuir's Tables for a Plane Diode with a Maxwellian Velocity Distribution, Phil. Res. Rep., Vol. 1, p. 81, Jan. 1936.

Langmuir, I., Scattering of Electrons in Ionized Mediums, Phys. Rev., Vol. 26, p. 585, Nov. 1925.

Langmuir, I., The Effect of Space Charge on Thermionic Currents in High Vacuum Tubes, Phys. Rev., Vol. 2, p.450, Dec. 1913.

Linder, E. G., Excess Electron Motion in High Vacuum Tubes, Proc. IRE, Vol. 26, p. 346, 1938.

Llewellyn, F.B., Equivalent Networks of Negative Grid Vacuum Tubes at UHF, B.S.T.J., Vol. 15, p.575, 1936.

Llewellyn, F.B., Operation of UHF Vacuum Tubes, B.S.T.J., Vol. 14, p. 632, Oct. 1935.

Llewellyn, F.B. and Peterson, L.C., Vacuum Tube Networks, Proc. IRE, Vol. 32, p. 199, 1944.

Llewellyn, F.B. and Peterson, L.C., Vacuum Tube Electronics, Proc. IRE, Vol. 21, p. 1532, Nov. 1933.

Llewellyn, F.B., Electron Inertia Effect, Cambridge University Press, New York, N.Y., 1933.

Miller, J., Solzberg, B., Measurement of Admittances at UHF, Vol. III, No. 4, p. 486, Apr. 1939.

Nergaard, L. S., Survey of UHF Measurements, RCA, p. 156, July 1938.

North, D. O., Analysis of the Effect of Space Charge on Grid Impedance, Proc. IRE, Vol. 24, p. 108, Jan. 1936.

Peterson, L. C., Equivalent Circuits of Linear Active Four Terminal Networks, B.S.T.J., Vol. 23, p. 593, Oct. 1948.

Peterson, L. C. and Llewellyn, F.B., Vacuum Tube Networks, Proc. IRE, Vol. 32, p.199, 1944.

Robertson, S. D., B.S.T.J., Vol. 28, p. 647, Oct. 1949.

Strutt, M.J.O., Vonder Ziel, A., The Cause for the Increase of the Admittances of Modern High Frequency Amplifier Tubes on Short Waves, Proc. IRE, Vol. 28, No. 8, p. 1011, 1938.

Thompson, B. J., Review of UHF Vacuum Tube Problems, RCA Rev., p. 146, Oct. 1938.

Tonks, L., Space Charge as a Cause of Negative Resistance in a Triode and its Bearing on Short Wave Generator, Phys. Rev., Vol. 30, p. 501, Oct. 1929.

Tyrell, W. A., Hybrid Circuits for Microwaves, Proc. IRE, Vol. 35, No. 11, pp. 1294-1306, Nov. 1947.

#### 4. Publications of Learned Societies:

Tube Admittances of Receiving Tubes, Tube Dept. Radio Corp. of America, New Jersey, Nov. 1946.

## INDEX

## A

- Acknowledgment, ii
- Appendices
  - I--Hybrid Circuits for Microwaves, 158
  - II--Discussion of Single Stream and Double Stream Electron Velocity Theory, 163
  - III--Maxwell's Velocity Theory, 163
- Application of Electron Stream Theory to Diodes, 73
- Application of Electron Stream Theory to General Tubes, 78

## C

- Comparison of Llewellyn and Peterson's Formulas with Experimental Results, 118
- Conclusions, 156
- Consideration of Displacement Current, 17
- Consideration of Lead Effects, 18
- Current Components of Electron Stream, 70

## D

- Decrease of Output at UHF, 15
- Derivation of Fundamental Equations, 41
- Derivation of General Impedance Formulas of Electron Stream Theory, 57
- D.C. Equation for Electron Stream, 66
- Diodes
  - Application of Electron Stream Theory, 73
  - Effect of Space Charge Upon Transit Time, 39
  - Measurements for, 121
  - Results of measurements, 125

## E

- Equivalent Circuit
  - Application to Triode at Low Frequencies, 11
  - First Concept of, 4
  - Grid Circuit Theorem, 8
  - Modification by Consideration of Transit Time, 25
  - Plate Circuit Theorem, 10
- Evaluation of Admittances of Electron Stream Equivalent Circuit, 84
- Extension of Electron Stream to Grid Wires of Vacuum Tube, 86

## F

- Four Terminal Networks
  - Application of Electron Stream Equivalent Circuit, 108
  - Application to Vacuum Tubes, 102
  - Definition of, 97
  - Extension to Higher Frequencies, 103
  - Fundamental Relations, 98

## H

Hybrid Functions, 159

## I

Introduction, 1

## L

List of Illustrations, iv

List of Tables, v

## M

## Measurements

Diodes, 121

Triodes, 129

Results of Diode Measurements, 125

Results of Triode Measurements, 137

Substitution Method, 141

Susceptance Variation Method, 150

## P

Plane Electrode Space Charge Flow, 37

## S

Space Charge, 35

Space Charge Factor Concept, 65

## T

Table of Contents, iii

## Tables

I--Values of Alternating Current Components of  
Electron Stream, 70

II--Complete Space Charge, 70

III--Space Charge Zero, 72

IV--Symbols used in Derivation of Electron Stream  
Equivalent Circuit, 72

V--Limiting Values of Admittances for Electron  
Stream Equivalent Circuit, 86

Title Page, 1

Transit Time 50

Triode Networks at Moderately High Frequencies, 114

## T

## Triodes

Discussion of Results of Measurements, 137

Current Law For Plane Triodes, 39

Four Pole Admittances, 126

Procedure in Measurement of Four Pole Admittances, 129

Transit Time Effect in Negative Grid, 48

## U

U.H.F. Effects in Conventional Vacuum Tubes, 14

## V

Vita, 175

## VITA

Vasil Uzunoglu was born on March 21, 1925 in Istanbul, Turkey, the son of Arangelos and Anastasia Uzunoglu.

His pre-college education was obtained in the elementary schools of Istanbul and he completed his secondary schooling at the "Deutsche Obereal und Handelshule" in the same city. After graduation in 1942, he enrolled in the Department of Commerce at St. George College in Istanbul. The college was closed two years later due to political reasons. Vasil then decided to elect a new career for himself, and applied at Roberts College for enrollment in the Electrical Engineering Department. After graduation in 1949, he decided to continue his studies in the United States of America.

In April 1950, he registered at the University of Missouri, School of Mines and Metallurgy and continued his studies in Electrical Engineering.